Master Thesis

Deposit modeling procedure for steep-dipping veins (lithium project Koralpe) using Surpac

Andrea Martínez Rodríguez

(22/03/2017)

Chair of Mining Engineering and Mineral Economics
Department Mineral Resources Engineering
MontanuniversitaetLeoben

A-8700 LEOBEN, Franz Josef Straße 18
Phone: +43 3842-402-2001
Fax: +43 3842-402-2002
bergbau@unileoben.ac.at

Declaration of Authorship

„I declare in lieu of oath that this thesis is entirely my own work except where otherwise indicated. The presence of quoted or paraphrased material has been clearly signaled and all sources have been referred. The thesis has not been submitted for a degree at any other institution and has not been published yet.”

Preface, Dedication, Acknowledgement

My deep gratitude goes first to Mine-IT Sanak-Oberndorfer GmbH, especially to Professor Thomas Oberndorfer, who expertly has guided me with invaluable dedication. Thanks for all his encouragement and the opportunity to learn so much, being a reference in the academic and personal dimensions.

I am also very grateful to ECM Lithium AT GmbH and Steve Kesler for making possible the development of this work.

I would also like to thank to Professor Philipp Hartlieb for his support and advices, and to all the members of Montan Universitaet Leoben who have contributed to my education.

I am highly indebted to my mom for her unconditional support, education and affection which have been my main guide all these years.

Thanks also to all the friends who have given me encouragement and joy every day.

Finally, I acknowledge myself for all the work and effort done, which makes me feel very proud.

Abstract

The 80´s exploration data of the Koralpe lithium deposit have been thoroughly analyzed in terms of consistency and interpretation. Through a detailed statistical assessment on a global and individual scale, former data have been compared to a new up-to-date standards exploration campaign and validated for its use for deposit modeling purposes according to the JORC compliant.

The required deposit model outputs are lithium grade and thickness. The selection of the suitable modeling method is mainly motivated by the spatial features of the deposit. It consists of a set of narrow veins which strongly resembles parallel planes: thickness varies from 0,25 m up to 5,5 m and the prominent dimensions are the extensions along the strike (up to 1,5 km) and in dip direction (around 450 m). An innovative 2D approach has been applied, neglecting the variations along thickness. Geo-statistics are used through a 2D block model definition which only extends along the strike and in dip direction of the veins. Vein thickness is calculated as another attribute to model, such as grade, whose results include reliability of the estimation and allow extrapolation. Therefore, the size of blocks may be optimized according to the data availability. The calculation is performed individually on a vein-by-vein basis conforming to a geologically based vein assignment of samples. Results visualization and checking is conducted in 3D through a surface triangulated by means of linear interpolation. This method also enables a high level of automatization, so easy incorporations of new exploration data and interpretations are possible.

Tonnage and lithium grade of the veins are provided. Local and global reliability of the modeling results are analyzed through indicator kriging and Monte Carlo simulation. Data validation and modeling results show good reliability and have been accepted by a competent person.

Zusammenfassung

Gegenstand der Untersuchungen ist die Lagerstätte des in den 80er Jahren explorierten Lithium Koralpe Projekts, welches aus eine Serie von steilstehenden geringmächtigen Gängen besteht. In einem ersten Schritt wurden die damals erhobenen Explorationsdaten überprüft und umfassend analysiert. Mit Hilfe dieser detaillierten Untersuchung konnten die verfügbaren Daten auf einen zeitgemäßen Standard gebracht werden, der auch den heutigen hohen Anforderungen des JORC Codes entspricht.

Für die Modellierung stehen Gangmächtigkeit und Lithiumgehalt im Vordergrund. Die Auswahl des dafür am besten geeigneten Modellierungsverfahren berücksichtigt insbesondere die räumliche Charakteristik der Gänge. Die Erstreckung im Streichen (bis zu 1,5 km) und im Einfallen (ca. 450 m) dominieren die Geometrie im Vergleich zur der dritten Dimension, da die Mächtigkeiten in einem Bereich von 0,25 m bis zu 5,5 m liegen. Für diese Situation wurde ein innovativer 2D Modellierungsansatz entwickelt, welcher die Variabilität in dieser dritten Dimension vernachlässigt. Die Modellierung mittels geostatistischer Methoden wird in einem einfachen 2D-Raum durchgeführt, welcher dem Streichen und Einfallen des Ganges entspricht. Die Gangmächtigkeit wird bei diesem Ansatz analog zu den üblichen Prognosewerten wie Gehalt ermittelt. Mit dieser Vorgangsweise stehen für alle Parameter sowohl Schätzwert als auch Schätzfehler zur Verfügung, und darüber hinaus sind auch Extrapolationen einfach möglich. Weiters kann damit die Blockgröße anwendungsbezogen optimal gewählt werden. Die Berechnungen erfolgen für jeden Gang getrennt, basierend auf den im vorhergehenden Schritt dem jeweiligen Gang zugeordneten Bohrlochdaten. Für die Visualisierung und Überprüfung werden die Ergebnisse in den 3D Raum rücktransformiert, wobei als Repräsentationsmethode die Dreiecksvermaschung gewählt wurde. Die entwickelte Vorgangsweise ermöglicht einen hohen Automatisierungsgrad, welcher die Einbindung künftiger Explorationsergebnisse erheblich vereinfacht.

Für jeden Gang werden Vorratsmengen und Gehalte ermittelt. Die globale Vertrauenswürdigkeit dieser Ergebnisse wird mittels Monte Carlo Simulation überprüft. Die für die bergtechnische Beurteilung wichtige lokale Variabilität wird mittels Indicator Kriging untersucht. Auf Basis der durchgeführten Untersuchungen wurden die Ergebnisse von dem verantwortlichen, externen Experten als den Anforderungen des JORC Codes entsprechend bestätigt.

Table of Contents

1 Goal and scope

The aim of this master thesis is to develop a standard and automated procedure to model a steep-dipping vein deposit, Koralpe lithium deposit, based on exploration data and geological interpretation. Surpac (GEOVIA Surpac™), a leader software application in the mining field, will be the computing tool used to this purpose. Due to the deposit is under continuous exploration, the model has to integrate new data quickly and smoothly as well as accept changes in its interpretation.

The available data (surface boreholes, underground boreholes, exploration drifts, trenches and channels) should be investigated and statistically analyzed to detect similarities and differences related to the geological situation, especially host rock type. Due to the existing data comes from different sources and time periods (from the 1980ies until nowadays), its reliability has to be checked. The deposit regularity in space should be also evaluated. The possible modeling techniques will be discussed to find the most preferable approach according to the deposit features. A suitable method to visualize the results should also be found.

This work will be the background calculation for the JORC-compliant resource classification of this deposit, which will take place in the near future. Thus, as preparation for this classification, lithium grade and thickness are the most relevant deposit characteristics to model. For this purpose, the modeling results reliability should be assessed. The relationship between the available exploration data and expected reliability of the model must be discussed. Finally, relevant key figures will be provided (tonnage, grade, …) as a result of the selected modeling method.

2 Introduction

The Koralpe deposit is the largest known lithium deposit in Europe (Al Maynard & Associates Pty Ltd, 2014). The lithium occurs in pegmatite veins up to 5,5 m wide

and the ore body remaining open in all directions. The deposit is located approximately 20 km to the east to the town of Wolfsberg, Austria (see Figure 1). This area, also called Weinebene, is part of the mountain chain Koralpe which makes the border between Carinthia and Styria regions. The topography is characterized by a gentle mountain ridge called Brandrücken at an elevation between 1.450 m and 1.750 m above the sea level.

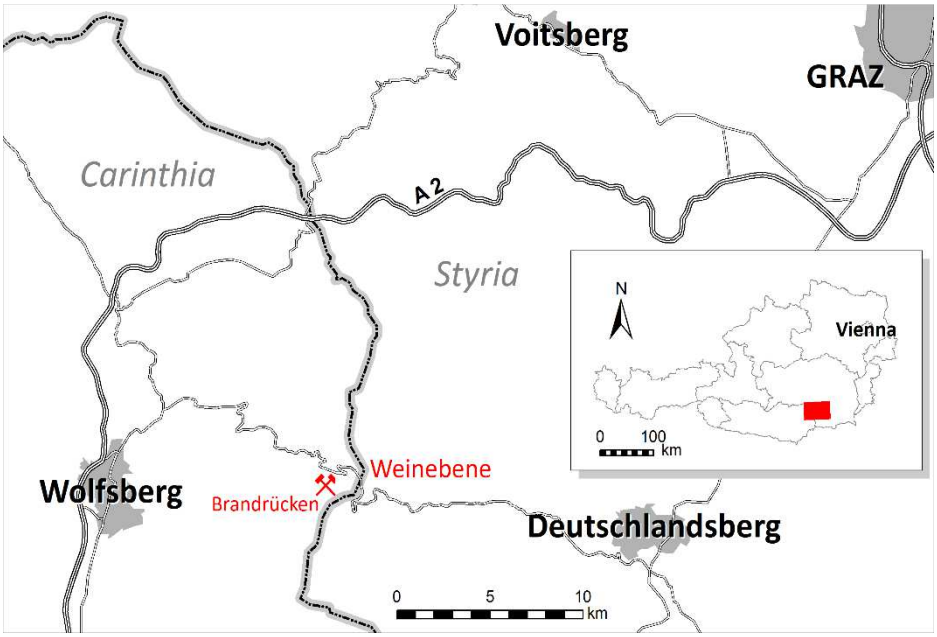

Figure 1: Location of the Koralpe deposit. Source: Göd.

The company Minerex (Minerex-Explorationsgesellschaft GmbH) performed an exploration campaign in this site between 1981 and 1988. At the initial phase, geological mapping, geophysical measurements, exploration trenches, and surface core drilling program was carried out.

In 1985, an underground exploration program was developed. It included a decline accessing the deposit, drifts along the strike and an underground core drilling program. Finally, two experimental stopes were also executed to analyze the feasibility and performance of cut-and-fill and long-hole stoping methods.

Afterwards, in 1991, all the exploration tenements and underground infrastructure was sold to “Kärntner Montanindustrie GmbH” (KMI), since then legal owner of all rights of the deposit. In 2004, 18 Mt JORC Code Inferred Mineral Resource estimate

was stated. Later, in 2011, the firm East Coast Minerals NL acquired the mining rights. Currently, the company European Lithium (EL) is investigating the feasibility of bringing the Koralpe lithium deposit into operation. For further investigations, EL needs a deposit model according to up-to-date standards. The resources will be classified through the JORC-compliant (Figure 2), allowing being listed on the Australian Securities Exchange (ASX).

The JORC code, Australasian Code, sets minimum standards for public reporting of mineral exploration results, mineral resources and ore reserves according to the levels of confidence in geological knowledge and technical and economic considerations. Its main application is to inform investors or potential investors and their advisors, emphasizing principles of transparency and materiality. All companies listed on Australian or New Zealand Stock Exchanges are required to comply with the JORC Code.

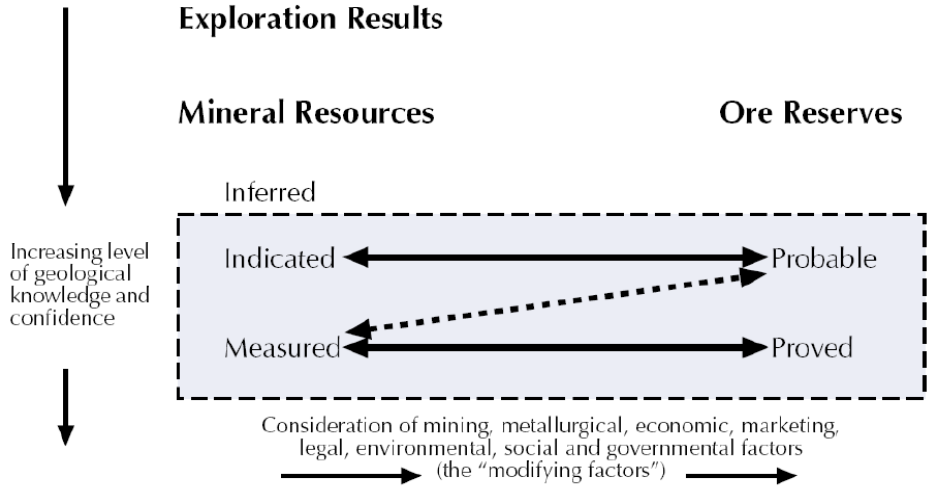

Figure 2: General relationship between exploration results, mineral resources and ore reserves (JORC 2012).

The main global end-use lithium markets are batteries and ceramics and glass, estimated as a 35 % and 32 % respectively (Jaskula, 2016). In recent years, the use of rechargeable lithium batteries has increased significantly due to its applications in the growing market for portable electronic, electric vehicles, and grid storage. In ceramics and glass applications lithium minerals were used directly as ore concentrates worldwide. Other uses of lithium are lubricating greases, air treatment,

continuous casting mold flux powders, polymer production and primary aluminum production. The main lithium import sources between 2011 and 2014 were Chile, 58 %, and Argentina, 38 % (Jaskula, 2016). Table 1 shows the world lithium production in 2014 and 2015 and the reserves per country.

Regarding the lithium markets trends, worldwide lithium production increased slightly in 2015 in response to increased demand for battery applications. Production raised about 17 % in Argentina and slightly in Australia and Chile. The expected lithium demand for 2015 was a 5 % increase respect to 2014, from 31.000 tons to 32.500 tons. Due to the increased demand spot lithium carbonate prices increased around 10 % to 15% from those of 2014 (Jaskula, 2016).

	Mine production		Reserves
	2014	2015	
United States	W [1]	W [1]	38 000
Argentina	3 200	3 800	2 000 000
Australia	13 300	13 400	1 500 000
Brazil	160	160	48 000
Chile	11 500	11 700	7 500 000
China	2 300	2 200	3 200 000
Portugal	300	300	60 000
Zimbabwe	900	900	23 000
World total (rounded)	31,700[2]	32,500[2]	14,000,000

Table 1: World Mine Production and Reserves (Jaskula, 2016).

3 Lithium geology

Lithium is the lightest metal, and has a high specific heat capacity. It may be produced from several geological sources which are divided in two broad categories of lithium sources: rock and brine sources. Rock sources include mineral sources such as spodumene, amblygonite, jadarite, as well as clay sources of lithium such as hectorite. Typical mineral deposits have a lithium content of around 0,5% to 2% Li (Mohr, 2010). Brine sources, includes lithium in salt water deposits, and include

[1]Estimated W Withheld to avoid disclosing company proprietary data. – Zero.
[2]Excludes U.S. production.

lakes, salars, oilfield brines, and geothermal brines. The Koralpe deposit corresponds to rock source category, namely the silicate spodumene (Figure 3), hosted in pegmatitic strata. Below it is given a short overview of the deposit characteristics.

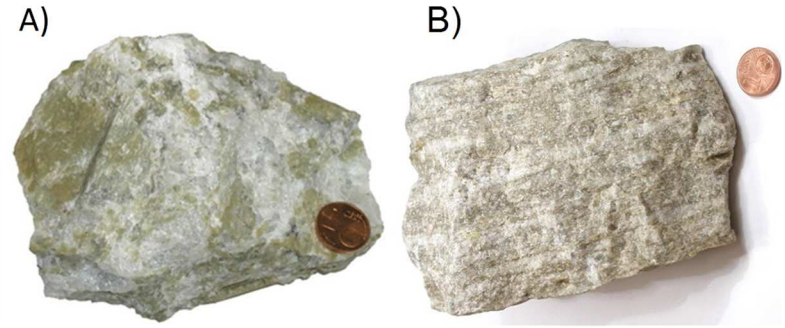

Figure 3: **Spodumene samples from Koralpe deposit. A) Coarse grain. B) Fine grain. Source: Götzinger.**

3.1 Regional geology

In the east of Austria, the Viennese and Pannonian Basins mark the eastern extent of the Alpine Belt, spine-like ridge stretching from east to west across central Europe. These basins are filled with the sediments product of the erosion of the uplifted Alps. The Alpine Belt consists of three main geological zones that relate to the thrust sheets (nappes) that have been thrust on to each other and over the crystalline basement. The oldest of these units is the Helvetic nappe which is composed of detached crystalline basement and metamorphic and igneous rocks that were metamorphosed during the Variscan Orogeny (~390-3l0 Ma).

The area under investigation is part of the eastern Alpine crystalline basement. The Koralpe area consists mostly of meso- to katazonal metamorphic rocks and is interpreted as a Variscan nappe. The crystalline complex comprises a great variety of paragneisses and micaschists as well as eclogites, amphibolites, and marbles. The metamorphic event causing the formation of the meso- to katazonal rocks is of Variscan age (Beck-Mannagetta 1980a).

3.2 Local geology of *koralpe* deposit

The area of interest is compouned by a sequence of more or less quartzitic, locally kyanite-bearing micaschists and eclogitic amphibolites. It is located at the northern slope of an anticline, so the strata uniformly strike WNW-ESE (average 120°) and dip moderately to the NNE at an average angle of 60° (Figure 4). The lithium is contained in spodumene-bearing pegmatites which form unzoned, dikelike bodies in eclogitic amphibolites and kyanite-bearing micaschists with concordant foliations (Göd, 1989). These pegmatites with form of dykes or veins have been traced over a distance of approximately 1,5 km and to a depth of about 450 m.

An extensive recrystallization took place in the micaschist-hosted pegmatites, probably caused by a younger Alpine metamorphic event. Nevertheless, it had a minor impact on the amphibolite-hosted ones. The amphibolites are finely laminated, mainly composed of amphibole, plagioclase, plus/minus garnet, and minor quartz. On the other hand, the micaschists, predominantly quartzitic are mainly composed of muscovite, quartz, garnet, and biotite. The amphibolite hosted pegmatites lie stratigraphically in the hanging wall position relative to the micaschist hosted ones, see Figure 4.

There is a NE-SW-trending fault cutting the amphibolite-hosted pegmatites which thin out in the west. Micaschist-hosted pegmatites are thin out also in the west and besides in the east. It is remarkable that the ore potential appears to be larger than the reserves known so far.

Their internal structure, degree of metamorphic overprint and the distribution of their major and trace elements differentiate pegmatites amphibolites to micaschists hosted. Nevertheless, there is no evidence suggests a different origin or intrusive stage. Their different reactivity during pegmatite emplacement and, therefore, regional metamorphic overprinting may account for the differences observed in the both pegmatite hosts.

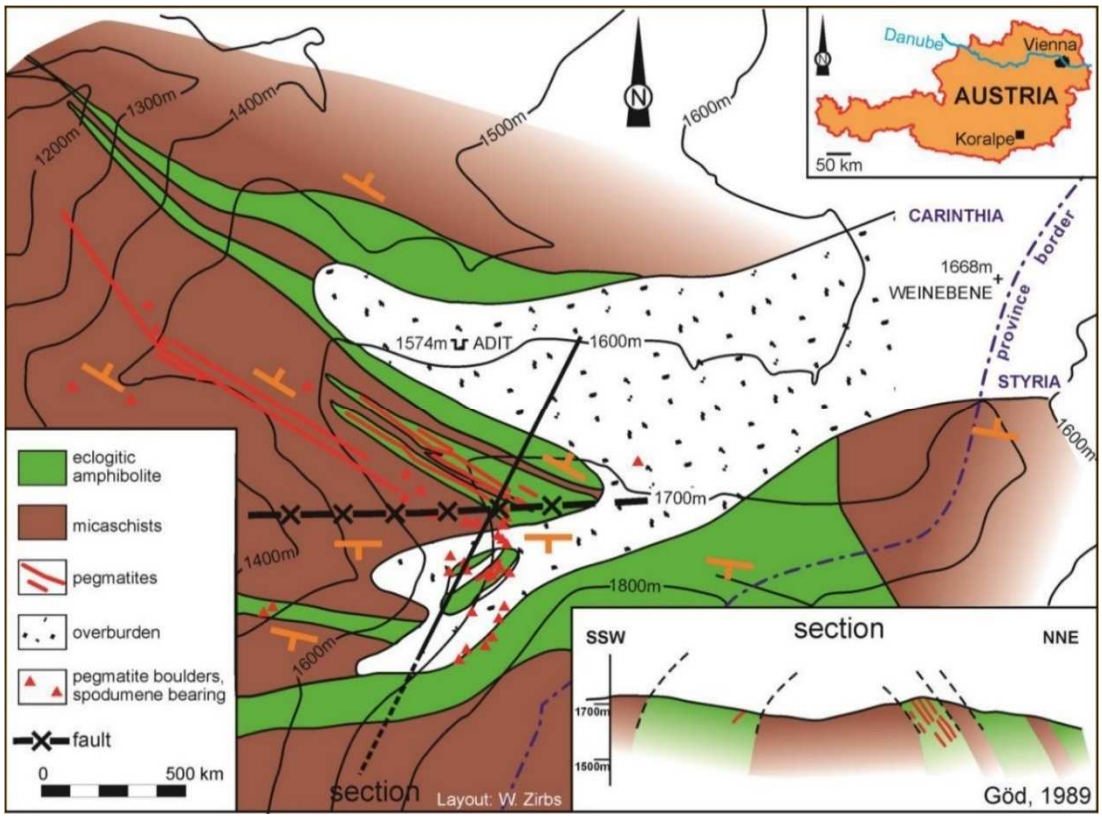

Figure 4: Geological map of the deposit area and cross section. Source: Göd, 1989.

It has been identified three main pegmatites dykes with economic interest hosted in the amphibolites (dykes 1.1, 2.1, and 3.1) and two more in the micaschists (dykes 6.2 and 7), see Figure 5. The dyke 7 is the largest and has been traced along strike continuously for approximately 1.250 m and to a depth of about 200 m. The thickness of the veins is around 2 m, with a maximum of 5,5 m. The disparity in thickness clearly depends on the host rocks shape.

In accordance with underground observations, the shape of the pegmatites seems to be rather uniform (Al Maynard & Associates Pty Ltd, 2014). The disturbances are found just locally by subordinate displacements ranging from a few decimeters up to a maximum of 3 m along NNW-SSE-trending faults. However, some veins show an inner discontinuity in certain areas denominated inter-bedding, see Figure 6.

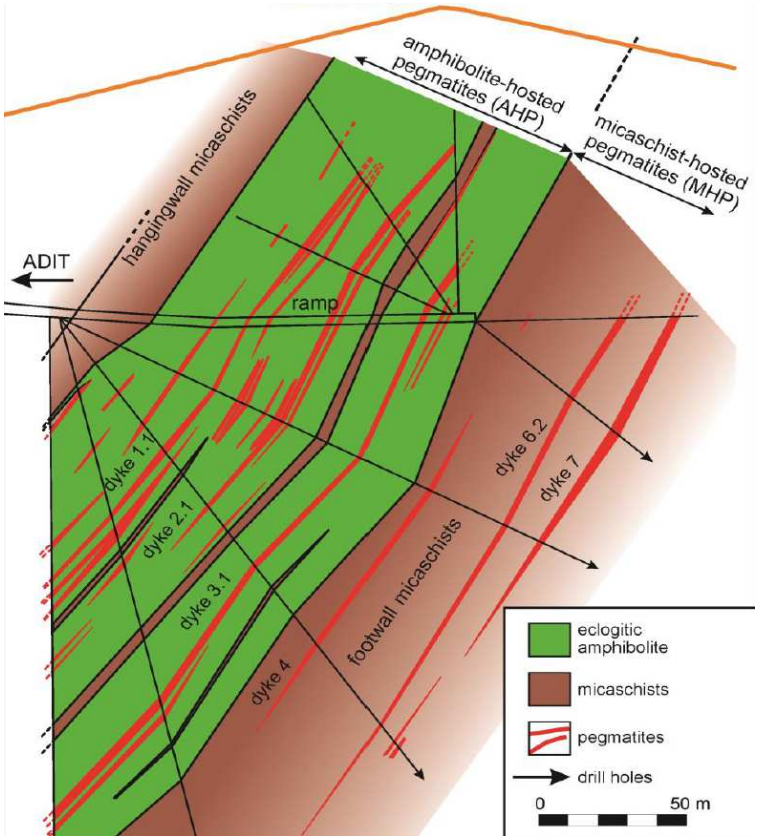

Figure 5: Cross-sectional profile of the Koralpe pegmatites. Source: Göd, 1989.

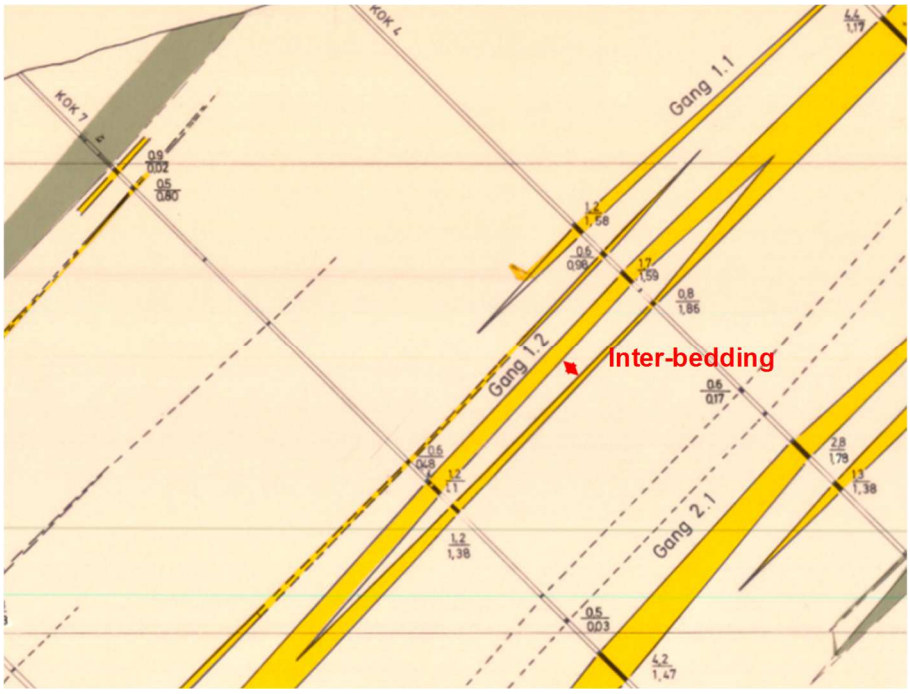

Figure 6: Example of geological interpretation of boreholes. Source: Minerex.

4 Review of deposit modeling techniques

Deposit modeling is a technology intended to calculate, document, and visualize the estimated characteristic of a deposit in the space generally by means of computer tools. The selected model approach must be in accordance with the relevant characteristics to model, that is to say its application, and deposit features. Expected accuracy and reliability are always important aspects to consider too.

Any spatial object can be represented through a surface element or a solid[3] element. The first may be defined like a boundary, while the second includes a volume and information of every inner point. However, both spatial elements can be used to represent a geometric surface or a geometric solid due to the fact that a geometric solid may be described by its surfaces using a surface element and a geometric surface can be represented as the surfaces which bounds a solid element. According to that, below it is explained the main modeling techniques for geometric surfaces representation and deposit deduction.

4.1 Geometric surfaces representation

There are two essential classes of surface representation: parametric and implicit. Parametric representations are defined by a vector-valued function $f: \Omega \rightarrow S$ where $\Omega \subset R^2$, that maps a 2D parameter domain to the surface $S = f(\Omega) \subset R^3$. On the other hand, an implicit, also called volumetric, is defined to be the zero set of a scalar-valued function $F: R^3 \rightarrow R$, i.e., $S = \{ x \subset R^3 \mid F(x)=0 \}$ (Botsch, 2010).

As an example of parametric versus implicit representation, both definitions for the unit circle are shown:

a. Parametric function: $f: [0, 2\pi] \rightarrow R^2, t \rightarrow \begin{pmatrix} \cos t \\ \sin t \end{pmatrix}$

b. Implicit function: $F: R^2 \rightarrow R, (x, y) \rightarrow \sqrt{x_2 + y_2} - 1 = 0$

For complex shapes finding a parametric function may not be possible. Thus, the domain is usually split in smaller extensions and then an individual function is defined to estimate the shape of every fragment locally. The global approximation

[3]Surpac uses the term solid to denominate a set of surfaces which envelope a close space. Both terms should not be confused.

to a given shape depends on the size and number of segments. A condition to generate these local functions is that they need to fit to its neighboring ones. Segmentation into triangles or quadrangles are the most common piecewise surface definition for the parametric method while hexahedral or tetrahedral cells are used for implicit cases (Botsch, 2010).

Both methods, parametric and implicit, have their own advantages and disadvantages, so the best option should be chosen according to the specific work aim and geometrical characteristics of the deposit.

4.1.1 Parametric surface representation

Parametric representations have the advantage of reducing 3D problems on the surface *S* to 2D problems in the parameter domain Ω (see Figure 7).

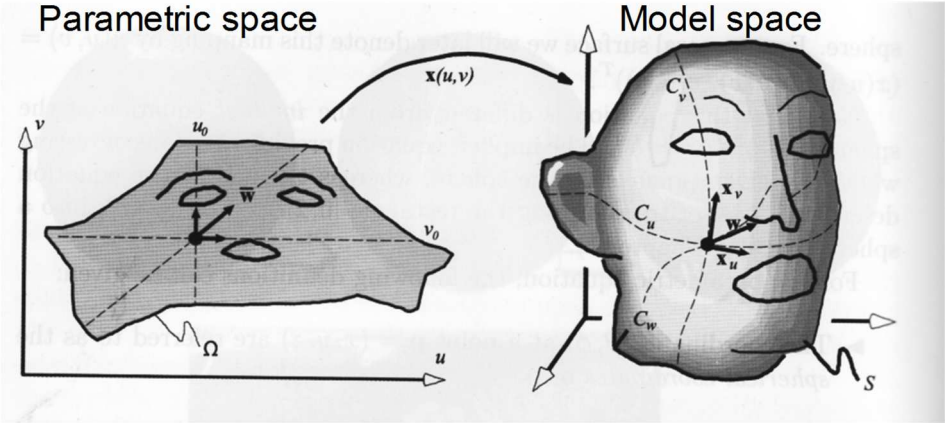

Figure 7: Example of transformation from parametric space into 3D. Source: Modified Horman et al., 2007.

Topology is the study of geometric properties and spatial relations unaffected by the continuous change of shape or size of objects. In topological terms, two objects can be considered equivalents if they can be transformed into the other through isometries without separating or joining any element compared to the original object. In Figure 8 is shown the difference between spatial and topological (geodesic) neighborhood. The point *a* has as spatial neighbor and equally distanced *b* and *c*, but only the point *b* is its topological neighbor.

In accordance, generating a parametric surface can be very complicated as it has to be fitted to the topological and metric structure. Due to the most of the surfaces

are defined as a set of parametrizations, if the topology is changed, also the domains have to be adjusted, which is an extremely complicated task.

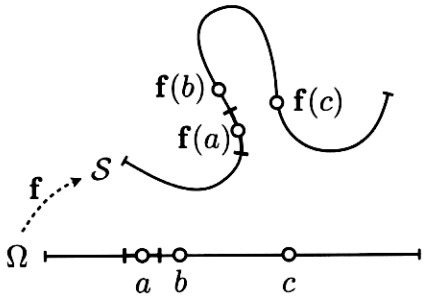

Figure 8: Spatial and topological neighborhood. Source: Botsch, 2010 p. 4.

Besides that, typical queries such as inside/outside or signed distance include also extreme difficulties as they require finding the closest point on *S* to the query point, also called foot print (Botsch, 2010). Therefore, the drawbacks of parametric surfaces are its difficulties to topological modification and spatial queries.

Three parametric representation styles can be described:

Spline surfaces or NURBS

NURBS, or none uniform rational B-splines, is the most widely representation system used in CAD systems. Tensor product spline surfaces are used to characterize high quality surfaces as well as freeform surfaces editing tasks. A tensor product split surface is the result of connecting several polynomial patches in a smooth manner and it always represents a rectangular surface in R^3. Each surface point is a convex combination of the so-called “control points” which have local influence only. The control points define the control mesh.

As consequence of the topological constrains, these models are typically a massive set of surface patches which have to be connected, complicating the surface construction. Another weak point is that in order to add extra control vertices, parameter intervals have to be split affecting an entire row or column of the control mesh tensor (Botsch, 2010).

Subdivision surfaces

The subdivision surfaces (Zorin, 2000) can be considered a generalization of spline surfaces due to the fact that they are also controlled by a coarse control mesh. Its advantage is that subdivision surfaces can represent surfaces of arbitrary topology. They are created by repeating the refinement of control mesh based on a set of local averaging rules (Botsch, 2010).

Hence, subdivision surfaces are not limited by topological or geometric restrictions, allowing highly efficient algorithms. Their restriction is to produce mesh with semiregular subdivision connectivity, i.e. product of the refinement of a coarse control mesh. As a consequence, the arbitrary meshes would have to be remeshed in a preprocessing step. However, this remeshing process leads to a resampling of the surface and, therefore, typically also a loss of information.

Working on arbitrary triangle meshes allows to avoid these limitations providing higher flexibility and still efficient surface processing.

Triangle meshes

Triangle meshes are defined as a collection of triangles without any particular mathematical structure (Botsch, 2010). Through the barycentric parametrization, each triangle defines a segment of a piecewise linear surface representation. Besides, every inner point p in a triangle can be defined as a barycentric combination of the corner points:

$$p = \alpha\, a + \beta\, b + \gamma\, c,$$

where

$$\alpha + \beta + \gamma = 1, \qquad \alpha, \beta, \gamma \geq 0.$$

Therefore, in order to define a complete triangle mesh it is sufficient to define a 2D position for each vertex. The linear mapping method from R^2 to R^3 chosen should cause the minimum distortion. It must be remark that even if vertices have assigned 3D positions, the resulting polygonal surface consist of triangles with linear parametrization functions. Accordingly, the approximation goodness of a mesh to a given shape depends on its curvature, that means flat areas are scarcely sampled, while curved areas need more amount of data. This involves a refinement splitting triangles. Thus, the approximation error of a mesh is inversely proportional to its number of triangles.

4.1.2 Implicit surface representation

In implicit or volumetric representations, any point in the 3D space is defined by inside, outside or exactly in the surface. In this kind of representation, the surface S is defined as the zero-level isosurface of scalar valued function $F: R^3 \rightarrow R$ and contains the points located exactly on the surface separating the inside from the outside (Botsch, 2010). Due to the function F is continuous there is no gaps in the

defined 3D space, and besides no geometric self-intersections can occur. Implicit representations allow constructing solid geometry of complex objects by using Boolean operations in object of simple geometry. Although the implicit function to a given surface *S* is not uniquely determined, the so-called *signed distance function* maps each 3D point to its signed distance from the surfaces.

An advantage of implicit surfaces is that they may be deformed through decreasing or increasing function of *F* locally. The topology and connectivity can be modified as well due to the structure of *F* is independent from surface topology. On the contrary, implicit methods present difficulties to generate sample points, finding geodesic neighborhoods or rendering the surface.

Implicit functions can be represented in several manners such as algebraic surfaces, radial basic functions, or discrete voxelizations (grid type). The most popular spatial data structures for representation are regular grids and adaptive data structures.

Regular grids

Representation through regular grids consist of discretizing the space in bounding box improving the efficiency of the process. Nevertheless, the memory needed by the data grows cubically if the precision is increased by means of reducing the edge length of grid voxels (Botsch, 2010).

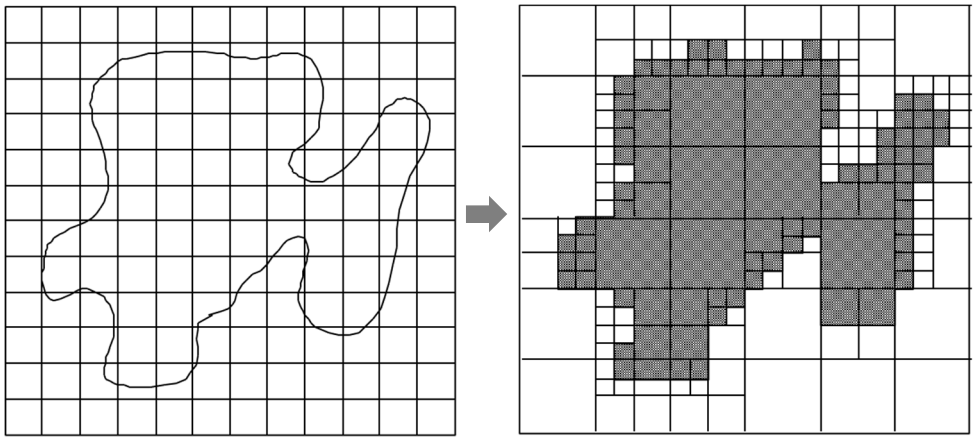

Figure 9: Additional precision just in the required locations in order to safe store capacity. Source: Botsch, 2010.

Adaptive data structures

In order to improve the memory consumption, sampling density is usually adapted to the local geometric significance. Because of more precise signed distance values are required in the vicinity of the surface, only in these regions more data density is needed. Extreme refinement is applied only in regions with high curvature. This

approach reduces the memory storage being even comparable to mesh representations.

Algebraic method

There is a popular software in the 3D geological modeling market, Leapfrog™, which through algebraic polynomial formulas provides an implicit method for modeling the space.

4.1.3 Parametric versus implicit representation

The parametric representations can be linked to surface elements while implicit representations resemble to solid elements because, even if they may represent a geometric surface, the model contains information in all the work space.

As explained above, parametric and implicit representations have complementary advantages. Parametric method allows simplifying 3D problems to 2D as it does not need to define all points in the space, but sampling just the surface. Therefore, the computing memory requirements are reduced. Besides, parametric method provides information about neighboring. On the other hand, implicit method is suitable for spatial queries, i.e. inside-outside of the surface, as includes information of all the working space. Moreover, through Boolean operations this method allows to characterize complex structures independently from topology.

4.2 Modeling deduction in Surpac

Surpac offers several deduction methods to estimate a deposit model. The methods most commonly used are linear interpolation, inverse distance and geostatistics. Linear interpolation method is applied through triangulation of surfaces, and thus it is a parametric method. Inverse distance method and geostatistics provides information about all the work space through block model, and therefore they both are implicit methods.

4.2.1 Linear interpolation (by means of triangulation)

Resource estimation techniques vary in complexity according to the amount of computation involved in deriving the estimate. The simplest techniques assign the value of a sample to its area of influence defined through intersections which other areas of influence. These methods are known as polygonal, area-of influence, or nearest-neighbour approaches and provide a discrete appearance (Figure 10). Besides that, these methods lack of applicability to thick, non-tabular bodies (Glacken and Snowden 2001, p. 189). On the other hand, linear interpolation offers a smoother version of estimation as is explained below.

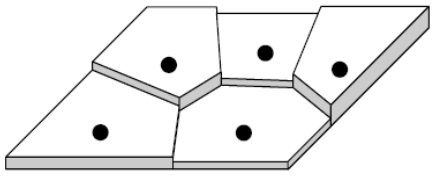

Figure 10: Estimation through areas of influence of sample points. Source: Berg et al., 2008.

A terrain can be interpreted as a 2D surface expressed in a 3D space with a special property: every vertical line intersects it in a point, if it intersects it at all (Berg et al., 2008). When a terrain height is sampled, the height of every point in its surface is not known so it has to be approximate at the other points in the same domain. Given a set of points with known elevations, it is created a planar subdivision whose bounded faces are triangles and whose vertices are the mentioned points. Afterwards, the vertices are lifted to its known elevation getting in the 3D space. The result is a polyhedral terrain as an approximation of the original terrain (Figure 11).

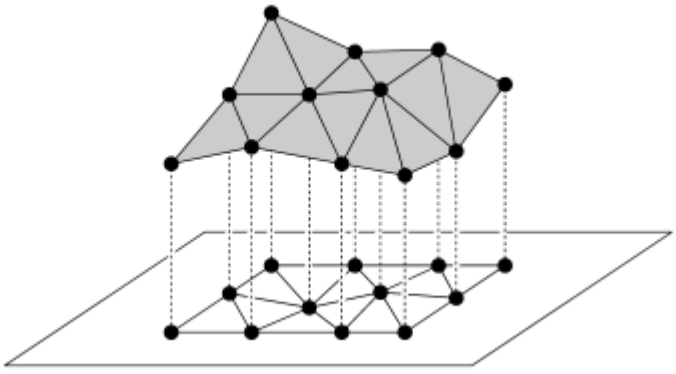

Figure 11: Obtaining a polyhedral terrain from a set of sample points. Source: Berg et al., 2008.

There are many different ways to triangulate a set of points. Due to the original terrain is unknown - only the sampled points are known – all possible triangulations that use the correct height at the sample points seem to be correct. Nevertheless, some triangulations look more appropriate than others. The Figure 12, taken from Berg et al., 2008, show an example of two interpretations for the same set of sample points. Intuitively the sample points seem to correspond to a mountain ridge. Triangulation (a) reflects this interpretation, however, triangulation (b), where only one edge has been modified, has included a little valley cutting through the mountain ridge. Triangulation (b) looks incorrect. The height of the point *q* is determined by two points that are relatively far away and in the edge of two triangles long and sharp. Hence, the optimal triangulation must have the triangles combination with the biggest angles, i.e. the maximization of the minimum angle, and requires a degree of interpretation by human participation.

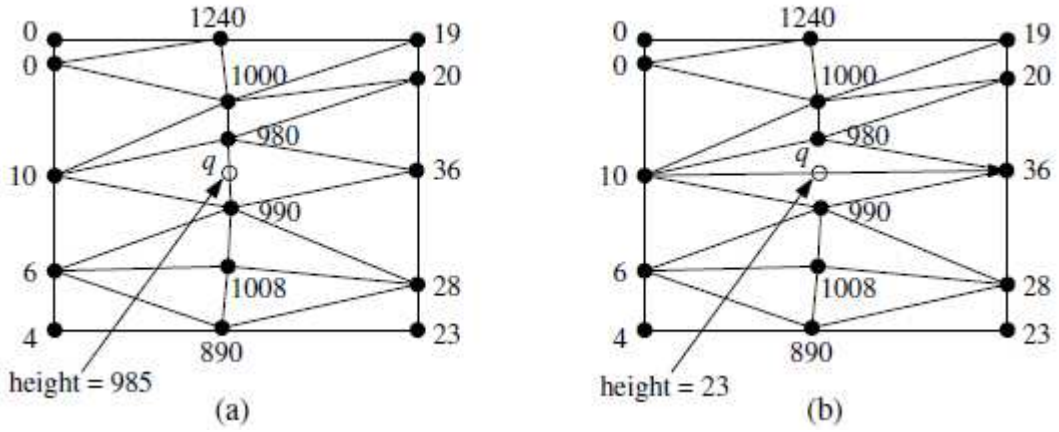

Figure 12: Two versions of triangulation for a same set of sample points. Source: Berg et al., 2008.

The most widely used method is Delaunay triangulation. It was created in 1934 and ensures the maximization of the minimum angle of the triangles. Given a set *X* of points in the plane, a set of Π configurations consisting of triangles formed by three non-collinear points in *X*. The Delaunay theorem can be summarized by these two conditions to a *P* set of points in the plane:

c. Given three points $p_i, p_j, p_k \in P$ are vertices of the same face of Delaunay graph of P if and only if the circle through p_i, p_j, p_k contains no other point of *P* in its interior.

d. Two points $p_i, p_j \in P$ are vertices of an edge of the Delaunay graph of *P* if and only if there is a closed disc *C* that contains p_i and p_j on its boundary and does not contain any other point of *P*.

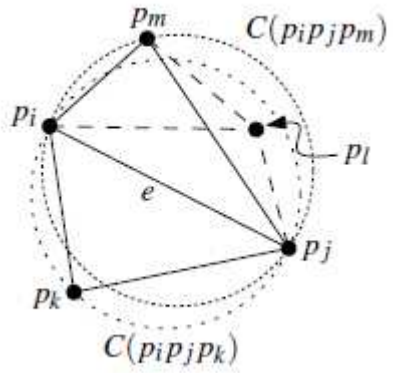

Figure 13: Example of Delaunay triangulation. If a point p_l exists, the triangulation drawn by continuous line is not valid because it lies inside the circles through the vertices of those triangles. Source: Berg et al., 2008.

Delaunay triangulation is linked to another important geometric structure, the so-called Voroni diagram, see Figure 14. Given a set *P* of sample points, the Voroni diagram built a subdivision of the plane into n cells, one for each point of *P*, where every point *q* inside the subdivision of the sample point *pi* satisfied dist(*q, pi*) < dist (*q, pj*) for each , $p_j \in P$ with $j \neq i$. For the two point in the plane, *p* and *q*, the Voroni diagram define a bisector of *p* and *q* as the perpendicular bisector of the line segment *pq*. Therefore, connecting the centers of each circumference where lies the three vertices of the triangles of the Delaunay triangulation it is produced the Voroni diagram.

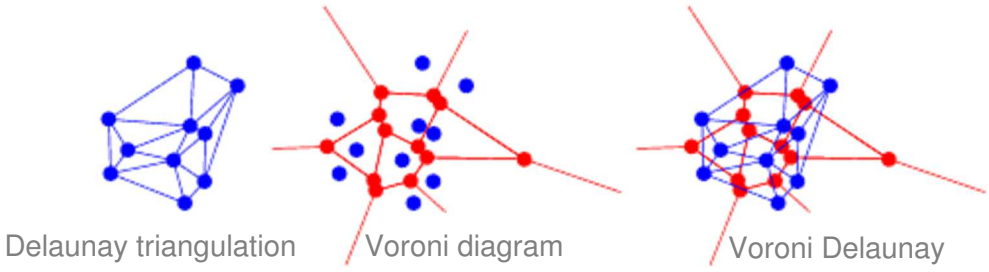

Figure 14: Example of Delaunay triangulation and Voroni diagram over the same set of sample points. Source: Wolfram Research, 2016.

Triangulation method may be considered a 2,5D method due to transform a 2D algorithm calculation method, considering just two coordinates of a triangulation plane (x,y), into 3D by giving a height perpendicular to the plane. Thus, its performance depends on the surface characteristics. If the surface is not parallel to the triangulation plane, such as steep areas of the terrain like a bench face, the approximation through triangulation is especially problematic. This problem is

particularly accentuated when the terrain to model do not show its topology from the triangulation plane view (Figure 15).

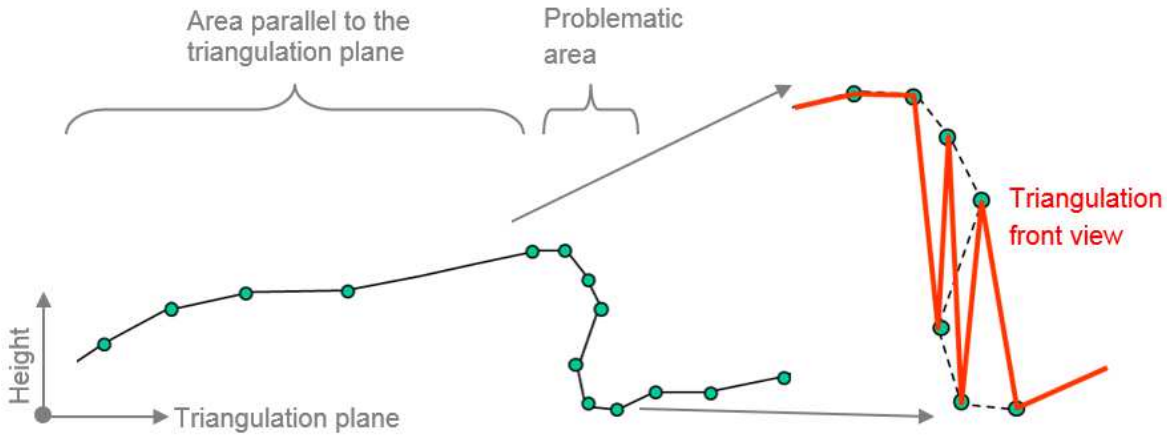

Figure 15: Example of problematic surface to model.

In other fields such as photogrammetry, where the sample data cloud is denser than in mining applications, triangulations can accept this kind of irregular shapes as well. Besides, note that Delaunay triangulation could also be applied in the 3D spaces by means of using spheres instead of circumferences and creating tetrahedrons 3D instead of triangles 2D. However, this alternative is not provided by Surpac.

Triangulation is also employed in the so-called cross section method. This method consists on the use of 2D profiles, likely product of geological interpretations, to create a boundary of the ore body by connecting through triangulation the cross sections (Figure 16). This method supports the 3D understanding of the deposit and enables spatial calculations, but it does not include any information about the deposit inside the surfaces.

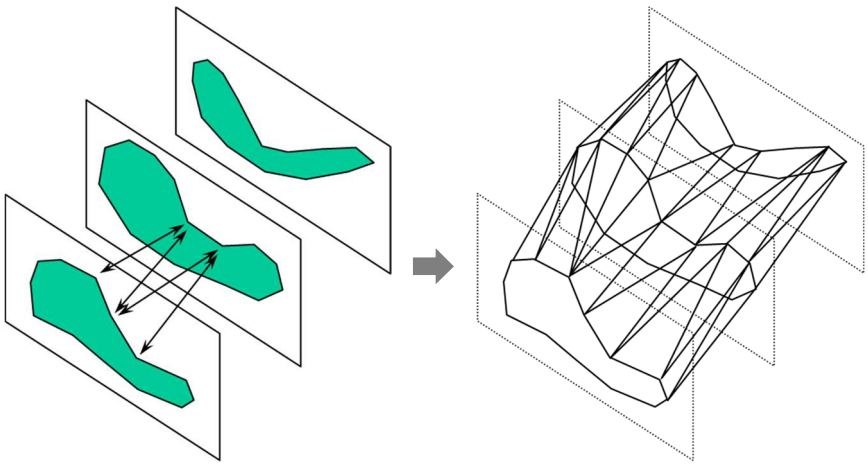

Figure 16: Example of cross section method.

Besides height, triangulation allows estimating any parameters such as grade or thickness through linear interpolation in a 2D perspective. The vertices of the triangulation surface contain the value of the samples. The estimation in the edges of the triangles is calculated as a linear combination of the value of its two vertices, while the points inside the triangle are estimated as a combination of the values of three vertices of the triangle (see 4.1.1).

4.2.2 Inverse distance method (by means of block model)

The next step up in computational complexity is to apply some weighting function to distribute the influence of the samples around the point to be estimated. A common weighting function is the inverse distance method.

In order to use the inverse distance method or geostatistic methods in Surpac, a bock model of the work space has to be defined. The space is discretized into blocks. Each of these blocks can have properties such as the estimated grade. All points inside the block have the same estimated value for a property. There are different manners of estimating the block properties:

e. Manual assignment: not a preferable due to the large number of blocks. For instance, an area of one square kilometer and 200 meters depth could mean 200.000 blocks.

f. Discrete properties or qualitative: usually by means of the relative situation to a surface.

g. Numerical properties or quantitative: deduction from a sample data. The possibilities to incorporate interpretations are limited. Deduction through geostatistics are included in this group.

Inverse distance method is the simplest weighting function in use. The weight is calculated as the inverse of the distance of the sample from the point to be estimated raised, generally, to the second powder. In this method, samples closer to the point to estimate get a higher weighting than the samples far away. Its main advantage is that is simple and speedy to calculate and that the exponent selection offers certain flexibility. The biggest disadvantages are that preferential sampling makes estimates unreliable and that extreme values create large halos of great estimates (Queen´s University, 2014). Besides, it does not include any output about the reliability of the results. This technique introduces issues such as sample search and declustering.

4.2.3 Geostatistics (by means of block model)

The use of geostatistical techniques, based upon the theory of regionalized variables, involves a further complexity in calculation. These techniques consist on the application of general univariate and bivariate statistical rules to make an estimation over a property dependent on its location, i.e. utilizing the spatial relationship between samples. Usually, the method is applied for numerical properties which have a gradual distribution over the space.

Due to the fact that the real properties between samples are unknown, the estimation approach may be considered subjectively more or less adequate, but not right or wrong, as they will reflect some assumptions. Once the extraction has taken place the quality of the estimation must be checked. Thus, estimation incorporates a degree of error which should be calculated in terms of statistical reliability. The main advantage of geostatistics is that they are based on mathematical foundations, offering a statistical result, i.e. reliability or confidence level. Besides, they are relatively simple to handle. On the other hand, it is not applicable to all kinds of deposit distribution and aims.

The regularity of a deposit describes the spatial continuity of a variable, i.e. adjacent samples are dependent to each other. It may be indicated by the correlation between one sample and the next. Comparing a sample with the sample after *n* sample steps might show the regularity on a longer scale interdependency. A statistical figure such as correlation factor or deviation variance could compile the characteristics into one single figure. A widely used mathematical model to represent the regularity is the variogram. A variogram represents a fitted model of the variance of the set of samples with *h* distance or step from each other as shown in Figure 17.

The graph starts with positive slope because samples close to each other are more likely to have similar values than those far apart. At some level, a maximum is reached due to it is not possible to find a larger dispersion than comparing minimum with maximum. This level is named sill and the *h* distance in which is reached is denominated range. In most of the cases, the model has also a variance at zero distance, indicating a small distance irregularity. Variograms refers to an entirety, so it might be useful to discriminate between different subsets such as geological formations or areas. In anisotropic situations, the variogram should also depend on a search ellipsoid orientation, not only distance between samples.

The kriging method is the most commonly used in geostatistics to approximate the values of a deposit. The main advantages of kriging are that provides a statistical

approach which include a measure of uncertainty and that includes geological knowledge by the use of the variogram. On the other hand, it requires an intense use of computing tools and highly depends on the selected parameters. (Queen´s University, 2014)

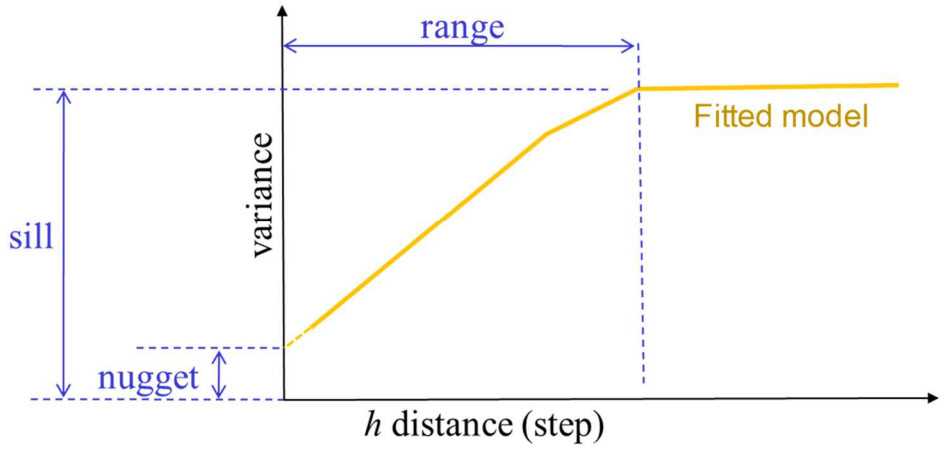

Figure 17: Outline of a variogram

Ordinary kriging method

The kriging method estimates a variable in the un-sampled points as a linear combination of values in the search radius of that variable with an assigned weight (Rostami and Habibi 2015, p. 184). The error of the estimation is approximated by the use of the variogram, and thus, the errors can be minimized, providing the optimal linear and unbiased estimations.

It is assumed that the data set has a stationary variance but a non-stationary mean value within the search radius. The covariances among the samples are consider to select the weights of a cluster of samples and minimize the effect of variable sample spacing. The success of kriging directly depends on a correct selection of the variogram parameters. Kriging weights are calculated by solving the equations shown below minimizing the variance of the estimation error:

$$g^* = \sum_{i=1}^{i=n} w_i * g_i \qquad \sum_{i=1}^{i=n} w_i = g_i \qquad R = g^* - G$$

where w_i = weights, g^* = estimate value, g_i = sampled value; R = estimate error, G = actual value.

For each point a set of linear equations are used to calculate the optimal weight according to the distance using the variogram. These equations are usually express through matrix notation, where the correlation matrix records all the redundancies between the samples.

$$\underbrace{\begin{bmatrix} C_{11} & \cdots & C_{1n} & 1 \\ \vdots & \ddots & \vdots & 1 \\ C_{1n} & \cdots & C_{nn} & 1 \\ 1 & & 1 & 0 \end{bmatrix}}_{\text{Sample redundancy}} * \underbrace{\begin{bmatrix} w_1 \\ \vdots \\ w_n \\ \mu \end{bmatrix}}_{\text{Kriging weights}} = \underbrace{\begin{bmatrix} C_{01} \\ \vdots \\ C_{0n} \\ 1 \end{bmatrix}}_{\text{Statistical distances}}$$

Indicator kriging method

The standard geostatistical procedure considers a block as a homogeneous item characterized by the mean and variance of the relevant parameters (here thickness and grade). It is however obvious that there will be some variation within a block. This aspect can be accomplished with a slightly modified estimation procedure called indicator kriging. This approach estimates the ratios of particular classes in every block. It is therefore based on a single threshold value, distinguishing the ratio above and below this value (e.g. for a thickness threshold of 1 m, the estimation describes the ratio above and below 1 m, see Figure 18).

Performing this calculation for a series of thresholds the ratio of classes can be determined. In this way, values on the tails of the distribution diagrams will appear, although only as a fraction of a total block. In consequence, the distribution as such resembles more to the reality and also to the samples.

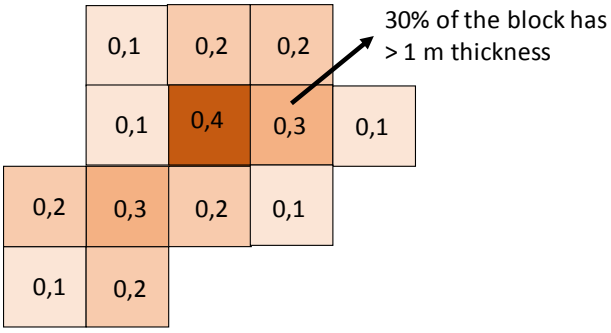

Figure 18: Example of ordinary kriging.

5 Available exploration data

The company Minerex (Minerex-Explorationsgesellschaft GmbH) conducted the exploration works in the Koralpe area between 1981 and 1988 including geological mapping, geophysical measurements, exploration trenches, and a core drilling program from surface as well as a detailed underground exploration: decline accessing the deposit, drifts along the strike of selected veins and an underground

core drilling campaign. In order to accept all Minerex data according to up-to-date standards, a selected subset from boreholes and drift samples will be compared by redoing sampling. The new drilling campaign will be carried out by the company European Lithium. It will consist of executing twin holes to the original boreholes and a drift face surveying through channel samples.

Besides, for a better representation of the topographic situation most recent surveying data of the surface topography of this area is used. These data are supplied by the Austrian Surveying Service "BEV". Basically these data comprise:

· Grid data and structural data of the exploration area (5.300m x 2.800m).

· Orthographic image of this area.

5.1 Surface topographic data

A topographic data extended to a size of 5.300 m x 2.800 m is used. The electronic data are provided by the Austrian Surveying Service (BEV) and consist of 10 m grid points and structural data (such as roads, etc.). For better orientation, the data is complemented by a satellite image of the same size (Figure 19).

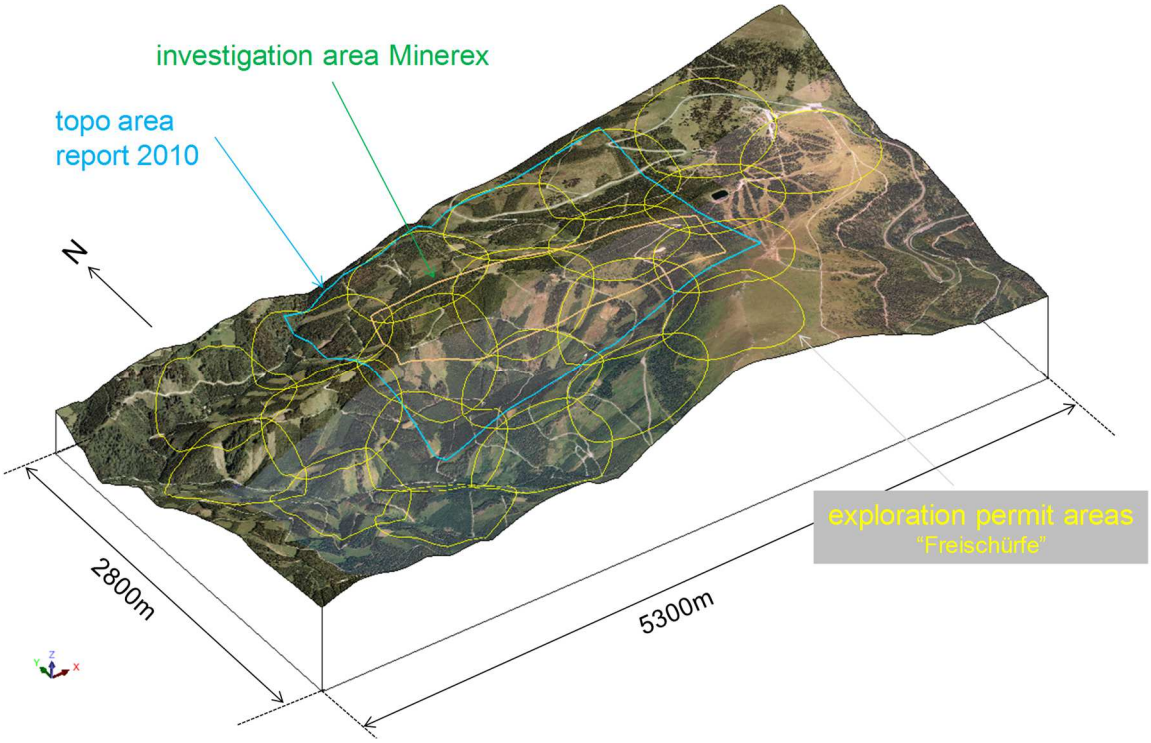

Figure 19: Topographic data. Source: BEV modified.

5.2 Original exploration data

The most prominent of Minerex data were:

- Overview of the regional geological situation (1:10.000).
- 22 geological profiles, covering a length of about 1.500 m along the strike of the veins (1:500).
- Site plan of the exploration area and the exploration works, including underground drifts (1:1.000).
- Geological database with positions of pegmatites and Li_2O grades.

Table 2 resumes the amount of data obtained from Minerex research works.

Exploration work	Parameters	
Exploration trenches (surface)	**Number / volume**	**35 / 9.940 m³**
Core drilling (surface)	**Number / length**	**64 / 12.012 m**
Decline drift from surface	**Length**	**417,6 m**
Decline underground (between veins)	**Length**	**119,2 m**
Drifts following vein (along strike)	**Length**	**853,7 m**
Core drilling (underground)	**Number / length**	**37 / 4.715 m**

Table 2: Summary of exploration works based on Minerex reporting. Source: Cerny et al., 1989.

5.2.1 Profiles

The profiles generated by Minerex are based on core drilling and observations during the extraction of the underground mine workings. Its layout follows a very regular pattern, generally oriented perpendicular to the general strike direction of the deposit.

The spacing ranges between 90 m and 130 m. In the eastern part of the investigation area additional profile lines are introduced at half-distance of the original spacing, reflecting the positions of the underground drillings. The profiles location is shown in Figure 20.

Profiles in the eastern part (investigation area I) are identified by capital letters (A to I). The supplementary profiles originating from the underground drillings are labeled with a character-combination denoting the neighboring profiles. E.g. profile C-D is located in between the main profiles C and D. Their orientation is 18° to the north. The profiles of the western area are labeled by numbers (0 to 9) and their orientation

has a bearing of 27°. Table 3 summarizes the existing profiles including the boreholes which effect the geological interpretation (i.e. which are close to the respective profile).

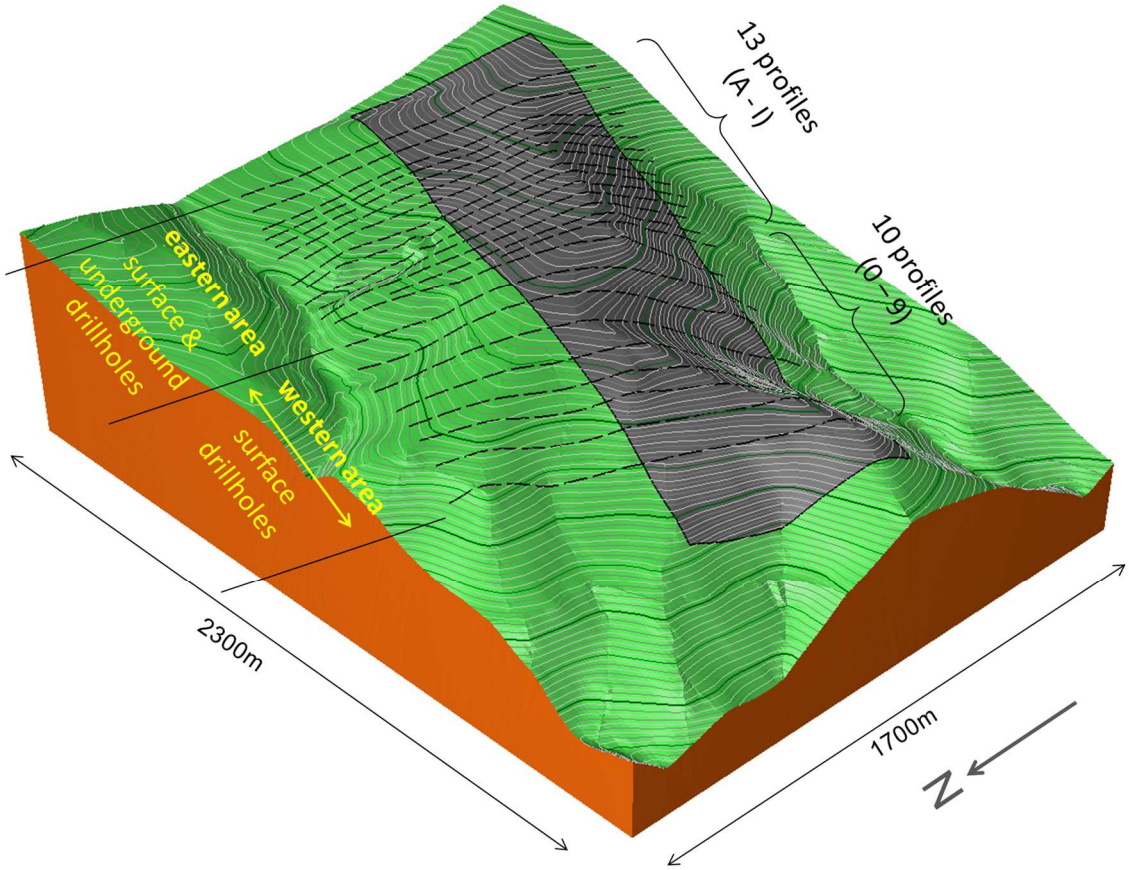

Figure 20: Location and nomenclature of the geological profiles.

These profiles show the borehole traces and the interpreted host rock (amphibolites and mica schist) and the trace of the veins interpreted by Minerex (Figure 21). The boundaries of these geological bodies have been digitized and converted into the corresponding 3D position in space through Surpac (see Figure 22). This information provides a basis to understand the general shape of the deposit. Likewise, the vein assignment done by Minerex along the boreholes will be also foundation for the geometric modelling of the deposit.

Profile	Area	Bearing	Boreholes			
			Surface		Underground	
			No.	Borehole name	No.	Borehole name
0	I (E)	27				
1	I (E)	27	3	46, 46A, 57		
2	I (E)	27	3	38, 38A, 47		
3	I (E)	27	3	39, 39A, 48		
4	I (E)	27	3	42, 42A, 49		
5	I (E)	27	3	44, 44A, 50		
6	I (E)	27	4	41, 41A, 51, 58		
7	I (E)	27	3	40, 40A, 52		
8	I (E)	27	2	53, 53A		
9	I (E)	18	2	54, 54A		
A	II (W)	18	1	23		
B	II (W)	18	6	24, 35, 35A, 35B, 43, 55	5	25, 28, 30, 33, 35
C	II (W)	18	5	21, 22, 33, 33A, 33B		
C-D	II (W)	18			7	26, 27, 29, 31, 36, 37, 38
D	II (W)	18	6	11, 13, 19, 19A, 19B, 32		
D-E	II (W)	18			9	12, 14, 15, 2, 32, 34, 4, 5, 6
E	II (W)	18	7	10, 12, 18, 18A, 26, 31, 31A		
E-F	II (W)	18			7	10, 11, 13, 16, 19, 23, 9
F	II (W)	18	8	1, 16, 17, 2, 3, 30, 30A, 30B		
F-G	II (W)	18			6	17, 18, 20, 21, 22, 24
G	II (W)	18	9	14, 14A, 15, 27, 29, 29A, 29B, 4, 7		
H	II (W)	18	4	28, 28A, 5, 8		
I	II (W)	18	2	6, 9		

Table 3: Summary of geological profiles (including effected boreholes).

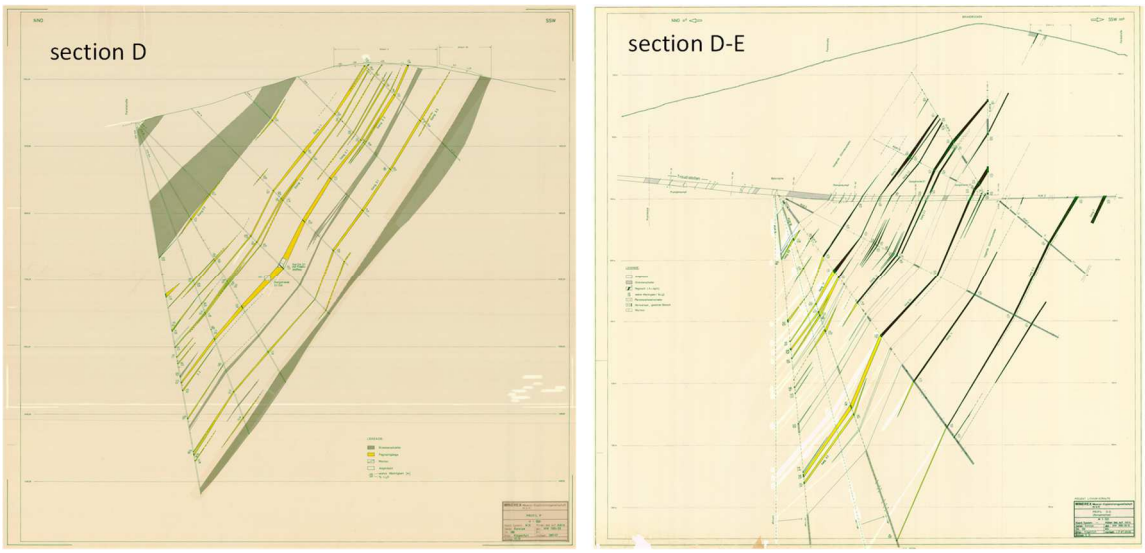

Figure 21: Examples of two geological profile done by Minerex.

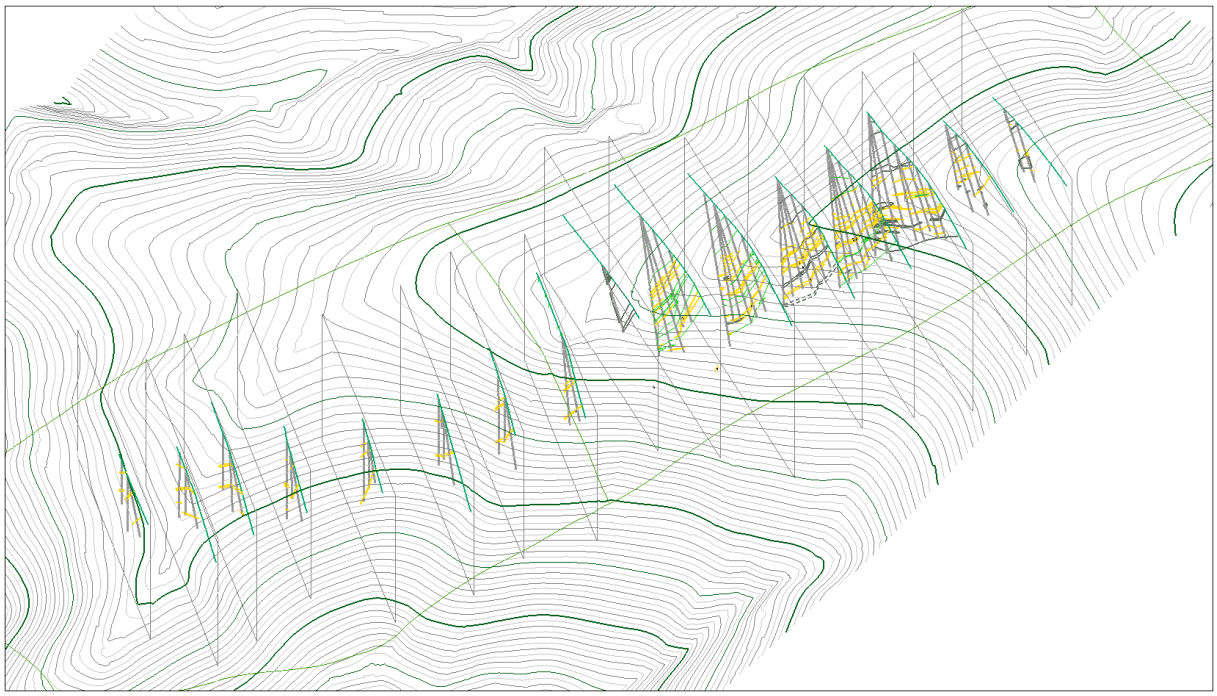

Figure 22: Illustration of the profiles in 3D space (only main profiles shown).

5.2.2 Boreholes

Core drilling was done both from surface, labeled as “KOK”, and underground, labeled as “KUK”. For the surface boreholes the geographic position (x/y coordinates of the collar) was digitized from the plan view maps. The elevation (z coordinate) was adjusted to the up-to-date topographic data (which slightly differs from the topography of the original Minerex maps). The position, length and dip of the underground boreholes could be taken exclusively from the profiles. For the orientation of the boreholes it had to be assumed that they are in alignment of the corresponding profile.

Figure 23 shows the position of the boreholes in 3D space. The borehole data have been converted into a MS-Access format for further usage. The pure geology data were complemented by the geometric data so that they can be used in a spatial context.

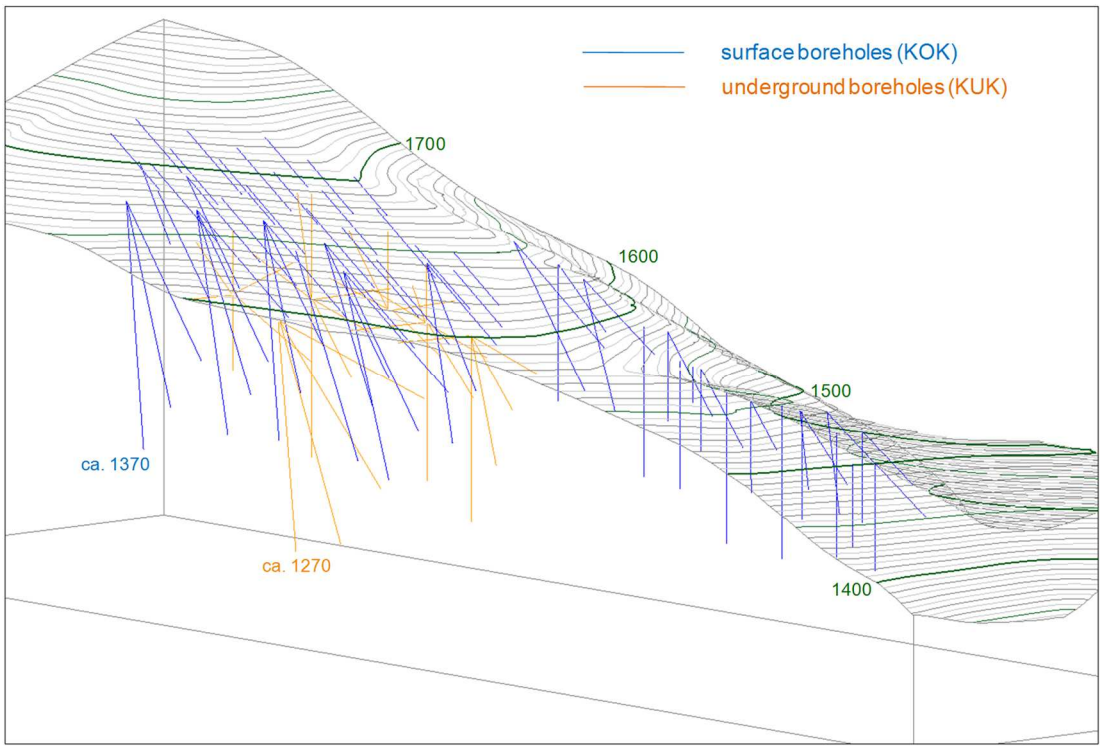

Figure 23: Detailed view on boreholes in exploration area.

Quite a lot of information was found for the geological mapping of the drill holes, however, varying in style or accuracy. Documents were categorized as raw sketch, draft sketch or final maps depending on its precision degree.

Raw sketches (Figure 24 a) were drawn on millimeter paper with 4 columns per page on A4 sheet size (scale 1:500). Lithology is indicated by hatches and/or color, but legend is usually not included. They also include often remarks on samples and structure.

Final sketches (Figure 24 b) are pretty similar to raw sketches, but have only one column per page (A4 sheet size), the lithology is shown by color/hatching and structural situation is indicated. Columns for lithological description, structure angle and remarks are prepared, but only rarely specified. Usually sampled pegmatites are specified, by sample number and from-to section.

Final drawings (Figure 25) are large scale sheets with logs neatly and precisely drawn. Sheets are about 1000-1500 mm in width and 300-600 mm in height. Drawing scale is 1:100. These drawings give a better overview on the total borehole. Lithology is indicated by hatches and the legend is included on each sheet. Additional information includes data such as mineralization, sample code, etc.

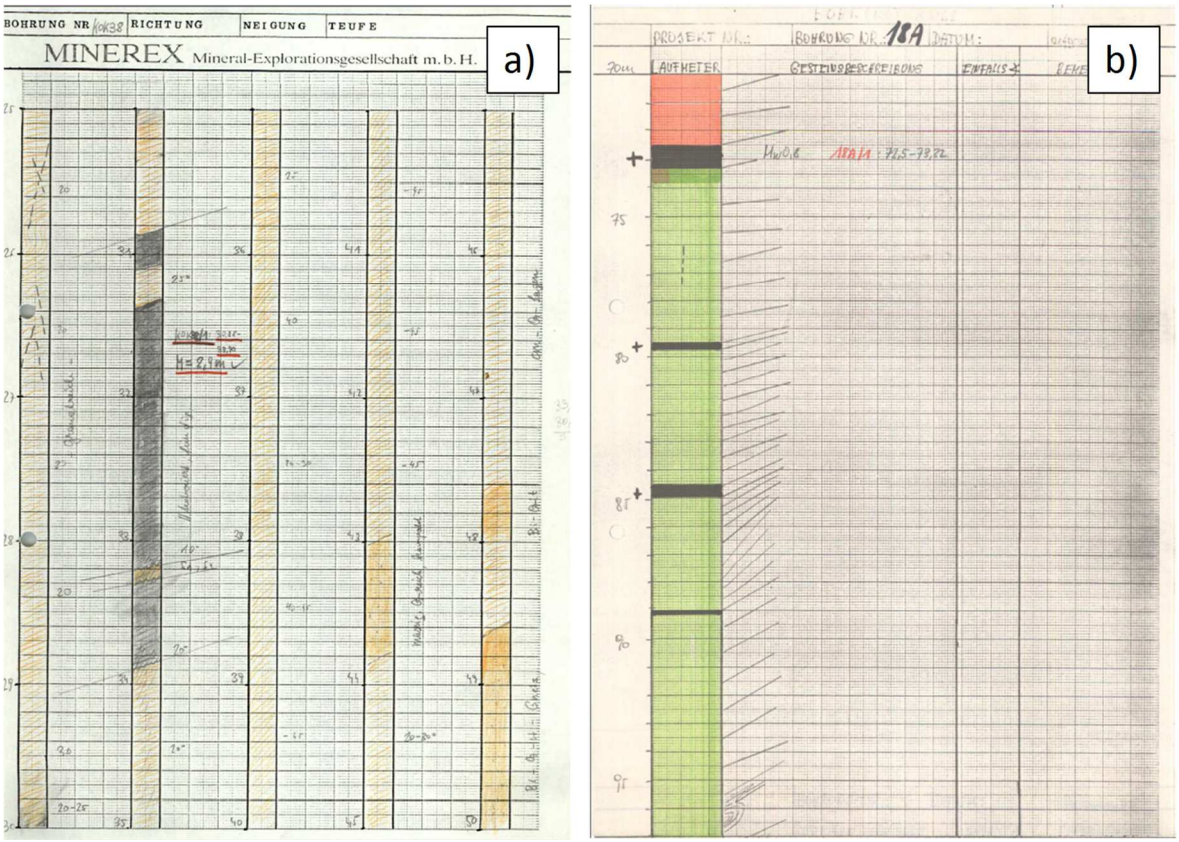

Figure 24: a) Example of "raw sketch" of geological drill log (KOK 38) and b) example of a "final sketch" of a geological drill log (KOK 18A).

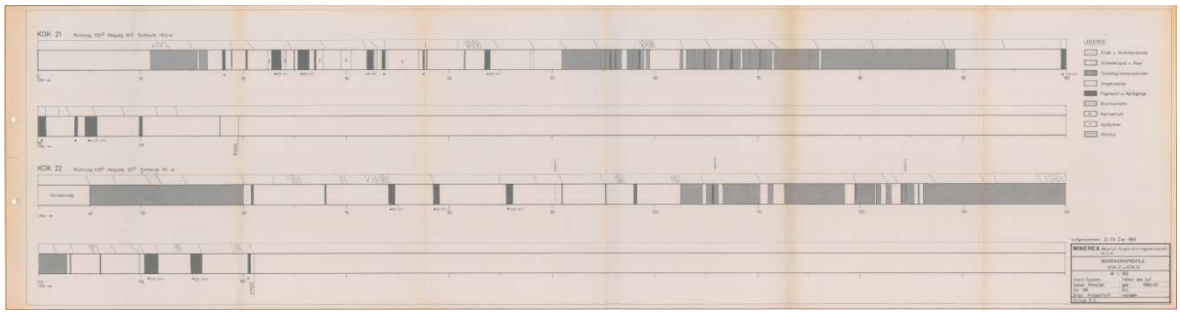

Figure 25: Example of a "final drawing" of a geological drill Log (KOK 21 & 22)

In case that more than one source document was available, the highest ranked format is used, i.e. the most preferable is the final drawing, followed by the final sketches. Table 4 provides an overview of the available data, where listing refers to 16 surface boreholes (KOK 46-58) where no geological information was recorded, so they are ignored. By the from-to values of the lithology sections were retrieved. The accuracy of this transformation is estimated to be approximately ±0,1m (slightly depending on the format).

document type	surface (KOK)		underground (KUK)	
	total	relevant	total	relevant
number boreholes	84		37	
final drawing	62	62	0	0
final sketch	18	0	0	0
raw sketch	52	6	37	37
listing	16	0	0	0
total	148	68	37	37
no doc		16		0

Table 4: Summary of exploration works based on Minerex reporting

5.2.3 Underground workings

The exploration work was extended and supported by underground adits to the deposit. The aim of this investigation was increase the level of knowledge of the deposit in terms of rock mechanical characteristics, mining performances, etc. As a result, it was produced detailed information such as variation of thickness and dip of the veins.

In order to provide a comprehensive description of the exploration activities, underground workings were included into the digital model in 3D. Thereby, it was made accessible the visualization of the areas with detailed information.

The underground works location, *x* and *y* coordinates, were digitized from the plan view map of Minerex. The *z* coordinates were manually entered and assigned as far as they were shown on the maps, which is the case for the majority of the points. The rest was deduced by linear interpolation. Both floor and top level of the drift were converted, so that the drifts can be represented as 3D objects, see Figure 26.

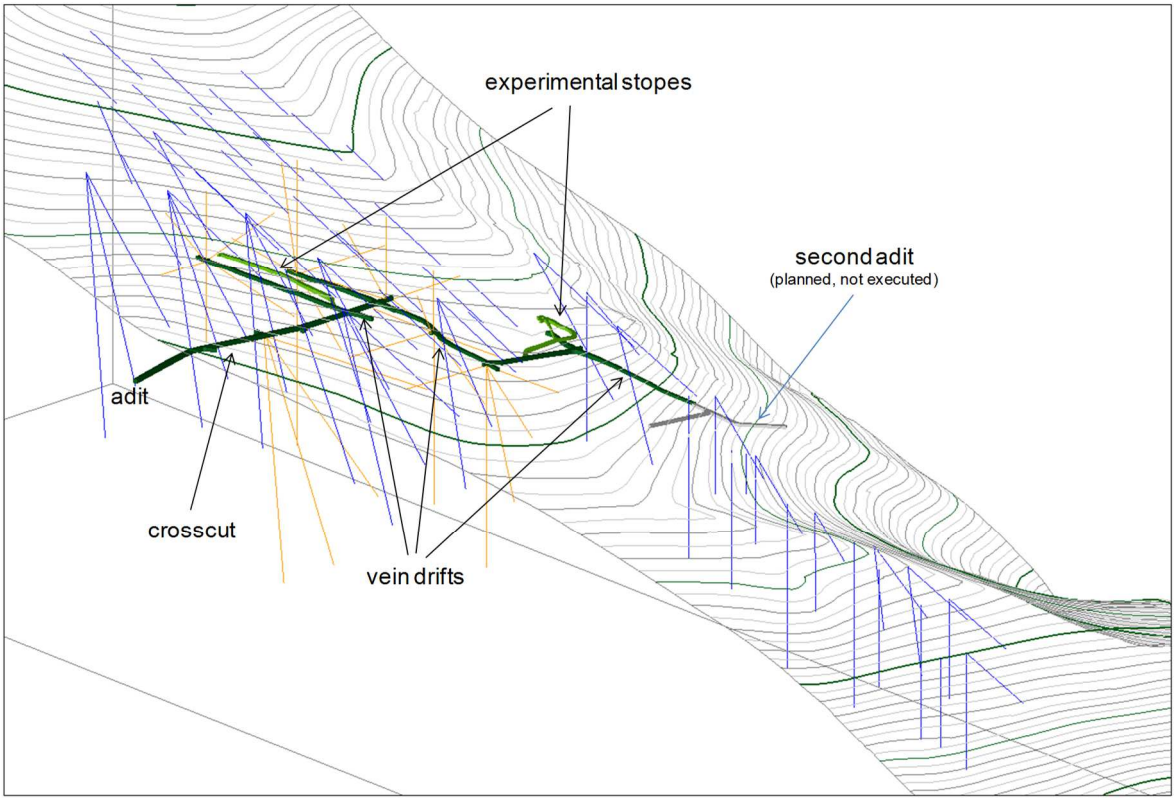

Figure 26: Overall view of underground mine workings, relative to exploration area and boreholes.

The underground drifts provide a good overall impression of the exploration area. The adit is in the north (hangingwall) of the deposit on a level of about 1.570 m. The cross cut accessing the deposit is a decline, so that the dominant level of the drifts along the strike of the veins reaches approximately 1.550m. This level reflects about the top third of the explored vertical extension of the deposit.

The 3D transformation of the underground works can be validated by comparing it to the profile data of Minerex (see Figure 27). No significant discrepancy could be observed, supporting the reliability of Minerex documentation.

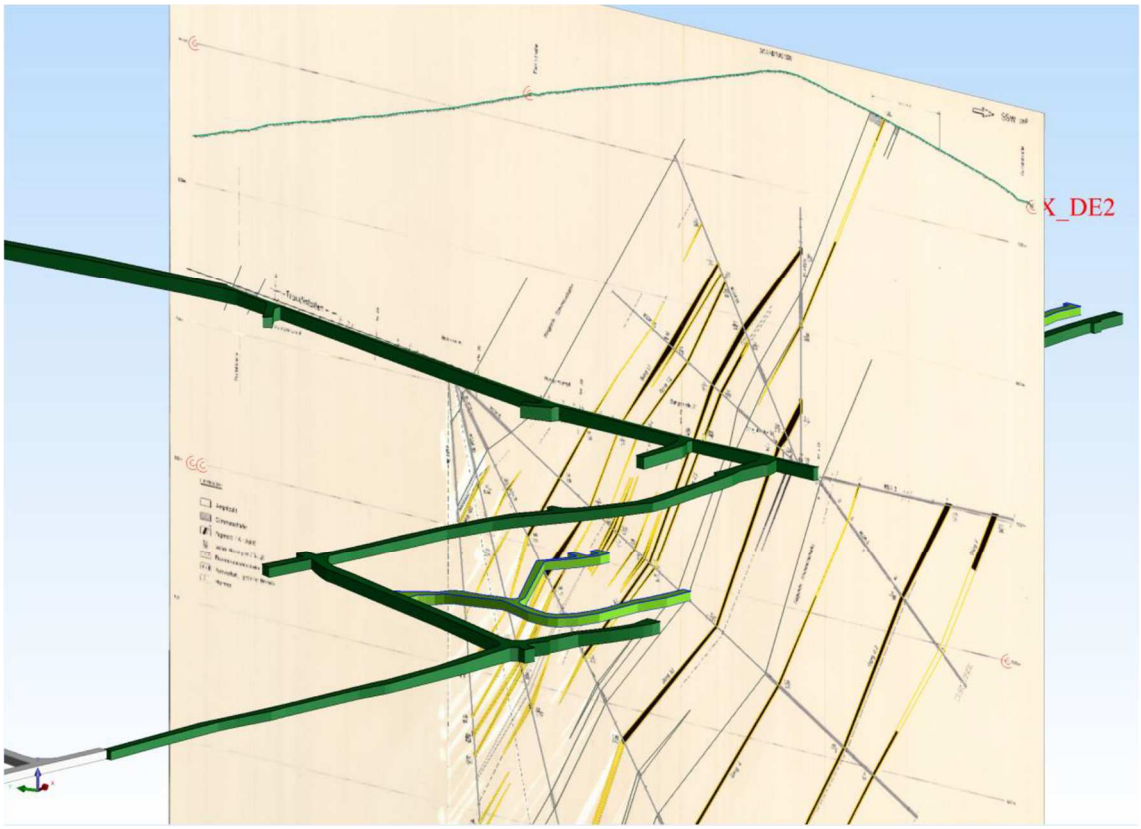

Figure 27: Diagram of alignment of underground mine workings and profile data.

Vein drifts were excavated along three veins: 2.1, 3.1 and 7. They are of special importance due to the process was accompanied by a detailed geological documentation, in particular for the face headings within the vein drifts, i.e. the drifts along strike where vein characteristics are shown exhaustively.

It has been named “drift face surveying” to the geological surveying of the face of each blast round during drift heading. It included sampling, generally between one to three samples per face, which was chemically analyzed.

For each face a standardized form sheet is completed including the date of blasting and geological surveying, the face position (via the underground station identification system) and other information such as host rock, vein dipping etc. Of particular interest is the sketch of the shape of the vein. This includes also the location of the channel samples taken (incl. sample ID) and the respective thickness. For the samples an additional table is destined holding important information as sample-ID, length, thickness, included interbedding, weight, grade etc. This is a valuable information for the sampling routine applied. In many cases photos of the face were also included.

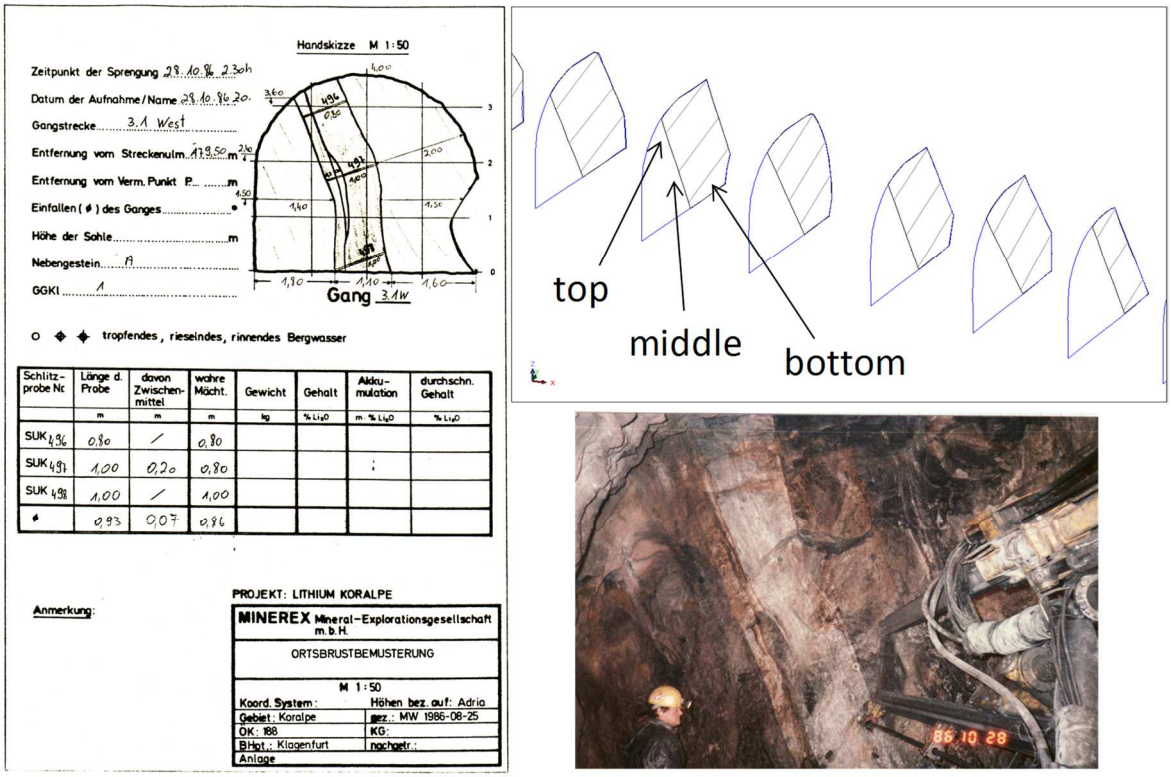

Figure 28: Example of a geological drift face surveying with photo documentation (vein 3.1 West) and sketch of sampling positions strategy.

5.2.4 Vein identification

Minerex performed the main interpretation work based on the exploration phase data. The outcome was an identification of several veins traced along the boreholes. The geometry of the veins was defined vertically through profiles and horizontally by labeling the veins. The transformation of these interpretations to 3D space confirmed the consistence of the all identified veins trace along the strike of the deposit.

In total, 15 veins were identified. There are several more pegmatite lenses shown in the profiles, but as long as they are not reasonably correlated samples in neighboring boreholes or the extension were not sufficiently long, they were not reported as veins. The identified veins show in general a pretty smooth shape both in strike and dip.

The positions of the modeled veins were checked with the available surface information, i.e. the geological mapping and the trenches without finding relevant

discrepancies. Table 5 shows to each identified vein its host rock, maximum extension in horizontal and vertical directions and in which profiles is reflected.

Vein	Host rock	Max. extension		Profiles																
		Horiz.	Vert.	1	2	3	4	5	6	7	8	9	A	B	C	D	E	F	G	H	I
0.0	A	460	175																		
0.1	A	640	160																		
0.2	A	100	180																		
0.3	A	500	180																		
1.1	A	590	190																		
1.2	A	590	190																		
2.1	A	590	235																		
2.2	A	310	180																		
3.1	A	460	350																		
3.2	A	460	310																		
4	M	500	225																		
6.1	M	500	80																		
6.2	M	1300	350																		
7	M	1300	250																		
8	M	260	80																		

Table 5: Summary of identified pegmatite veins (“A” = Amphibolite, “M” = Micashist).

The distinction between separated veins or vein interbedding is a critical aspect in the vein assignment. Figure 29 shows some extreme examples of geological profiles were the interpretation is especially sensitive due to their proximity.

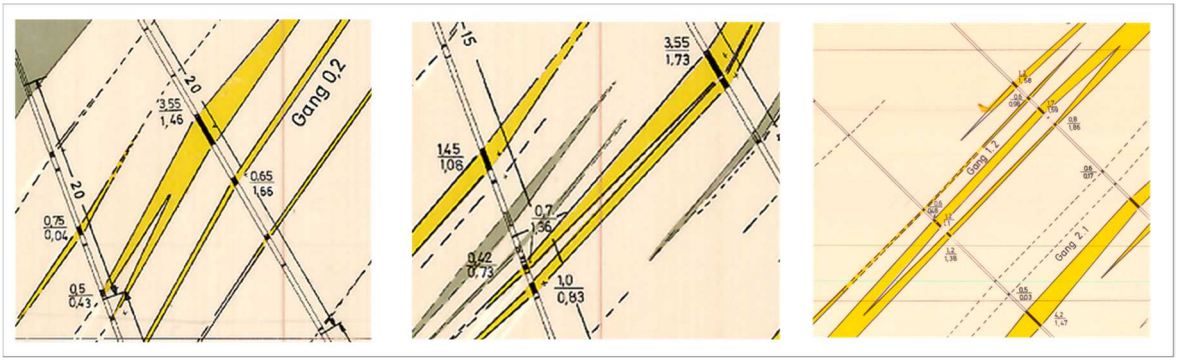

Figure 29: Details of geological profile which illustrate the difficulties of vein and interbedding assignment

Regarding sampling, the possible situations related to vein assignment are (Figure 30):

a) Single: the vein is assigned to one single sample. The vein grade is identical with the sample or pegmatite grade.

b) Multiple: the vein is assigned to several consecutive samples (sample splitting was done by Minerex usually when pegmatite thickness exceeded 1m). The vein grade is calculated as the average of the sample grades weighted by the sample length.

c) Interbedding: the vein is assigned to several samples which are separated by a gap in between. The gap is defined by the section positions of the samples, independent from the geology (because geology is not always known). The vein grade is calculated as in case b) as weighted average, applying a Li_2O grade of 0 for the gaps between the samples.

d) and e) Geology: eventually no samples were taken for some pegmatites, but by geological consideration an assignment to a vein seems plausible. This happens typically when veins are supposed to thin out. This is a pure geometric information where no further calculation is required. The focus of the vein assignment or vein identification is of course on massive mineralization. This is because these veins are easier to trace over some distance, but also because of their economic relevance. Nevertheless, also some smaller intersections are assigned to veins by geometric assumption and interpretation. Usually this geometric relation is identified at a later date and hence these sections were not sampled and consequently also not seen in the sample analysis. However, they can be of relevance for deposit modeling process.

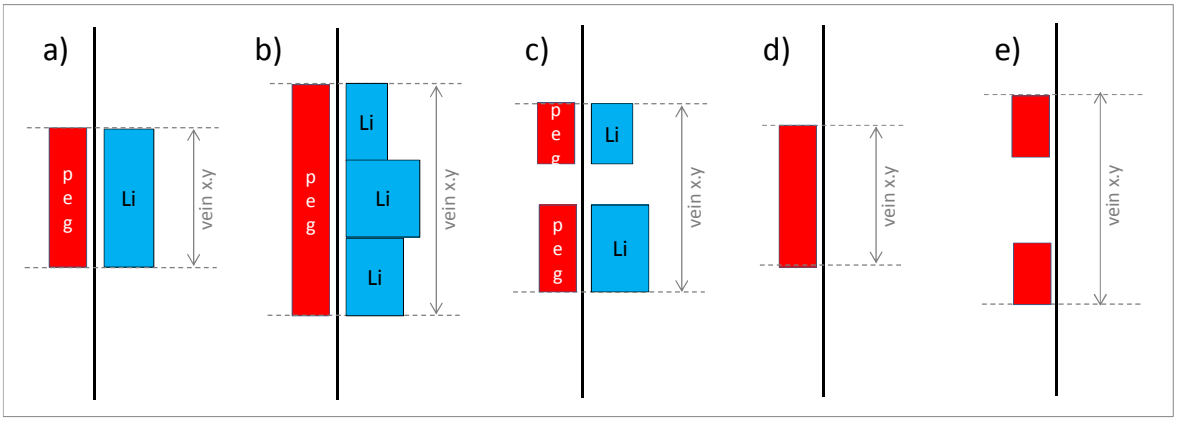

Figure 30: Sketches of types of geometric vein assignment.

Accordingly, the term “pegmatite grade/thickness” will be use only to refer to the portions where a pegmatite has been identified excluding any interbedding while “vein grade/thickness” and composite would consider the interbedding if there is any, diluting the grade. Therefore, if there is no interbedding, pegmatite grade/thickness is equal to vein grade/thickness. On the contrary, if there is any, the vein grade will be equivalent to the pegmatite grade diluted by interbedding, i.e. lower grade, and the vein thickness will be equal to the pegmatite thickness increased by the interbedding thickness, i.e. greater thickness.

Besides the previous, there are also cases where geology was identified or a sample was taken but they were not assigned to a vein.

5.3 Additional exploration data (up-to-date standards)

A total of seven twin holes to the original boreholes was executed using a Sandvik DE 130 drill rig. It was used wire-line cored in the entirety of 50 mm double-tube core barrel. The total length was 829,6 m. Down hole surveying was performed. The flow sheet for handling core from rig side to storage is the following:

1. At drill rig site core is extracted and placed into boxes. Drilling and handling induced brakes are marked on the core.

2. Transport: core loaded and transported to the core shed facility.

3. Recovery: Quick run length recovery log performed to ensure drill depth markers are correct and identify position of core loss.

4. Depth marks written on the core at 1 m interval.

5. Geotechnical logging.

6. Geological logging.

7. Sample mark up: Sample intervals based on visible mineral estimates of upper and lower contacts for the units and sub units.

8. Density sampling of small sections of core at 3 m interval using the hydrostatic dry and submerged method to calculate the density.

9. Photography: undertaken on the wet core with all marks visible.

10. Core cutting.

11. Core sampling.

12. Secure sample storage.

On the other hand, channel sampling was conducted every 3 m in the drifts along the strike of the pegmatite veins number 2.1, 3.1 and 7. Samples were cut perpendicularly to the strike direction using a remote-controlled diamond saw. Sample dimensions were 5 cm and 10 cm depth. After cutting, samples were extracted by the use of hammer, chisel and a small jackhammer.

Analytical and data quality control was performed by the execution of duplicates, standards with different Li_2O grades and blank samples.

6 Original data analysis and validation

In order to evaluate a mineral resource, the estimator has to be convinced of the soundness of the foundations underlying the estimation process. Therefore, the quality of the data, density and database of sampling as well as the geological interpretation must have integrity and robustness. The definition of a consistent geological model must be based in a complete geological data which explain the observed arrangement of lithological and mineralogical domains and support the distribution of mineralization seen in the sampling. The process of resource estimation involves the definition of mineralisation constraints or geological domains, the statistical and/or geostatistical analysis of the sample data, and the application of a suitable estimation technique of its features. Then, the final stage of the process is to classify the resource according to the JORC Code. (Glacken and Snowden 2001, p. 189)

Statistical analysis may support the definition of the nature of the domain boundaries. Once the domains have been consistently identified, the numerical characteristics of the mineralization should be assessed. Statistical analysis should be done in accordance with the defined domains. It is required that data represent an equal volume to be analyzed. Regarding this requisite, compositing the samples into equal lengths is a well-accepted methodology. If sampling was performed on fixed lengths, the compositing should be on multiplies of the original sampling interval to reduce the excessive smoothing. When the boundaries in a deposit are strict, such as in a narrow vein, compositing by zone is critical to avoid dilution. On the other hand, the original length of sampling should not be split into smaller composite lengths due to the fact that it would result in an unreal low variance.

Due to the tendency to intensify the exploration activities or take more samples of the higher grade portions of the mineralization, the irregular distribution of samples in the space is quite likely. Thus, there are some declustering approach to make each sample represent an equal volume, avoiding biased results. In the same way, different drilling types within the same domain are recommended to be examined independently.

After compositing and declustering, statistical assessment may offer key information about trends in the domains, data distribution, comparison between sample types or relationships between multiple variables. (Glacken and Snowden 2001, p. 189)

Due to the Koralpe deposit was explored in the 1980ies, the data generated at that time was transferred from one to other archive location when the company Minerex disappeared until ending up in “Montanbehörde” (now BMFWF: Bundesministerium für Wissenschaft, Forschung und Wirtschaft, Sektion III, Federal Ministry of Science, Research and Economy), where it still resides. The archive comprises only paper work and no electronic data of any type. Originally the archive comprised 729 folders and 13 map boxes, however, some of the documents got lost over the years. For the recent reactivation in the project, relevant documents were scanned and catalogued for its later analysis. Besides that, an electronic dataset, mention as “Zier database”, with valuable information on sampling was kept by the responsible geologist at Minerex. These data should be investigated in order to be useable to provide the basis for a resource estimation and a feasibility study which satisfies nowadays quality standards. In particular, the international “JORC code” is used as a guideline for the resource estimation as mentioned before.

The chemical sampling analysis work was mainly executed by two laboratories, one Austrian and one American:

- ARS: Bundesversuchs- und Forschungsanstalt Arsenal (arsenal research)
- MRL: North Carolina State University, Minerals Research Laboratory

A very reduced number of samples were analyzed in other labs, e.g. Bondar-Clegg (Canada). Because of the very low quantity and poor documentation these sources were not considered.

The lab analysis data includes some duplicates between labs and some internal duplicates which allow to prove the quality of the results as well as the new exploration drilling campaign. The assessment performed is described in next sections.

6.1 Borehole data analysis

Regarding borehole lab analysis, 880 samples are recorded, about 2/3 performed by ARS and 1/3 by MRL. Surface borehole samples (KOK) were analyzed by both labs, while exclusively ARS data was found for underground (KUK). For surface boreholes, 280 samples executed by both labs. A summary of the data situation is given in Table 6.

	ARS	MRL	both
batch	12	3	
total samp	557	322	
internal dup.	0	0	
KOK	372	322	280
KUK	185		

Table 6: Available laboratory results of exploration boreholes.

The sample data has been subject of a general statistical analysis. This refers to the mere sample data and does not yet incorporate any geological aspects. No distinction is made between surface and underground samples, because they are somewhat different in respect of the space covered and hence a comparison might me misleading. However, the investigation focuses rather on differences of the two laboratories involved. Figure 31 shows the comparison by means of a box plot of the distribution of the KOK data. In a box plot diagram, the median of each dataset is represented through the horizontal line inside the box. The notches around it describe the 95 % confidence interval of the median. Note that if the notches of two datasets do not overlap, and thus their medians are different from a statistical point of view. Dispersion and skewness are characterized with the 1st and 3rd quartile (upper and lower limits of the boxes) and the whiskers. The whiskers include the lowest datum still within 1,5 interquartile range of the lower quartile, and the highest

datum still within 1,5 interquartile of the upper quartile. Values out of this range, called outliers, will be represented as circles if there is any. It shows slightly higher values for the samples analyzed by MRL.

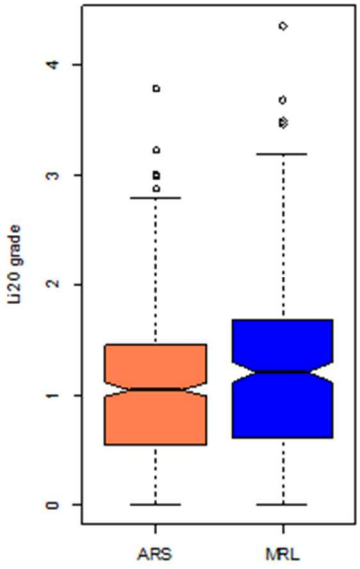

	Min	1st Q	Median	Mean	Sd	3st Q	Max
ARS	0,01	0,54	1,05	1,04	0,67	1,45	3,79
MRL	0,01	0,61	1,21	1,18	0,77	1,68	4,36

Figure 31: Box diagram of comparison between ARS and MRL results for surface borehole samples.

In order to eliminate the risk of using biased datasets (in spatial or geological respect), the comparison was done also for the 280 samples which can be directly assigned to each other, i.e. to those analysis results which refer to the same sample. The comparison is done by correlation and the result is shown as scatter plot in Figure 32. A linear regression has been calculated as function type *MRL data=a*ARS data* drawn in blue color. The grey line passing through the origin with slope one is plotted as a reference of the ideal case where both datasets are equal. The confident limits of the fit value *a* have been included, as well the determination confident R^2, which shows the goodness of the fit. The R^2 is quite high, 0,96, and therefore acceptable, although the visual inspection of the data shows a considerable dispersion. According to the linear regression the MRL results are in general about 10% higher than the ones from ARS.

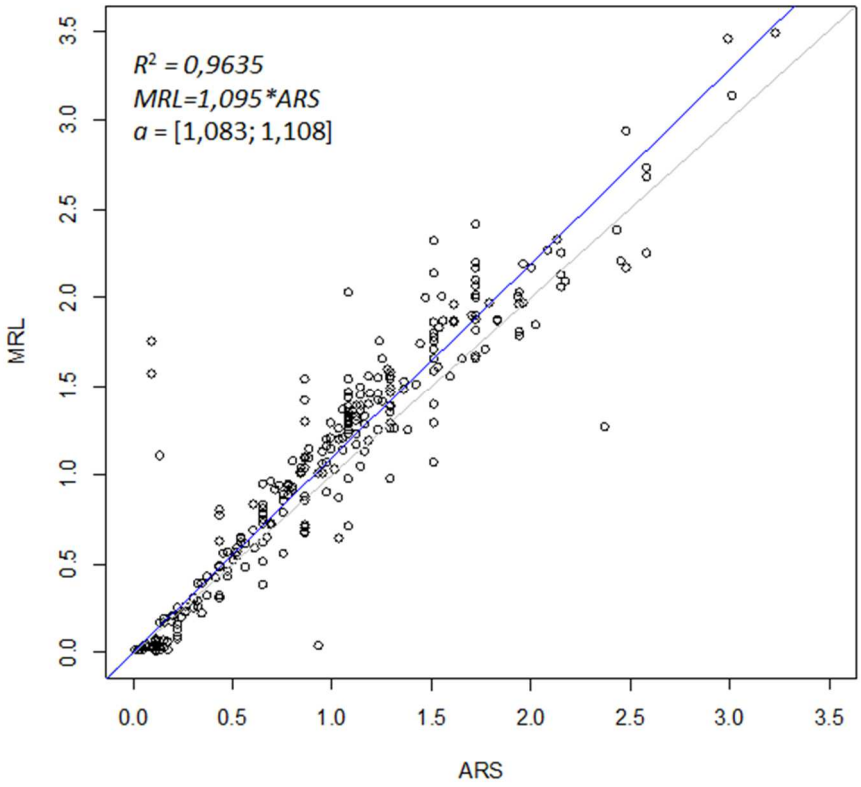

Figure 32: Box diagram of comparison between ARS and MRL results for surface borehole samples.

The investigation is completed by applying two statistical tests to assess the equality of the distributions of the results of the two labs, Kolmogerov-Smirnov and Wilcox test. For reasons of completeness this was done for both data sets, i.e. all KOK samples and for only those which can be positively paired. Table 7 gives the result of these tests. The calculated figures are basically below the generally accepted threshold of 0,05 for the *p*-value, which concludes that the compared datasets come from different distributions from a statistically view. As expected, the results for the correlated dataset are slightly better but still indicate a significant difference. Therefore, the selection of lab data for its use must be made cautiously.

	KOK	MRL (all)	MRL (corr)
KS	ARS (all)	0,0008247	
	ARS (corr)		0,003673
W	ARS (all)	0,008231	
	ARS (corr)		0,05186

Table 7: Kolmogerov-Smirnov and Wilcox test *p*-values for the comparison of surface boreholes lab results.

According to the definition of different vein assignment types expose in section 5.2.4 it has been analyzed the sample grade distribution to each case (see Figure 33) including the samples unassigned as well. The key statistical values of this analysis are shown in Table 8.

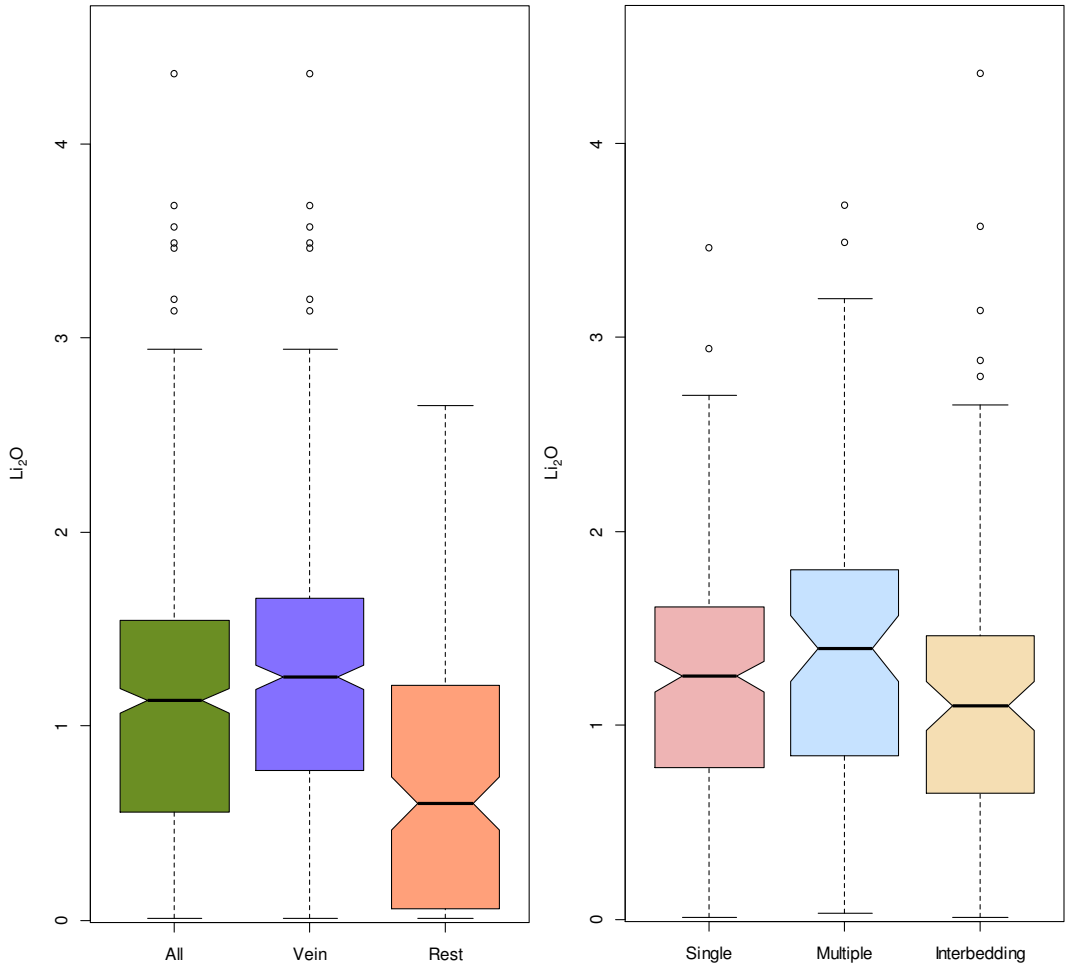

Figure 33: Sample/pegmatite Li_2O grade distributions to distinct vein assignment situations.

In the left part, the grade distribution of all samples is represented in green, the purple one refers only to the samples which has been assigned to a vein and the orange to the samples which remain unassigned. It seems like only samples with higher grade are assigned to distinct veins. Unassigned samples show a significantly lower grade. This is probably also because thin zones with a more aplitic characteristic are included.

In the right part, the different vein assignment types are assessed. The pink box refers to single samples. The blue one corresponds to multiple samples (i.e. thick intersections split into several samples) and shows slightly higher grades, while

samples form areas with interpreted interbedding tend to lower grades (yellow box). It is important to note that these are sample grades, i.e. dilution by interbedding is not yet incorporated. Consequently, it could be deduced that thicker areas have higher Li_20 grades.

	Min	1st Q	Median	Mean	3rd Q	Max	Sd	num
All	0,01	0,56	1,13	1,10	1,55	4,36	0,73	651
Vein	0,01	0,77	1,25	1,24	1,66	4,36	0,69	470
Rest	0,01	0,06	0,60	0,73	1,21	2,65	0,68	181
Single	0,01	0,79	1,25	1,23	1,61	3,46	0,64	282
Multiple	0,03	0,85	1,40	1,40	1,80	3,68	0,76	82
Interbed.	0,01	0,65	1,10	1,16	1,46	4,36	0,77	105

Table 8: Sample/pegmatite Li_2O grade statistical values to distinct assignment situations.

From a mining point of view, the analysis of the composite grade has a particular relevance due to the limitations in the selectivity of mining techniques and equipment, which require to mine blocks of a minimum size. In Figure 34 the effect of compositing in the grade distributions has been evaluated.

In the left part, it is compared the grade obtained directly from samples versus the composite, which is diluted as vein grade and therefore reduced. Nevertheless, the decrease is limited due to the low ratio of vein sections with interbedding and usually the interbedding is relatively small compared to the total vein (see Table 9).

vein assignment			samples			composites		
			KOK	KUK	total	KOK	KUK	total
located samples			466	185	651			
vein assignment			358	112	470	243	105	348
	single	(a)	184	98	282	184	98	282
	multiple	(b)	82	0	82	19	0	19
	interbedding	(c)	92	14	106	40	7	47
no assignment		(d+e)	108	73	181			

Table 9: Number of sampling items according to the vein assignment.

Analogously to the previous figure, the right part shows the grade distribution of the composite for single, multiple and interbedding samples. The situation of single composite is of course identical with the sample grade as in these cases no dilution occurs. Naturally, multiple samples distributions tend to averaging after compositing. On the other hand, the grade of the veins with interbedding drops significantly although it still remains on an acceptable level.

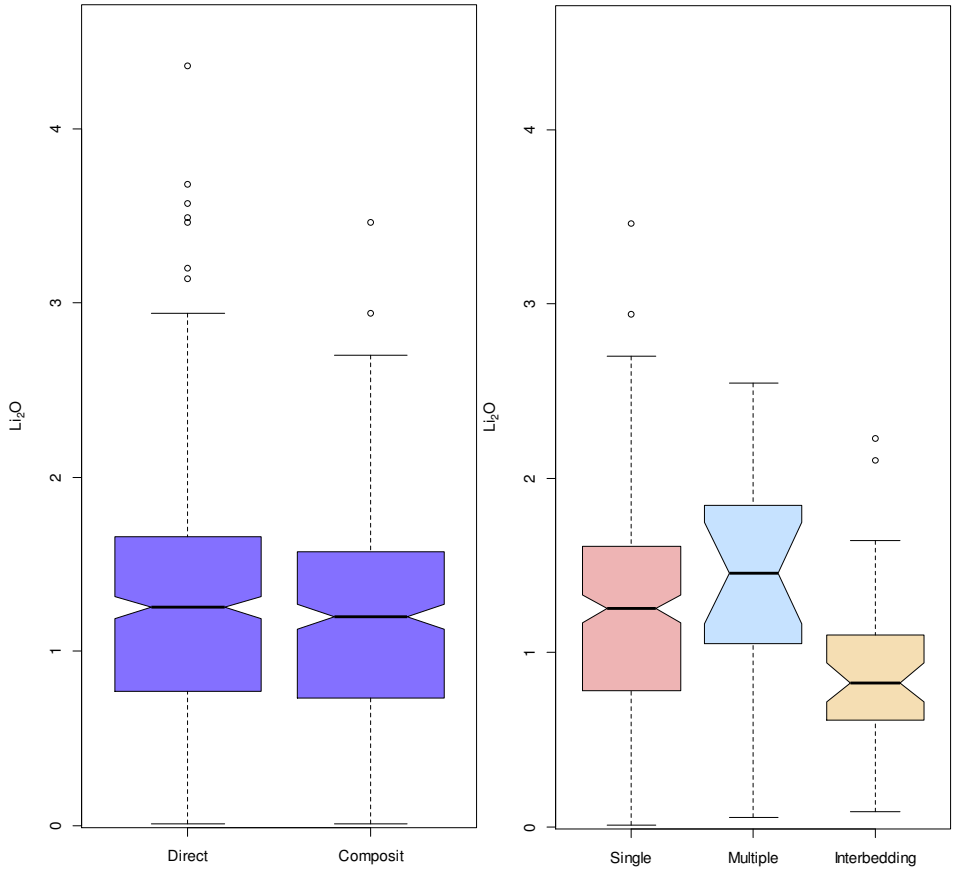

	Min	1st Q	Median	Mean	3rd Q	Max	Sd	num
Direct	0,01	0,77	1,25	1,24	1,66	4,36	0,69	470
Composi.	0,01	0,73	1,20	1,19	1,57	3,46	0,63	348
Single	0,01	0,79	1,25	1,23	1,61	3,46	0,64	282
Multiple	0,06	1,05	1,46	1,43	1,84	2,55	0,65	19
Interbed.	0,09	0,62	0,83	0,85	1,08	2,23	0,48	46

Figure 34: Vein/composite Li_2O grades by distinct vein assignment situations.

In order to investigate the influence on Li_2O grade of the geology, the composites have been grouped by host rock type according to amphibolite (AHP) or mica schist (MHP) hosted pegmatites. The veins 0.0 to 3.2 are considered AHP, and vein 4 to 8 are counted as MHP. Figure 35 shows, by means of a boxplot in blue for AHP and in yellow for MHP, that there is a significant difference in grade, being greater AHP grade. This confirms the statements from Minerex and other previous investigations.

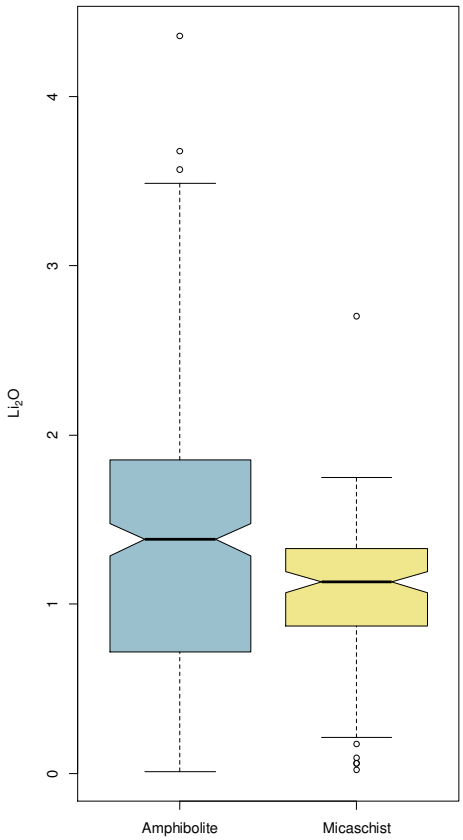

	Min	1st Q	Median	Mean	3rd Q	Max	Sd	num
Amphib.	0,01	0,72	1,38	1,32	1,85	4,36	0,77	331
Micasch.	0,02	0,87	1,13	1,06	1,33	2,7	0,39	139

Figure 35: Sample/pegmatite Li_2O grade by geology (host rock).

Besides lithium grade, thickness is the other parameter subject of interest for later deposit modeling. Due to the location and shape in small scale of the veins is an unknown feature at this stage of the investigation, the intersection length of the boreholes in the veins will be accepted to be used for assessment purposes as a preliminary approximation of the actual vein thickness, see Figure 36.

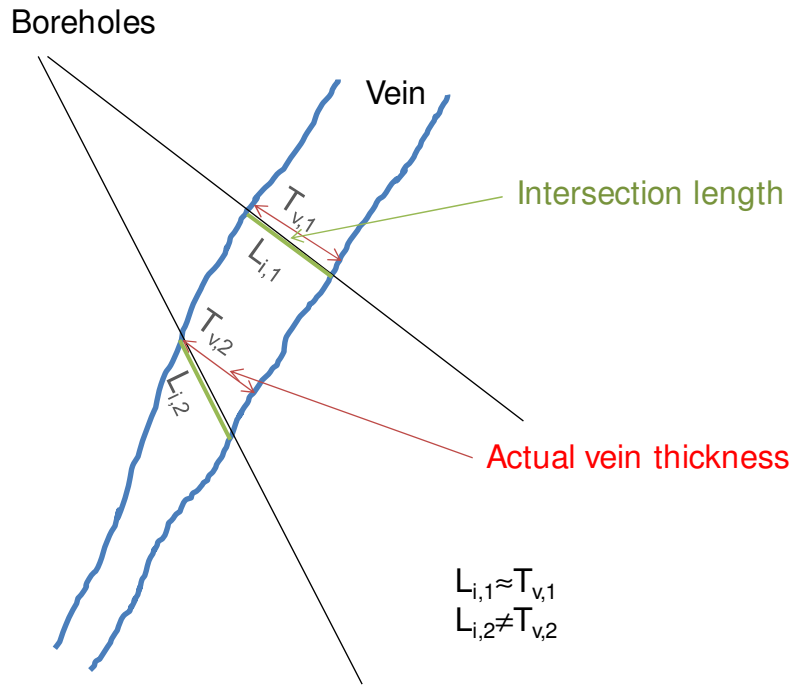

Figure 36: Intersection length of a borehole in a vein versus actual thickness.

As was mentioned in section 5.2.4 massive mineralization intersected by boreholes were usually identified like veins instead of the slim pegmatites and major subject of interest for sampling. This is illustrated in the Figure 37 where the green box refers to the length distribution of all composites, the blue one refers to only the composites with Li_2O analysis result and the orange one to those without it. Sections assigned to a vein without a sample grade have very low section lengths, such as in the example of illustration a). The illustration b) depicts the effect of composing in the vein thickness when the interbedding is relevant. Because this assignment was done by Minerex assumingly by geological considerations, the interbedding ratio can be in some cases considerably high. This situation occurs very seldom. A final assessment must take both thickness and grade into account; hence assignments like the exemplified will not have serious consequences. Nevertheless, the isolated evaluation of thickness can be eventually misleading.

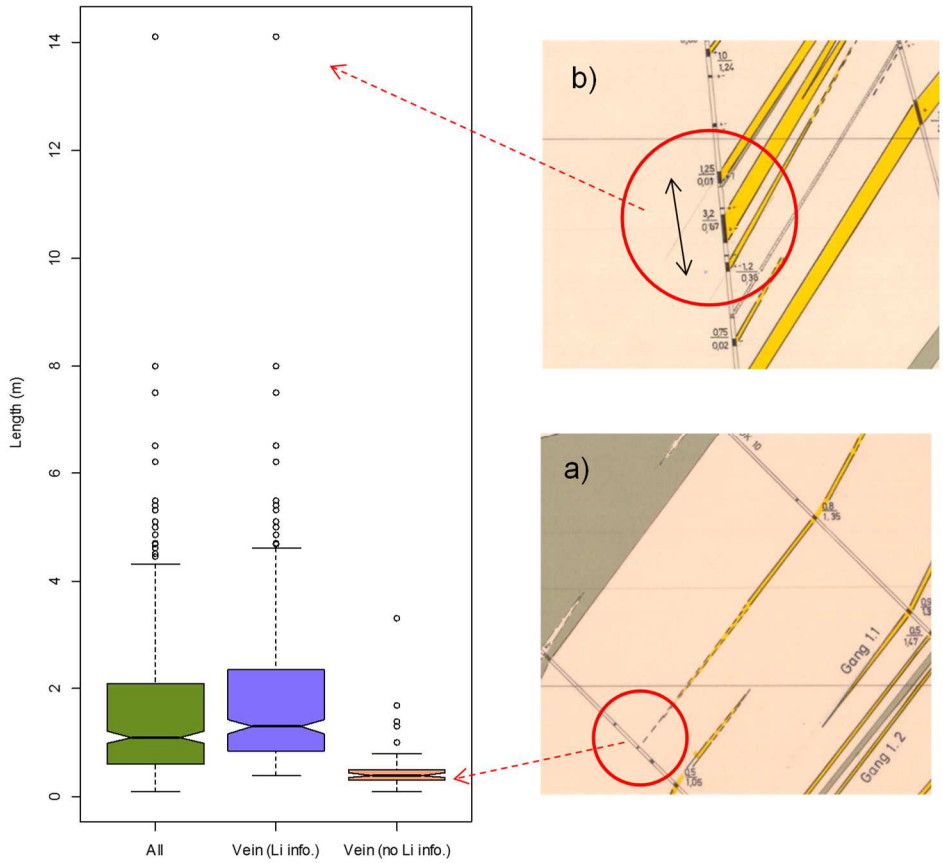

	Min	1st Q	Median	Mean	3rd Q	Max	Sd	num
All	0,10	0,60	1,10	1,59	2,10	14,10	1,42	405
Vein Inf.	0,40	0,85	1,30	1,78	2,35	14,10	1,44	347
Vein no I.	0,10	0,30	0,40	0,47	0,50	3,30	0,48	58

Figure 37: Borehole intersection length distribution of assigned veins distinguished by existence of grade analysis.

The investigations on the intersection length is done analogously to the grade. Figure 38 represents the variation of length according to the vein assignment and sample type.

The left part of Figure 38 shows in the green plot the distribution for all measured lengths, in blue only the corresponding to vein-assigned samples and in orange the not assigned. Samples assigned to veins have a significantly larger length compared to the unassigned samples as expected. The lengths of the unassigned samples however are still in a range that justifies further investigations, because at the current stage of assessment they are dismissed, not contributing to any kind of resources.

In the right part the different assignment types are again demonstrated. Single sample veins show typically a length between 0,7 m to 1,7 m. According to the

Minerex sampling procedure the designed length of samples from multiple sampling is approximately 1 m. In reality, the length is sometimes smaller because the full vein length was distributed in equal shares. Samples from sections interpreted as veins with interbedding are less in length than the single samples, but still have remarkable dimensions.

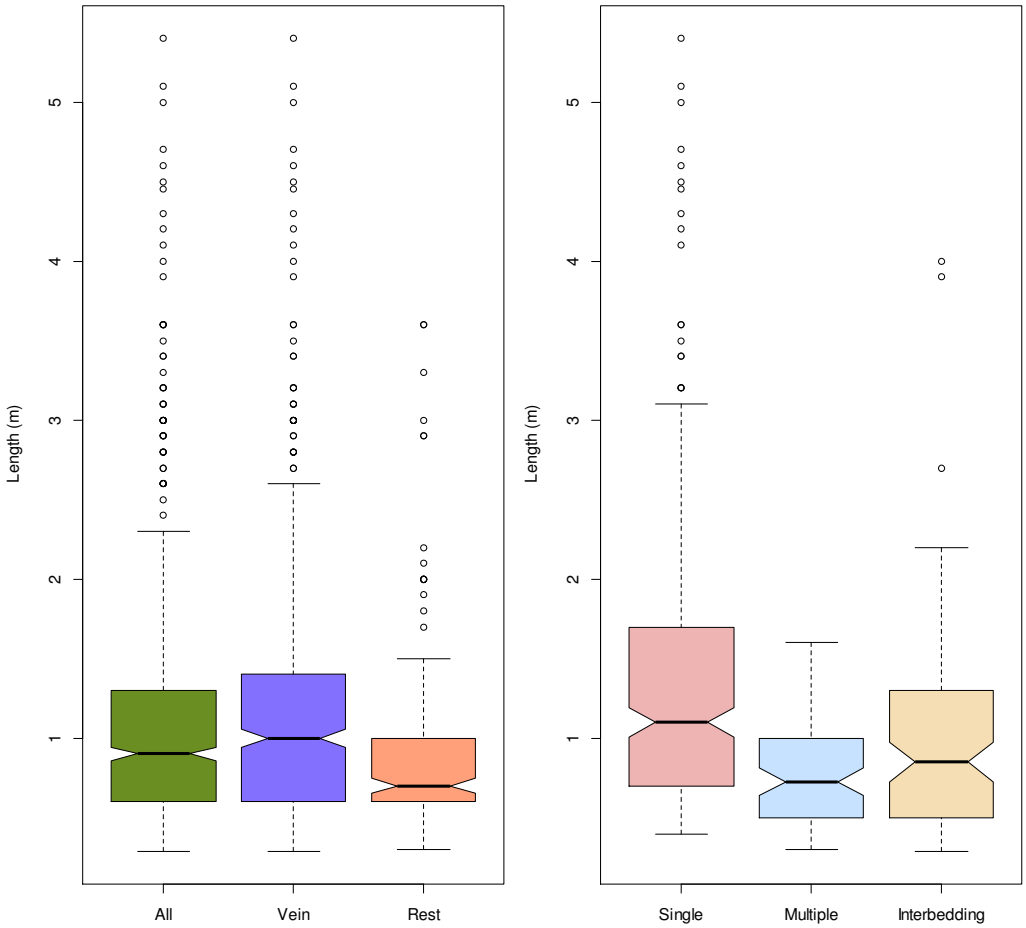

	Min	1st Q	Median	Mean	3rd Q	Max	Sd	num
All	0,29	0,60	0,90	1,12	1,30	5,40	0,80	651
Vein	0,29	0,60	1,00	1,21	1,40	5,40	0,86	470
Rest	0,30	0,60	0,70	0,90	1,00	3,60	0,57	181
Single	0,40	0,71	1,10	1,41	1,70	5,40	0,97	282
Multiple	0,30	0,50	0,73	0,78	1,00	1,60	0,33	82
Interbed.	0,29	0,50	0,85	1,03	1,30	4,00	0,67	105

Figure 38: Sample/pegmatite lengths by distinct vein assignment situations.

The comparison between the distribution of the length of direct samples and composites is illustrated in the right side of Figure 39. In the composites is reflected the length of the assigned vein, which is very relevant for mining purposes.

Composites have of course larger lengths than the direct samples due to multiple and interbedding samples are consider. This difference is notable for the 3rd quartile but not for the median because the relative scarce number of these cases. The right side of the figure shows in detail that only the composites of multiple samples correspond to larger sections, while short sections were sampled as single. On the other hand, the length distribution of multiple and interbedding type is comparable, exposing the low influence of interbedding. Accordingly, it is very reasonable to compilate close-by samples into diluted veins from a mining point of view.

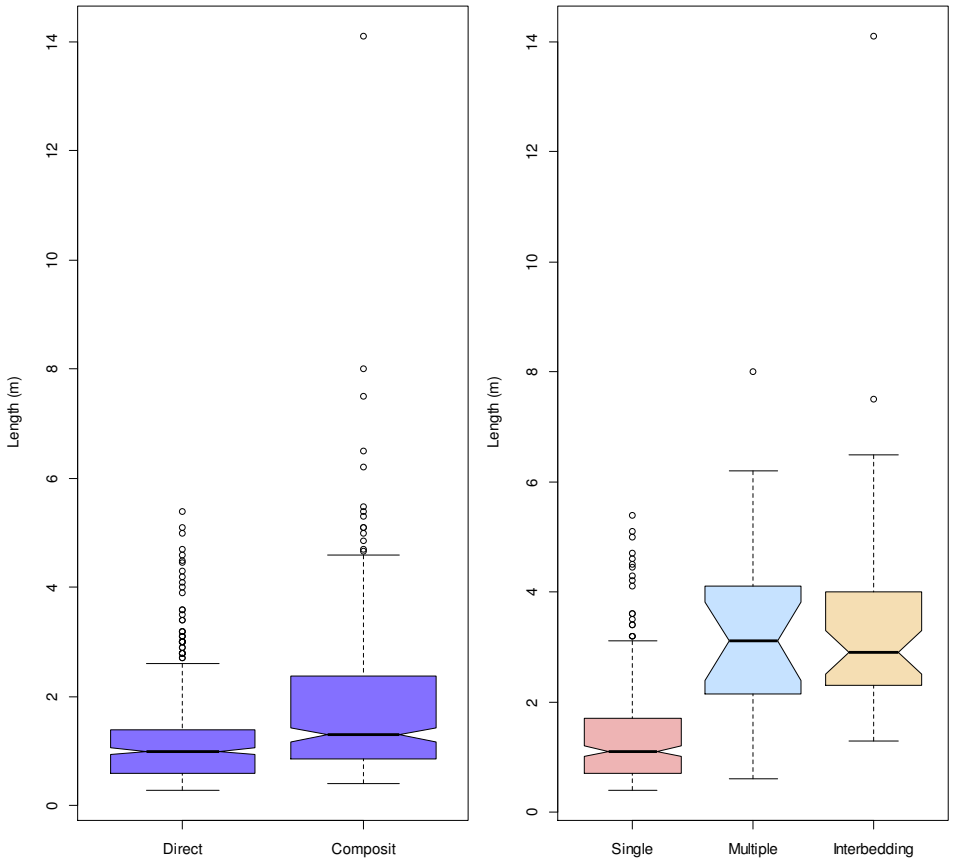

	Min	1st Q	Median	Mean	3rd Q	Max	Sd	num
Direct	0,29	0,60	1,00	1,21	1,40	5,40	0,80	470
Composi.	0,40	0,87	1,30	1,78	2,36	14,10	0,86	348
Single	0,40	0,71	1,10	1,41	1,70	5,40	0,57	282
Multiple	0,60	2,15	3,10	3,35	4,10	8,00	0,97	19
Interbed.	1,29	2,31	2,90	3,39	3,98	14,10	0,33	46

Figure 39: Vein/composite lengths according to vein assignment type.

Thus, for the investigation of the geology influence, i.e. primarily the host rock, composited data are used. The results displayed in Figure 40 depict clearly the differences between these two geological situations. The majority of the composites

of AHP has lengths in the range of 1 m to 2 m, while MHP go up to 3 m (based on 1st and 3rd quartile). Maximum thickness (excluding outliers) of the MHP is almost fifty percent more than in AHP.

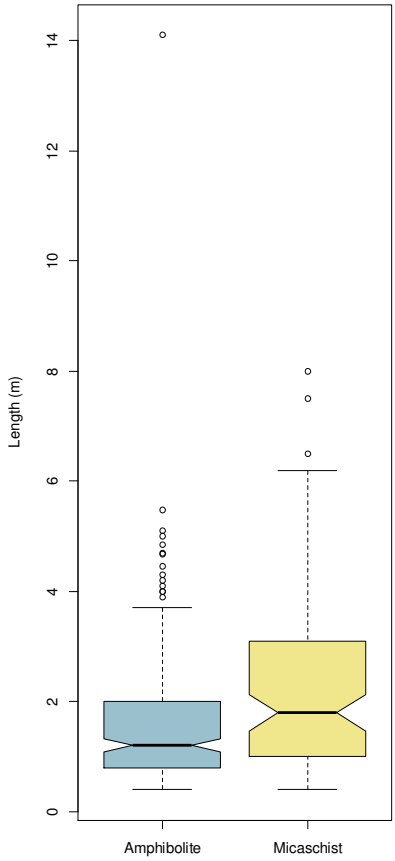

	Min	1st Q	Median	Mean	3rd Q	Max	Sd	num
Amphib.	0,40	0,80	1,20	1,58	2,00	14,10	1,32	249
Micasch.	0,40	1,00	1,80	2,28	3,10	8,00	1,63	99

Figure 40: Vein/composite lengths by host rock.

6.2 Drift face sampling

The aim of the underground exploration campaign developed by Minerex was obtaining detailed information of the vein characteristics, specifically shape, grade and continuity in the space. These works, which were documented in detail in paper, have been transferred into modern computer supported data. Drift face sampling (SUK) was performed along two AHP veins (2.1 and 3.1) and one MHP vein (7), see Figure 41.

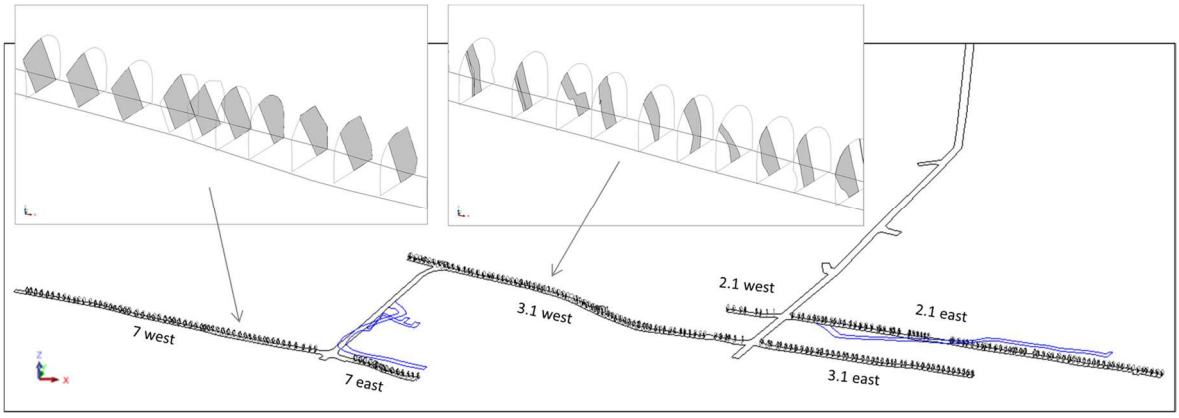

Figure 41: 3D overview of drift face survey with two examplary details

In total 2.276 data from ARS and 128 data from MRL were collected. The total sampling data from ARS includes 1.384 internal duplicates. Apparently, ARS laboratory split most of the samples after crushing and both sub-samples were sent for analysis as duplicates. For those samples, the grade was calculated as the average of each set of duplicates. As a result, 892 samples from ARS and 119 samples from MRL are available to use. MRL was used as verification lab (see Table 10).

	ARS	MRL	both
batch	12	2	
total samp	2276	128	
internal dup.	1384	0	
SUK	892	119	115

Table 10: Available laboratory results of underground channel samples (face surveying).

The distribution of the Li_2O grade to the results of each lab is represented in the Figure 42. It is important to note that this comparison does not yet consider any geological background (i.e. host rock family). Since the samples analyzed in both labs correspond to the veins in a different proportion, the distributions are slightly different, having means quite similar.

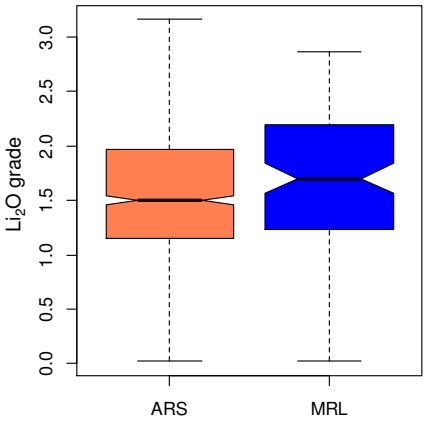

	Min	1st Q	Median	Mean	Sd	3st Q	Max
ARS	0,02	1,15	1,50	1,51	0,63	1,96	3,16
MRL	0,02	1,24	1,70	1,57	0,79	2,19	2,86

Figure 42: Box plot of the ARS and MRL underground channel samples

The results of the grade for internal duplicates done by ARS are plotted in the Figure 43 in a comparison one to one. A linear regression function type *dataset1=a+dataset*2b* is drawn in blue color. The grey line passing through the origin with slope one is plotted as a reference. The confident limits of the fit values *a* and *b* have been included, as well the determination confident R^2, which shows the goodness of the fit. Ideally, both dataset should be equal (grey line). This involves that the 95 % confidence interval of *a* must comprise zero, and the interval for *b* must embrace one. In this case, the comparison of both sets provides a difference to the ideal case that can be consider negligible. Besides, due to the high value of R^2, 0,983, the fit can be interpreted as accurate.

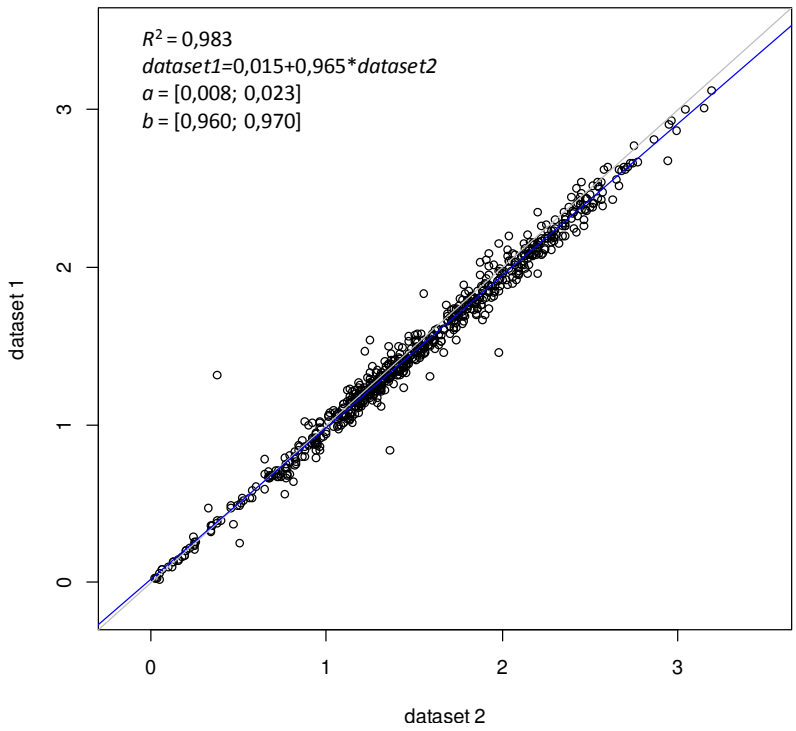

Figure 43: Linear regression for the Li_2O grade of ARS internal duplicates.

The differences between the results of the analysis of the original samples and duplicates by the same lab show a random effect in a degree of ±0,1, which indicates that they should not be interpreted extensively at this level.

A second source for an appraisal of the quality of the two labs and hence the reliability of the received figures are the duplicates analyzed by MRL. The comparison of the results of the two labs provides 95 % confidence intervals of the estimated coefficient which indicate that the regression is statistically meaningful (*MRL=a+b*ARS*), i.e. for *a* includes zero and for *b* includes one (Figure 44). R^2 is also high in this case, 0,969. Thus, there is not a significant difference between both analyses.

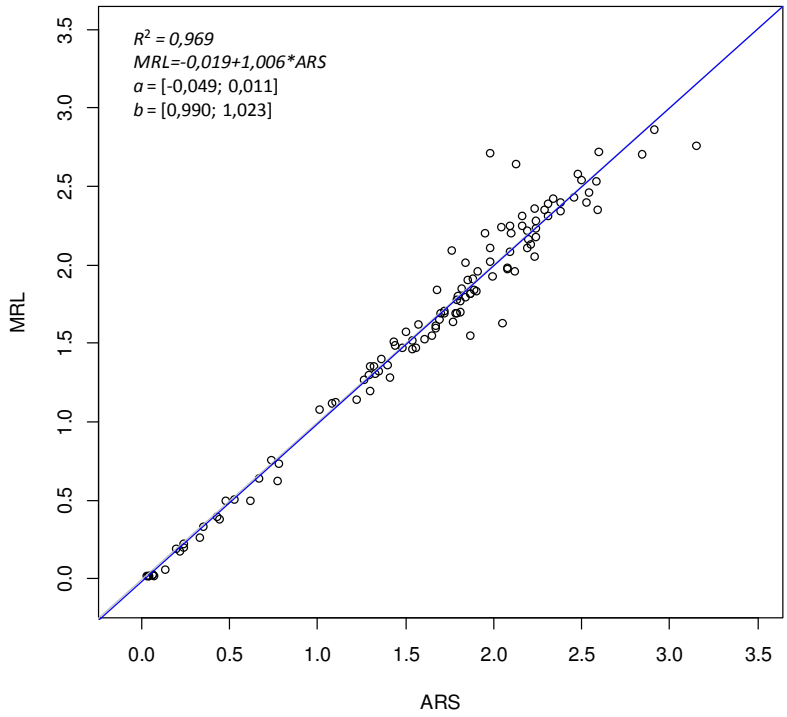

Figure 44: Linear regression the Li_2O grade of ARS versus MRL underground channel samples analysis.

In order to assess the influence of the geology in the measured grade, ARS results distribution has been calculated vein by vein, see Figure 45. The distributions of veins 2.1 and 3.1 are comparable while vein 7 has lower values and less spread. This is in accordance to the fact that veins 2.1 and 3.1 are hosted in amphibolite and vein 7 in micaschist. The samples were taken at three different levels of the tunnel face (bottom, middle and top).

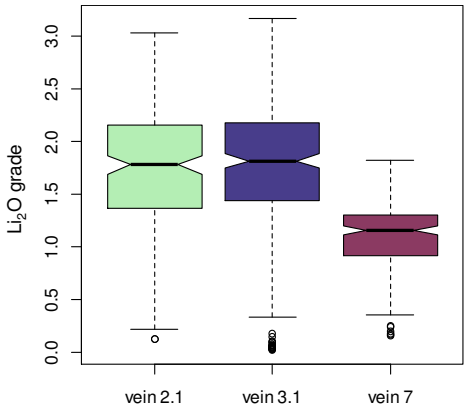

	Min	1st Q	Median	Mean	Sd	3st Q	Max
Vein 2.1	0,13	1,37	1,78	1,72	0,65	2,16	3,03
Vein 3.1	0,02	1,44	1,82	1,72	0,67	2,18	3,16
Vein 7	0,16	0,92	1,16	1,09	0,33	1,31	1,82

Figure 45: Box plot for ARS drift face samples of Li_2O grade in veins 2.1, 3.1 and 7.

With the aim of visualizing the variation of grade in small scale, the box plot of the grades obtained to the three levels in each vein is represented (see Figure 46). Each box is identified with the name of the vein and B, M and T in reference to bottom, middle and top sample. The grade difference along a face is especially notable in vein 2.1, where the middle samples have a remarkable higher grade. The results in vein 3.1 and 7 shows a lower variability along the three different levels as the medians are comparable, i.e. the notches around the medians overlap.

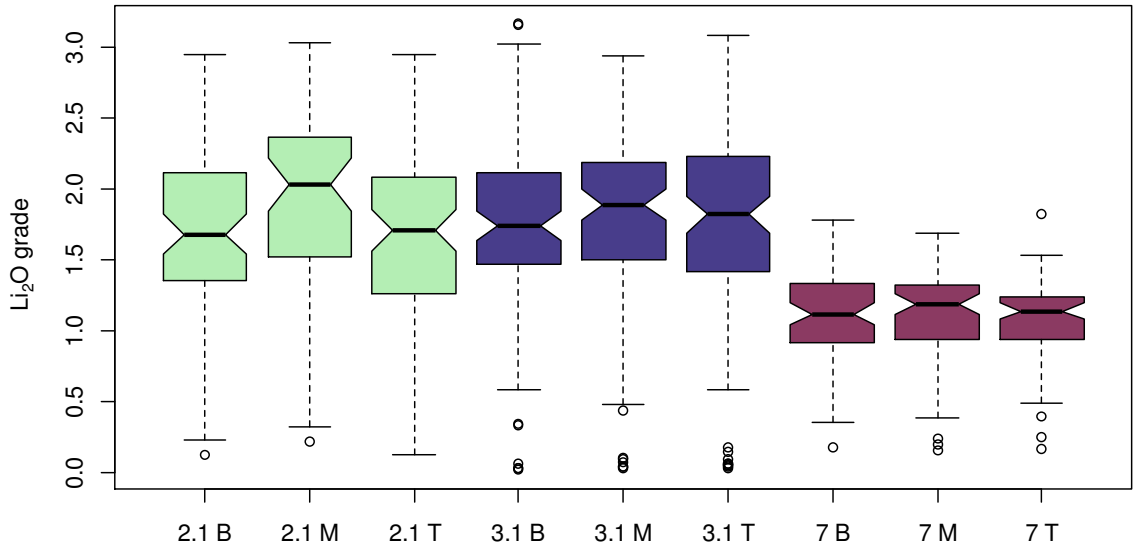

Figure 46: Box plot for ARS drift face samples in veins 2.1, 3.1 and 7 differencing by bottom, middle and top samples.

This global (distribution based) investigation can be sharpened by a more individual point of view. Because the samples are arranged on a blast-by-blast basis, the three samples of each face can be directly linked to each other. Figure 47 shows the comparison between the grade at the bottom, middle and top samples in a same drift face. The low R^2 express the high inaccuracy of the linear regressions due to

the huge variability in the measurements. This oscillation in the grade distributions shows a strong random effect in the small scale though the three veins.

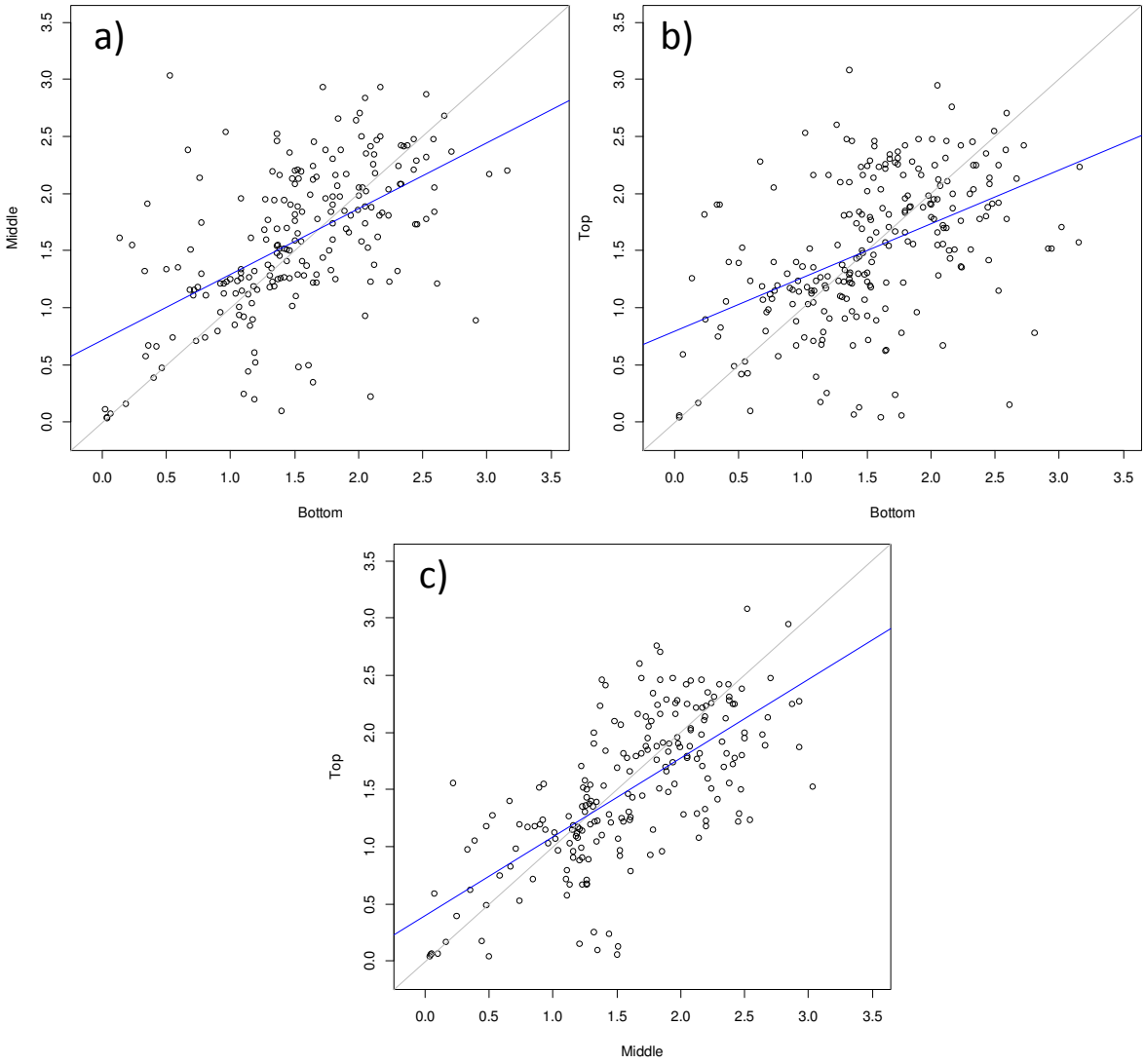

Figure 47: Linear regression of the Li_2O grade of bottom versus middle samples (a), bottom versus top samples (b) and middle versus top samples (c) for each face along the drift in veins 2.1, 3.1 and 7.

This result illustrates a remarkable scattered correlation on small scale. In contrast, on a larger scale has been observed a consistent conformity which infers that the erratic effect in small scale is partially balanced for larger areas.

7 Up-to-date data validation

In order to verify the quality of the exploration campaign done by Minerex, during the Summer 2016 EL carried out an investigation program according to updated standards covering the two main sources of exploration data: boreholes and drift face sampling. Twin holes as close and parallel as possible to seven of the underground boreholes of Minerex were drilled to provide a large-scale assessment of the deposit, while, the small-scale characteristics were represented by channel sampling at the drift areas were Minerex performed the drift face sampling.

7.1 Channel samples

Channel samples were intended to verify the drift surveying data of Minerex and to investigate the local distribution and grade of the veins. The actual face surveying data cannot be reproduced because the material was already mined during drifting. The approach was to apply channel samples along the vein thickness in the roof of the drifts to enable comparisons to the three samples of Minerex located at the bottom, middle and upper part of the veins. The location of the channel sample program is shown in Figure 48.

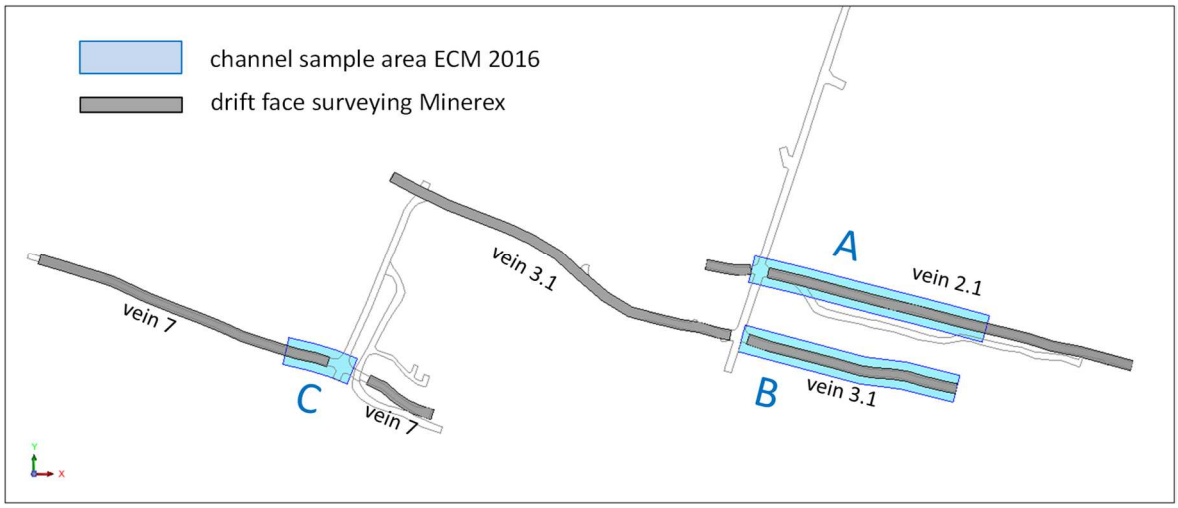

Figure 48: Location of the channel sample program

There are 3 dedicated zones labeled A (vein drift 2.1), B (vein drift 3.1) and C (vein drift 7). These zones are represented by the blue shaded areas and exaggerated in

width for better visibility. The grey shaded polygons reflect the drift extension where face surveying data from Minerex are available for comparison. The extension of zone C was considerable reduced due to safety issues. The essential key figures of the data for the 3 areas are shown in Table 11 and plotted in form of box plot in in Figure 49 for its comparison.

	Data	Min	1st Q	Median	Mean	3st Q	Max	Sd	No. Samp.
Vein 2.1	ARS(btm)	0,13	1,37	1,78	1,72	2,16	3,03	0,65	203
	ARS(av)	0,47	1,29	1,78	1,67	2,03	2,61	0,52	79
	ARS(bmt_cz)	0,13	1,51	1,92	1,85	2,29	3,03	0,60	130
	ARS(av_cz)	0,87	1,65	1,92	1,85	2,11	2,61	0,42	44
	EL(all)	1,01	1,57	1,83	1,80	2,06	2,70	0,38	40
	EL(cz)	1,01	1,53	1,84	1,80	2,06	2,70	0,39	37
	ARS(t_cz)	0,24	1,51	1,90	1,80	2,15	2,95	0,58	44
Vein 3.1	ARS(btm)	0,02	1,44	1,82	1,72	2,18	3,16	0,67	288
	ARS(av)	0,04	1,53	1,84	1,71	2,05	2,74	0,58	100
	ARS(bmt_cz)	0,35	1,57	1,90	1,88	2,22	2,87	0,46	129
	ARS(av_cz)	1,06	1,63	1,93	1,88	2,08	2,55	0,34	43
	EL(all)	0,97	1,69	1,82	1,82	1,95	2,34	0,28	40
	EL(cz)	1,42	1,69	1,84	1,85	1,95	2,34	0,23	36
	ARS(t_cz)	0,89	1,64	2,05	1,95	2,25	2,70	0,42	43
Vein 7	ARS(btm)	0,16	0,92	1,16	1,09	1,31	1,82	0,33	202
	ARS(av)	0,17	0,97	1,10	1,09	1,28	1,62	0,27	68
	ARS(bmt_cz)	0,16	0,92	1,12	0,99	1,20	1,64	0,37	24
	ARS(av_cz)	0,17	1,00	1,10	0,99	1,13	1,28	0,35	8
	EL(all)	1,16	1,23	1,30	1,31	1,37	1,49	0,11	9
	EL(cz)	1,16	1,19	1,23	1,24	1,30	1,34	0,08	5
	ARS(t_cz)	0,17	1,06	1,15	1,02	1,18	1,24	0,58	44

Table 11: Summary of the key figures of the distinct data sets used for drift-sample vs channel sample comparison (ARS(t_cz) refers to samples taken by ARS in the top position).

The label ARS(bmt) represents the grade distribution of ARS samples considering all samples (bottom, middle and top) and reflects the geological background of the respective vein in detail. Note that not in all the locations were taken the tree of them. ARS(av) stands for the average value of set of existing ARS samples at each position. Logically, the use of the average value reduces the spread of the distribution and the influence of grade changes on a small scale disappears. In ARS(bmt_cz) are considered all ARS samples which are located in the area where EL also sampled, or common zone, to comparison purposes. This is relevant due to the fact that the EL investigation area is considerable smaller than the Minerex data. ARS(av_cz) correspond to the average value of ARS samples in the common zone to both sampling programs.

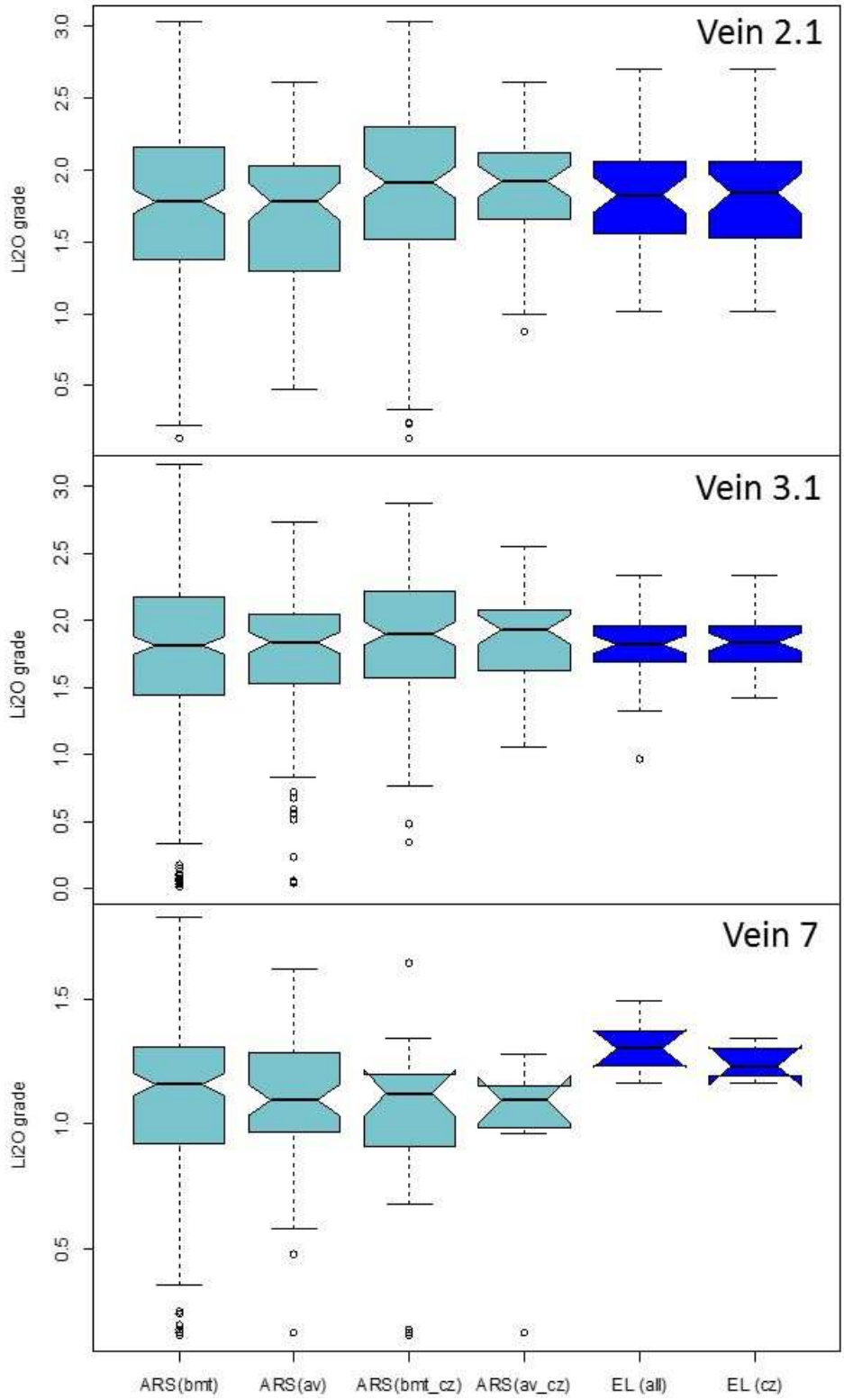

Figure 49: Box diagrams of various datasets for channel samples of veins2.1, 3.1 and 7.

EL(all) includes all samples taken by EL program while EL(cz) only those in the common area, mainly excluding samples in the crossing sections. It is added for reasons of completeness and theoretical correctness (strict comparability).

The results in AHP (veins 2.1 and 3.1) are pretty consistent though the grade in the common zone has a slightly higher grade. They show good correlation with EL samples, which are only slightly lower. In the case of the samples taken in the vein 7 the interpretation is complicated because only few samples executed by EL. According to Minerex data the grade of the investigation area is quite similar to the general characteristic of the total vein. It is remarkable that the new sampling results from EL tend to have a significant higher grade but it must be considered as well the reduced amount of available data for this vein.

The samples taken in the top position and the average results of ARS, both in the common zone, are used as basis for a deeper statistical comparison with the new channel sample data. Average results are used because the small-scale variations are balanced though it includes larger volume in relation to new measurements. The top samples are considered because its proximity to new samples in space. Figure 50 shows the boxplot for comparison and Table 12 the statistical values of its distribution. For veins 2.1 and 3.1 the median value of EL is very similar to the ARS results and it is included in the confidence intervals. However, it is not the case of the vein 7 where EL obtained higher values. Thus, the use of ARS values in vein 7 for calculations is quite conservative but it must be noticed the limited number of data (8 samples from ARS and 5 from the new campaign).

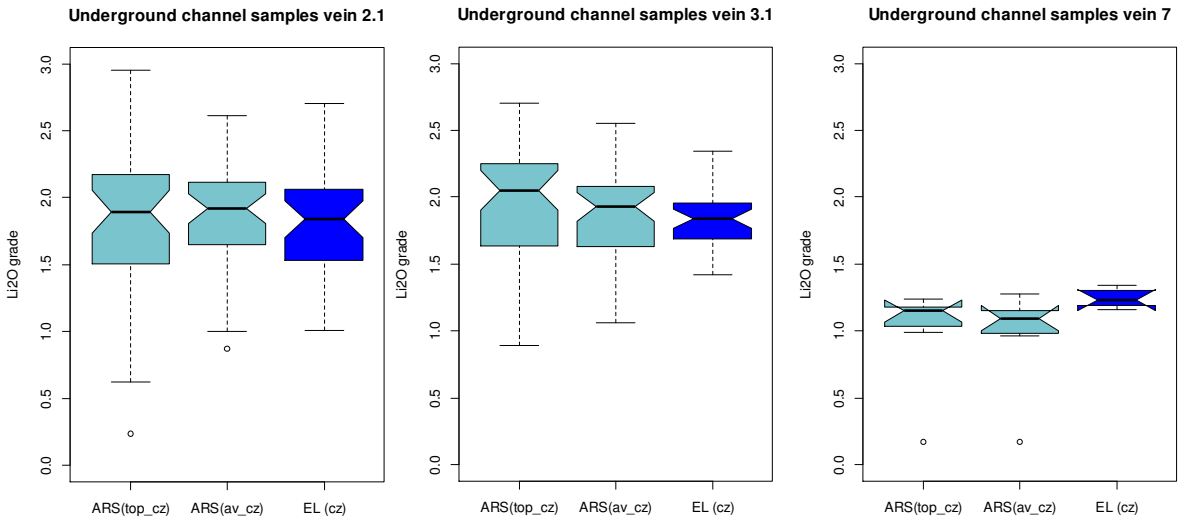

Figure 50: Summarizing result of the comparison and verification investigation for all three veins (2.1, 3.1 and 7).

		Min	1st Q	Median	Mean	Sd	3st Q	Max	No. Samp.
Vein 2.1	ARS	0,87	1,65	1,92	1,85	0,42	2,11	2,61	44
	EL	1,01	1,53	1,84	1,80	0,39	2,06	2,70	37
Vein 3.1	ARS	1,06	1,63	1,93	1,88	0,34	2,08	2,55	43
	EL	1,42	1,69	1,84	1,85	0,23	1,95	2,34	36
Vein 7	ARS	0,17	1	1,1	0,99	0,35	1,13	1,28	8
	EL	1,16	1,19	1,23	1,24	0,08	1,30	1,34	5

Table 12: Summary of statistical key figures for the verification of channel samples (ARS correspond to the average values).

The Kolmogorov-Smirnov test has been applied to compare ARS average and top values of the grade to EL results. Table 13 shows the *p*-values of the test. Values higher than 0,05 – appear in bold - means both data sets come from a same distribution in statistical terms. The equality of vein 2.1 results is validated for average and top data. El data of vein 3.1 is only comparable to the average values, probably due to the asymmetry or lack of uniformity in the distribution of the top samples noted in its 1st quartile (see Figure 50). On the other hand, the new data from vein 7 corresponds exclusively to the top samples.

Kolmogorov-Smirnov test		ARS (av.)			ARS (top)		
		vein2.1	vein3.1	vein7	vein2.1	vein3.1	vein7
EL	vein2.1	**0,348**			**0,583**		
	vein3.1		**0,404**			0,017	
	vein7			0,042			**0,310**

Table 13: Distribution equality test for channel sample verification

One to one correlation of the samples is not possible due to they come from different positions in the drift. In any case, the Figure 47 showed such individual comparison has limited significance. For visual analysis, it has been plotted how the grade results changes along the veins 2.1 (Figure 51) and 3.1 (Figure 52). Vein 7 has not enough data to produce such meaningful chart. For this exercise, the samples of Minerex and EL were projected to the central axis of the drift so that the position along the vein is comparable. The used Minerex data consist of the average of the three samples per face (bottom, middle and top). For easier readability, the course of the grade along the drift is smoothed by means of a moving average with a spread of 3 (i.e. for each sample the one before and the one afterwards is included as well). These data are displayed as solid thick lines. The individual sample results are shown as thin-dotted lines.

In general, this visual comparison reveals a good congruency. Zone B seems to have good continuity or regularity, which is well reflected by both data sets. The situation in zone A is more complex and shows a higher variability. Nevertheless,

most of the significant ups and downs of the grade variation is again reflected by both investigation series. Some differences can be observed from position 70 m to 90 m. This section is poorly represented by the Minerex faces due to a 15 m spacing gap.

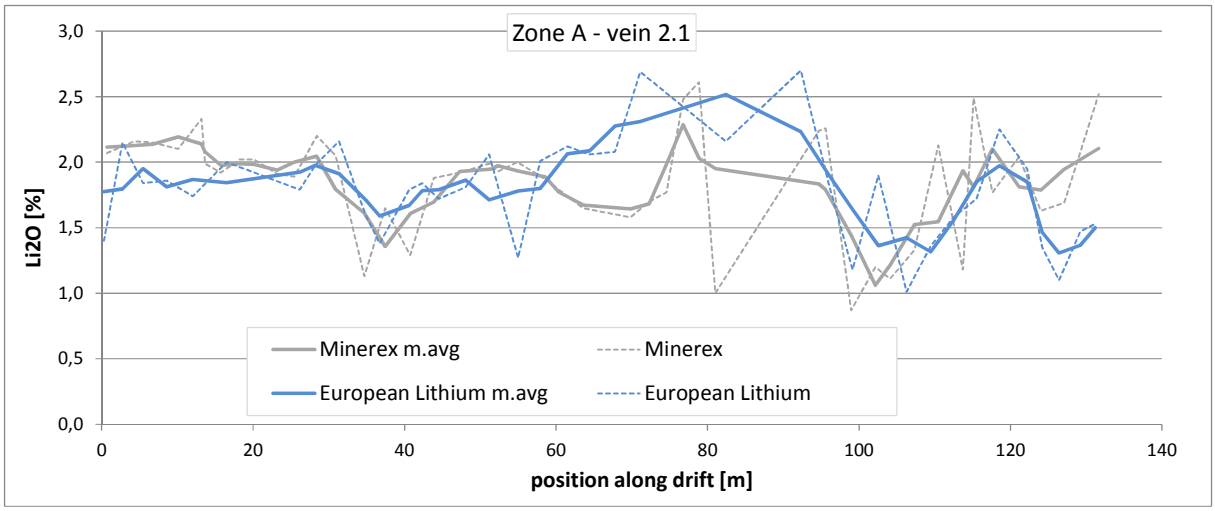

Figure 51: Comparison of the Minerex and European Lithium campaign for the trend of the Li2O grade along the drift of Zone A (vein 2.1).

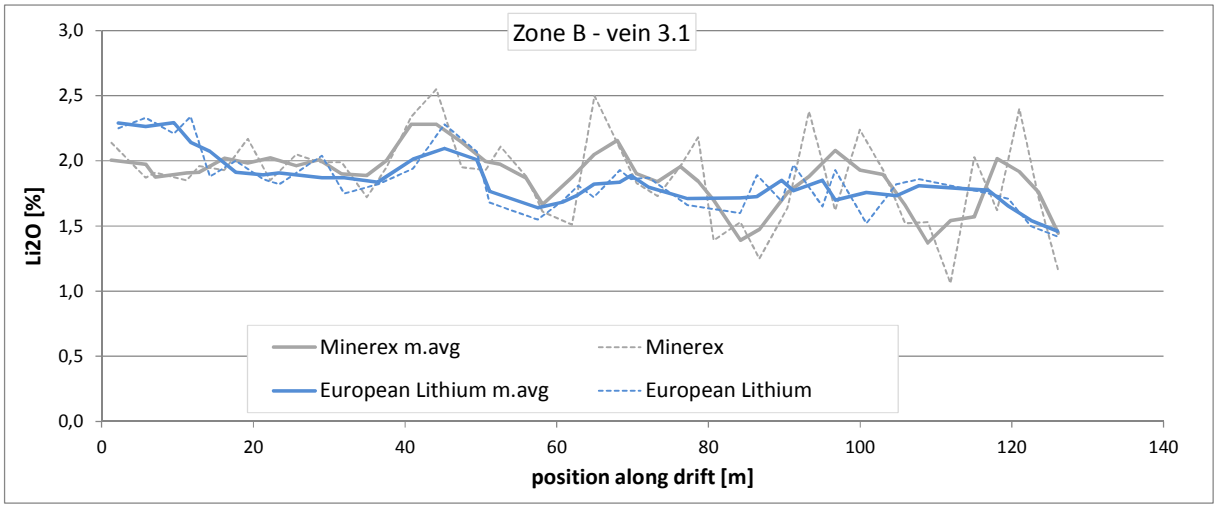

Figure 52: Comparison of the Minerex and European Lithium campaign for the trend of the Li2O grade along the drift of Zone B (vein 3.1).

7.2 Twin holes

A total of 7 boreholes were twinned. They were selected by practical (accessibility, space, infrastructure) and geological (number of expected pegmatites to be intersected) aspects. Besides, underground boreholes combine high information level with reasonable borehole length. In total the twin hole drilling program

exceeded 800 m of drilling length. The design reflects exactly the borehole geometry of Minerex, with the exception of P15-25, which was cut in length by about 70 m against KUK-6 for budgeting reasons (Figure 53).

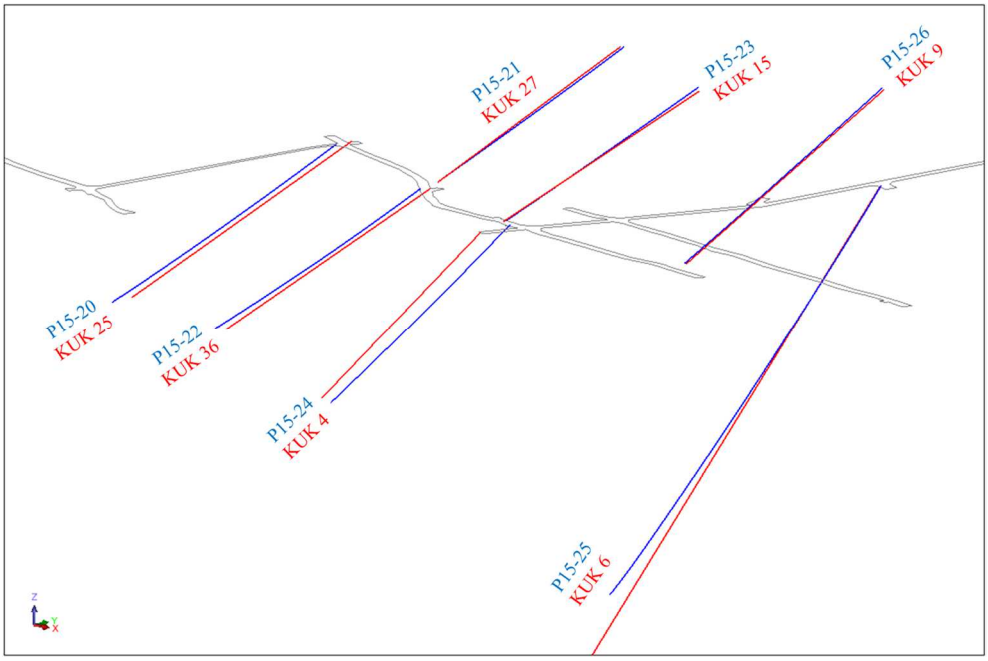

Figure 53: Visualization of the geometric relation between Minerex and European Lithium twin holes.

As a starting point data from the Minerex campaign are compared with the twin hole results on a global basis, i.e. no consideration of the location of the sample occurrences. This is based on the fact that the drill holes of both series intersect the same geological formation and hence should show in general a similar characteristic.

Figure 54 shows EL Li_2O grade and the length of the samples directly compare to Minerex. Lithium grade shows a very good similarity between both sets with almost identical medians. Only the spread of the EL samples is slightly lower than those of the Minerex. The distribution of the sample length however is significantly different. This reflects merely the different sample strategies used in the two series. EL was following a very detailed analysis procedure, i.e. thicker intersections were readily split into sub-samples. Minerex has applied a similar strategy, but only during the beginning phase of the exploration project.

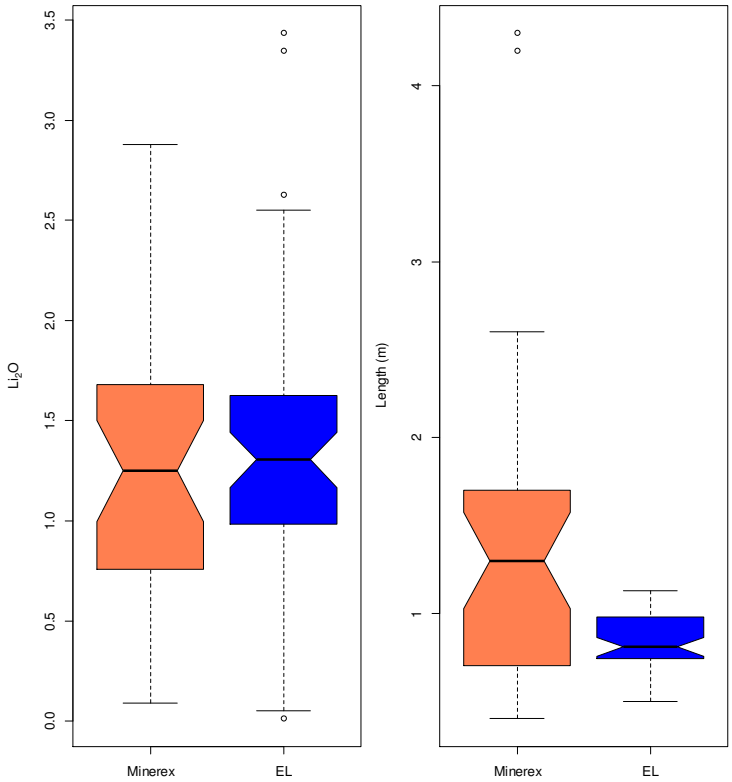

Figure 54: Comparison of lithium grade and length of the samples of twin hole data sets

Accordingly, the subsequent investigation focuses on the composites which provides a more meaningful point of view. The lithum grade from the composites do not change excessively compare to the provided by direct samples. In Figure 55 shows that the median grade for EL is slightly lower, but the distribution has a skewness to higher grades. These changes are caused by the fact that for the distribution of the direct samples the sample length (which varies to some degree) is not considered. The confidence intervals of the medians are almost identical which means that with high reliability they are the same for both data sets.

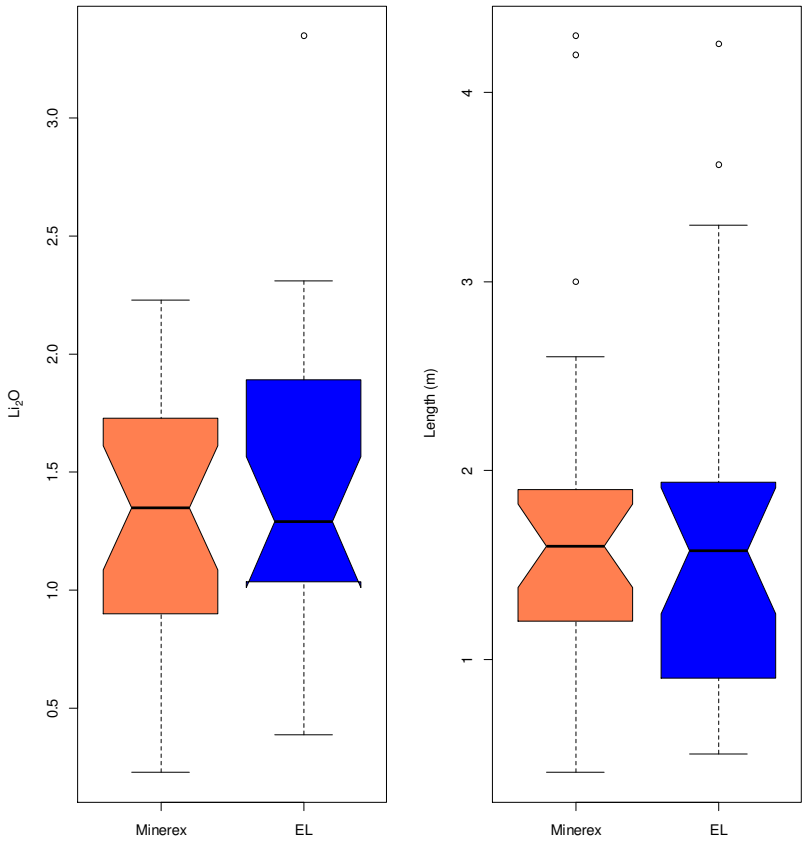

Figure 55: Comparison of lithium grade and length of the composites of twin hole data sets

Result characteristics are represented by the key statistical figures of the respective distribution of lithium grade and pegmatite thickness (Table 14).

Twin holes			Min	1st Q	Median	Mean	3st Q	Max	Sd	num
Li2o Grade	sample	Minerex	0,09	0,76	1,25	1,24	1,68	2,88	0,66	33
		EL	0,01	0,98	1,31	1,32	1,62	3,43	0,66	53
	composite	Minerex	0,23	0,90	1,35	1,34	1,73	2,23	0,59	25
		EL	0,39	1,06	1,29	1,39	1,89	3,35	0,59	24
Length	sample	Minerex	0,40	0,70	1,30	1,42	1,70	4,30	0,66	33
		EL	0,50	0,74	0,81	0,82	0,98	1,13	0,66	53
	composite	Minerex	0,40	1,20	1,60	1,72	1,90	4,30	0,95	25
		EL	0,50	0,95	1,58	1,68	1,93	4,26	0,95	24

Table 14: Compilation of statistical key figures for the twin hole validation

The comparison is supported by testing the equality of distribution using the Kolmogerov-Smirnov test. The resulting *p*-values are shown in Table 15 confirming the previous conclusions with the exception of the direct sample length (which has no practical relevance). Therefore, the tests provide a high probability that both data sets are identical.

Kolmogorov			El			
			sample		composite	
			Grade	Lenght	Grade	Lenght
Minerex	sample	Grade	0,905			
		Lenght		<< 0,05		
	composite	Grade			0,778	
		Lenght				0,839

Table 15: Equality test for grade and length of twin hole validation

The most stringent comparison of the two data sets refers to an analysis of direct pairs of samples, i.e. that a distinct section of Minerex is directly aligned with a corresponding section of the twin holes. In order to assist the geometric alignment, it was first tried to allocate the boreholes in such a way that the differences of the collar position are compensated.

This adjustment is modified in addition in favor of a good geometric fit of the pegmatite or sample positions respectively. The principle of the geometric compensation is shown in Figure 56 The main basis of the correction is the assumption of the general orientation of the veins (respectively the dominant geological formation). The shifting vector is the given by the intersection point of the borehole to be aligned with the plane defined by the collar of the corresponding borehole and the vein orientation. Applying this shift the borehole and thus creating a theoretical comparison scale, ideally intersections of the same vein (or geological feature) should be found on the same position. The calculated geometric shift values and the additional individual adjustment are listed in Table 16 where the label KUK refers to the original boreholes and P15 are the new ones. The additional adjustment is based on a visual inspection targeting at a good alignment of the geological features along the borehole. The interpretation of this manual correction relates mainly to the eventual inaccuracies of collar position of the Minerex boreholes.

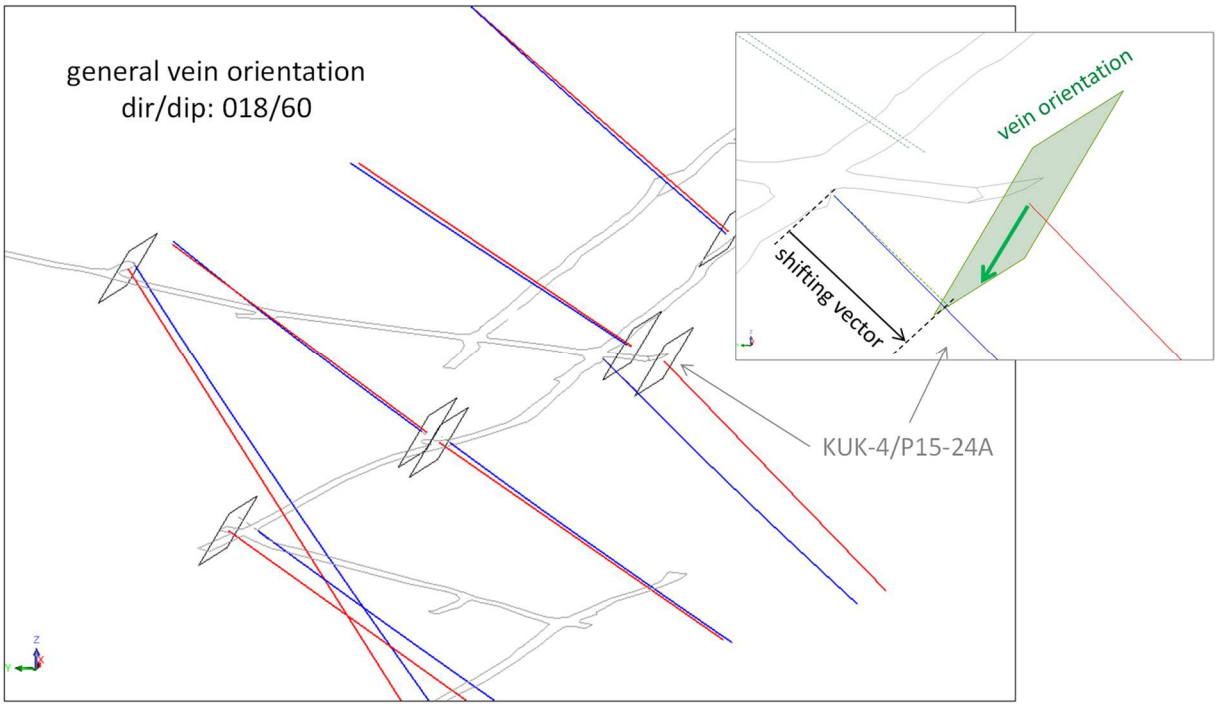

Figure 56: Borehole collar compensation for geometric vein alignment

borehole twins		geom.	indiv.	total
KUK-25	P15-20	7,3	3,9	3,4
KUK-27	P15-21	1,7	1,7	0,0
KUK-36	P15-22	3,2	-0,4	3,6
KUK-15	P15-23	1,5	-0,8	2,3
KUK-4	P15-24A	-14,8	-0,6	-14,3
KUK-6	P15-25	1,0	1,0	0,0
KUK-9	P15-26	0,2	-1,5	1,7

Table 16: Shifting values for data comparison along twin boreholes

For an easier readability, the boreholes are position parallel in 2D, with the collar position shifted according to the geometric and individual adjustment, see Figure 57. The Li_2O grade is represented in green, the pegmatites of the original boreholes in blue and pink is used for the pegmatites found in the twin holes. Connection lines between boreholes indicate the intuitive assignment of the sections of the boreholes considered comparable done on a visual basis. The vein assignment done by Minerex is also shown. The graph illustrates a very nice alignment between most of the pegmatite occurrences. There are only few exceptions, such as the section range 65 m to 110 m of the borehole twins KUK-6 and P15-25. In this section, the structure visible at the cores shows also some irregularities which indicate that the deviations are based on geological effects rather than measurement or monitoring problems (see Figure 58).

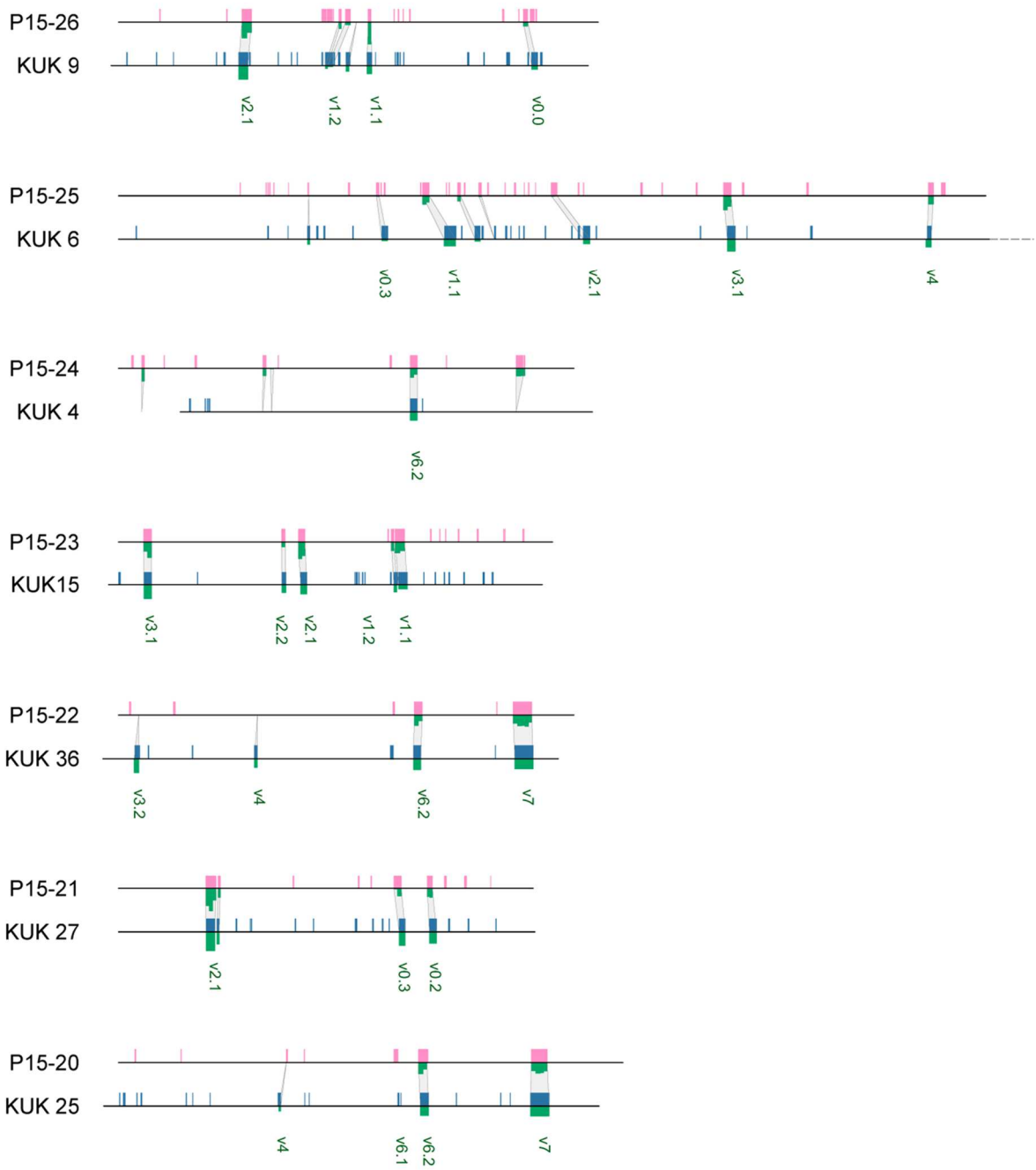

Figure 57: Paired alignment of original (KUK) and new (P15) boreholes.

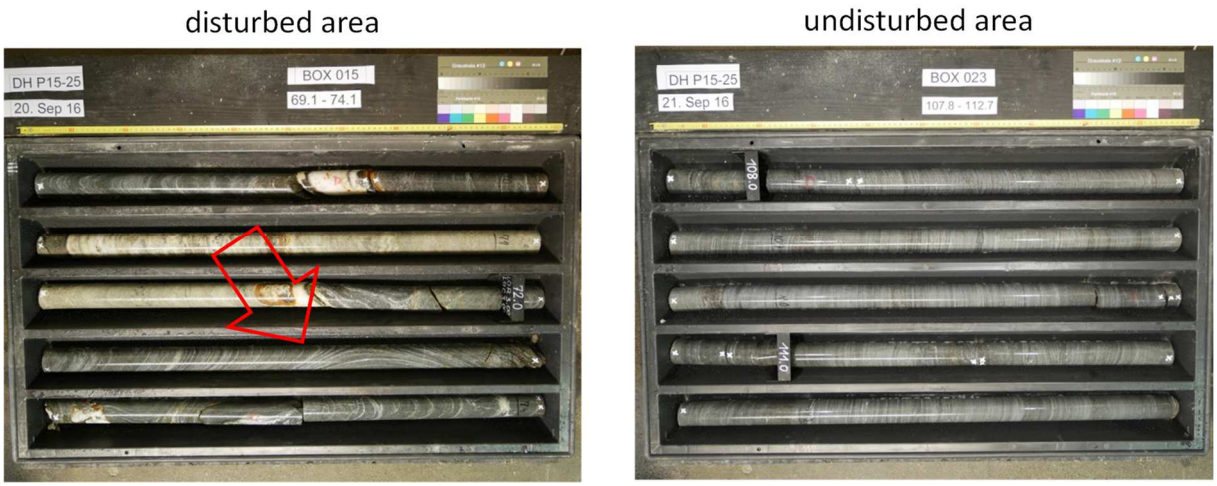

Figure 58: Examples of drill log images illustrating irregularity zone of P15-25.

In total, 35 alignments were defined. Examples of sections without corresponding part in the respective borehole are balanced, i.e. there are 5 samples of KUK with no correspondence in P15, and 5 samples the other way around. This leaves 25 alignments for direct comparison. The 10 none-corresponding samples are of lower length and lower grade compared with the rest. It must be noted that the assignment is a first appraisal and necessarily subjective. It is also to some degree influenced by the different sampling strategy in both campaigns. In Table 17 a summary the selected sections are given including length and average grade incorporating dilution.

alignment	num	Minerex		European Lithium	
		length	Li2O	length	Li2O
Missing in P15	5	0,66	1,18		
Missing in KUK	5			0,91	0,87
paired	25	1,52	1,30	1,65	1,32

Table 17: Summary of alignment of borehole twins

Due to the limitations of the assignment currently no detailed statistics are applied for this individual comparison. A one to one comparison of the results of EL and Minerex is plotted in Figure 59. Taking into account the short-scale dispersion observed during previous investigations the correspondence between the former Minerex results and the new European Lithium data is considered as very good.

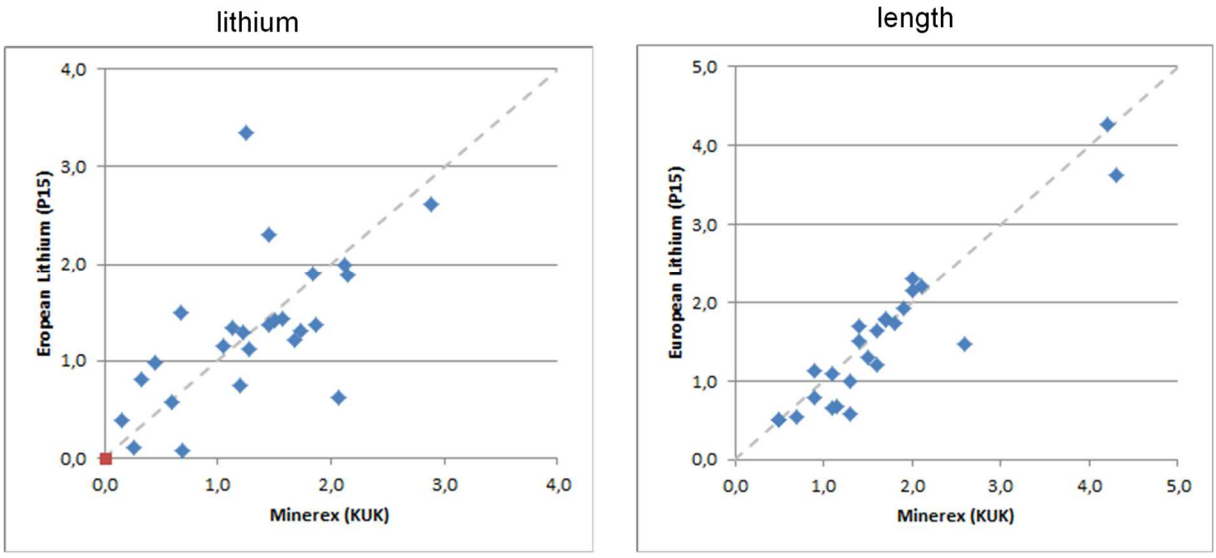

Figure 59: Comparison of lithium grade and length of aligned sections of borehole twins (KUK vs. P15)

7.3 Summary

The aim of proving the quality of Minerex data, obtained during the 1990ies, to be compliant with the requisites of the JORC code, has been achieve through a thoroughly statistical analysis and comparison to the duplicates performed by Minerex and the new data acquired according to update standards. For this purpose, it has been mainly use the lithium grade results of drift face and borehole samples.

For drift face samples, ARS was used as primary lab. Lab results are very well confirmed by the duplicates from MRL, which cover approximately a 20 % of the total. Original samples and duplicates have been compared on a general basis by distribution comparison through box plot diagram and on individual basis by the calculation of linear regression of the one to one evaluation, providing congruent and similar values.

On the other hand, the data validation of drift samples through the new exploration campaign was conducted by the use of channel samples in three areas. For these samples, taken in the roof of the drifts by European Lithium during the 2016, the results have been confirmed in statistical terms as well. This has consisted on a general comparison of the distributions through box plot diagram and Kolmogorov-Smirnov test and individual comparison of the obtained lithium grade one to one. For zone C (vein 7) this conclusion is less stringent, because only few samples were drawn and even fewer can be directly compared with the Minerex samples. For these data, the EL results show considerably higher grade, although this result

should not be overemphasized due to the lower reliability provoked by the high variability on small scale of the deposit. Taken the comparison as a total, the assumption that the sampling quality and reliability of Minerex for vein 7 can be expected of as good level as for the other two veins is acceptable. The samples of EL, and therefore the comparison, was focused on AHP veins. However, there is a very reasonable likelihood of the existence of same quality conditions during the MHP sampling.

The borehole data have also been subject of analysis. The analysis for Minerex was distributed among the two labs, about 2/3 performed by ARS and 1/3 by MRL, including about a 30 % of duplicates between them. Surface borehole samples (KOK) were analyzed by both labs, while exclusively ARS data was found for underground (KUK). Thus, due to the different spatial location and density of the samples of both sets, the distribution of the results of both labs does not fit. However, the one to one comparison for the duplicates analyzed by both labs is quite favorable.

Besides, it has been compared the former borehole data of Minerex and the new twin holes data of EL. On a general basis, distributions of new and former data have been compared through boxplot and Kolmogorov-Smirnov test providing very satisfactory results. Both sources may be considered statistically equal providing high confidence intervals. On an individual analysis, both groups have been assessed visually providing quite acceptable similarity between both datasets, especially if the high level of small-scale variability is taken into consideration.

On the whole, statistic comparisons of the distributions (former duplicates and new versus old data) are satisfactory while one to one comparison is rather acceptable.

As a consequence, the data selected for the resources calculation are:

- Surface boreholes analyzed by MRL lab which were also documented in the aforementioned „Zier database“
- Underground boreholes analyzed by ARS lab.
- Drift face sampling analyzed by ARS (which was duplicated in a 20% by MRL).

8 Deposit regularity

The previous data investigations have shown a high level of variability in small scale, but a good consistency in the large scale. In this section, this result is contrasted by the data analysis through variograms. Due to the difference in the

representativeness of face sampling and borehole data, they are analyzed separately.

8.1 Variability of drift face sampling data

The search parameters of the variogram were selected in a way that only the comparison of data from the same vein was allowed. Primary search direction is along strike (bearing 108°) and the cone angle is relatively small with 30°, with a maximum limit of 25m perpendicular to search direction. The results are shown in Figure 60, where term detail refers to bottom, middle and top data – drawn in black lines – and face avg. refers to the average value of the set of measurements at each face – red color lines.

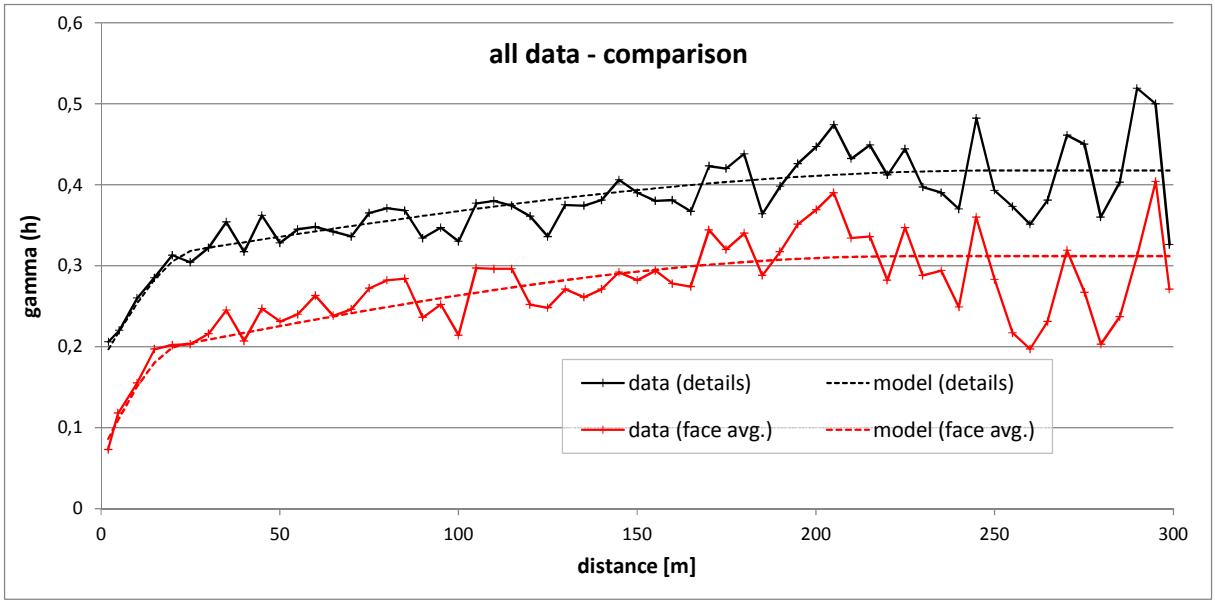

Figure 60: Variogram of face sampling lithium grade (detailed and face average).

Due to the averaging calculation, the variance of the "face avg." is more reduced, so that the corresponding graph is on a lower variance scale, but in essence both data sets show the same characteristics. This supports the theory that the consideration of the mere face average is sufficient to reflect the deposit characteristics.

The variogram shows a considerable nugget effect and a pretty sharp rise on small scale. This means that within relatively short distance (20 m – 30 m) almost 2/3 of the total variance is already reached. Hence, it is confirmed that the mineralization

can be described as pretty volatile in short distance. In consequence, the prediction of volumes at this scale necessarily incorporates a considerable level of uncertainty.

On the other hand, it is remarkable that, in the long-distance level, another systematic correlation can be detected. The range of this structure is significantly larger and was estimated to be approximately 150 m – 200 m. This supports the idea to generate a meaningful deposit model despite of the mineralization complexity. Thus, the model should be based on a reasonable volume space, or block size, to absorb some degree of the short scale variability.

From the data analysis of previous sections, it is deducted a significant difference between amphibolite and mica schist hosted pegmatites. Accordingly, it is also investigated their behavior in respect of variability separately, see Figure 61. Based on the insights of the previous investigations, this analysis is only executed for the average data. Notice the different number of samples available, 179 for AHP and 58 for MHP.

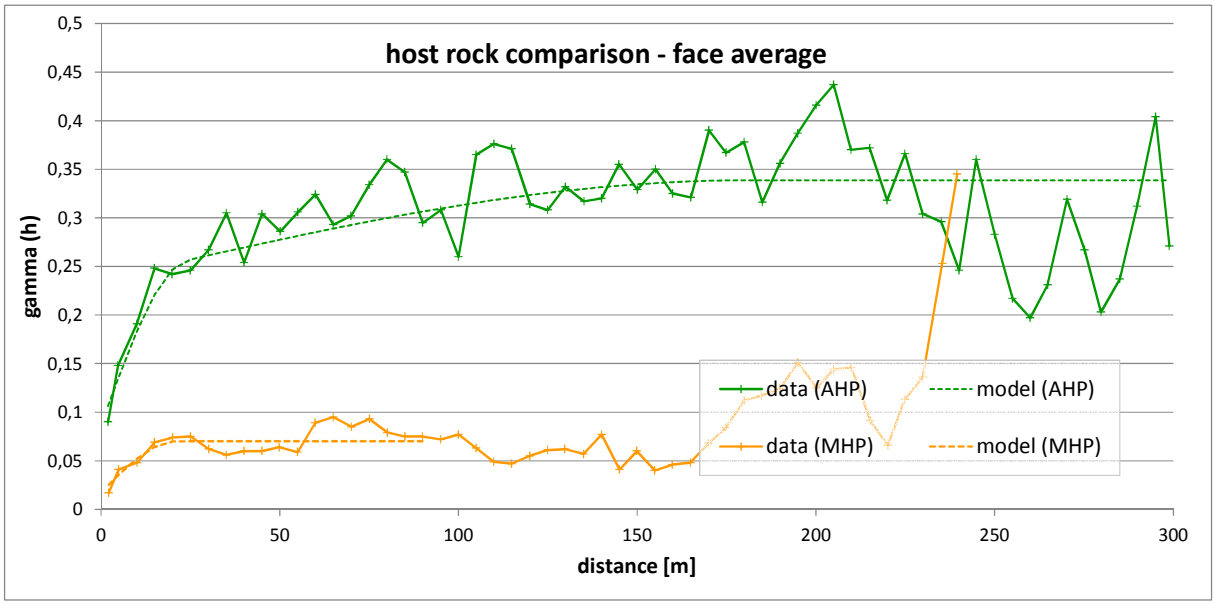

Figure 61: Variogram of face sampling for AHP and MHP lithium grade.

As expected due to the dominant number of AHP samples, the variogram of the AHP shows a very similar behavior as the one of the total data set. The MHP variogram is similar in the small-scale range showing the already described sharp rise in the beginning. However, no systematic large scale correlation similar to the AHP is clearly identifiable. Instead there are some indications for some degree of cyclicity. However, the main aspect is the dramatically lower total variance.

This is partly due to the slightly lower average grade in MHPs but mostly it reflects the much lower spread of the general grade distribution of MHP. This continuity

effect was already clearly identified in the data analysis (section 6, Figure 35 and Figure 45). This means that even if the modeling of spatial distribution is still very problematic, mineralization within the global range is very reliable.

8.2 Variability of borehole data

The number of samples (and vein composites) is too small to enable a vein by vein analysis on a statistical basis. Table 18 gives an overview of the available data assigned to each vein.

vein 0.0	vein 0.1	vein 0.2	vein 0.3	vein 1.1	vein 1.2	vein 2.1	vein 2.2	vein 3.1	vein 3.2	vein 4	vein 6.1	vein 6.2	vein 7	vein 8	total
17	12	8	17	34	31	42	19	45	24	18	6	31	39	5	343

Table 18: Number of borehole intersections per vein.

When all samples are considered, due to the proximity of veins in space, samples of two different veins would be included into the comparison - which would clearly violate the underlying idea of the veins investigation. This is due to the fact that veins are so close to each other that adjustments of the parameters of the search direction cannot prevent a blend of data in the examination.

For this reason, it was applied a geometric rearrangement that allows to use all data for variography and prevents mixing samples from different veins (Figure 62). This is done by positioning data of each vein as a group along a vector with sufficient space in between, but keeping the relative 2D distance between samples of each vein. The space is determined by the maximum search distance (500 m). For reasons of simplicity, the arrangement was done in a linear manner (using a common vector to all veins).

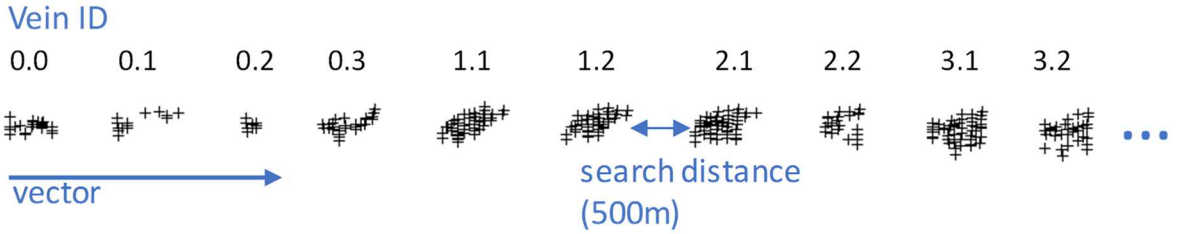

Figure 62: Tabular rearrangement of samples (composites) for variography

In the case of borehole data, variograms of Li_2O grade and also thickness are assessed, due to borehole data show the complete extension of its intersection with veins, in contradistinction to drift face data.

8.2.1 Lithium grade investigation

For this purpose, Li_2O grade of the vein composites is used directly from the database. Figure 63 shows the results of the global variogram that, due to the geometric rearrangement, is in essence a 2D analysis. The search is uniform in all directions, i.e. no anisotropy is assumed. Maximum search distance is 500 m, with a lag interval of 15 m.

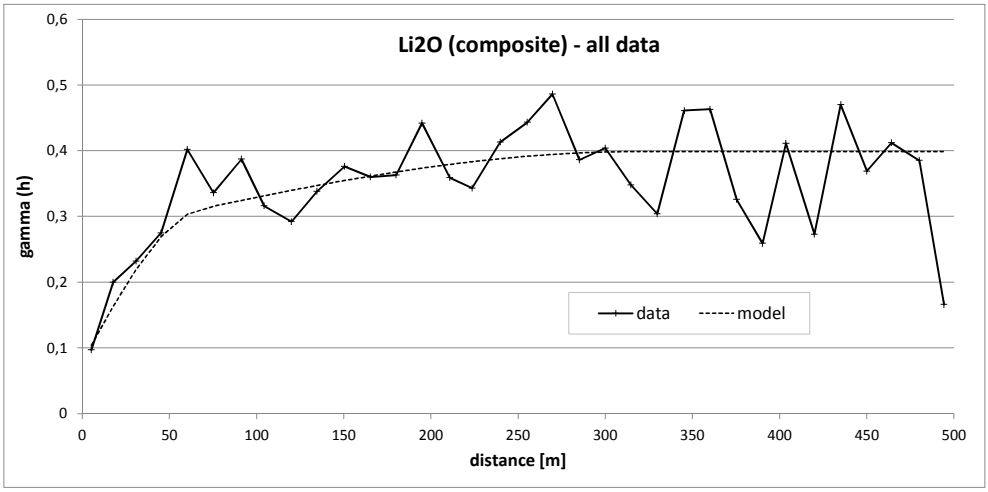

Figure 63: Variogram of lithium vein grade (borehole data).

The graph has a conspicuous similarity with the one generated for the face sampling data (Figure 60). The current interpretation is again a two-tiered structure. The first structure is characterized by a considerable nugget and a comparatively steep increase within relatively short distance (approximately 50 m – 70 m). This is followed by a gentle increase with a range of about 300 m. Nugget accounts for about 25% of total variance (random or unexplained variation of grade). The first structure covers about 50% and the second on about 25% of total variance. In particular, in the small range section of the graph the structure is not completely clear because of the reduced number of sample pairs at this section. The interpretation and resulting variogram model can be therefore subject of debate.

As already mentioned, there are many indications that the AHP and MHP differ in their characteristics. Accordingly, these two groups were investigated separately. The results are shown in Figure 64.

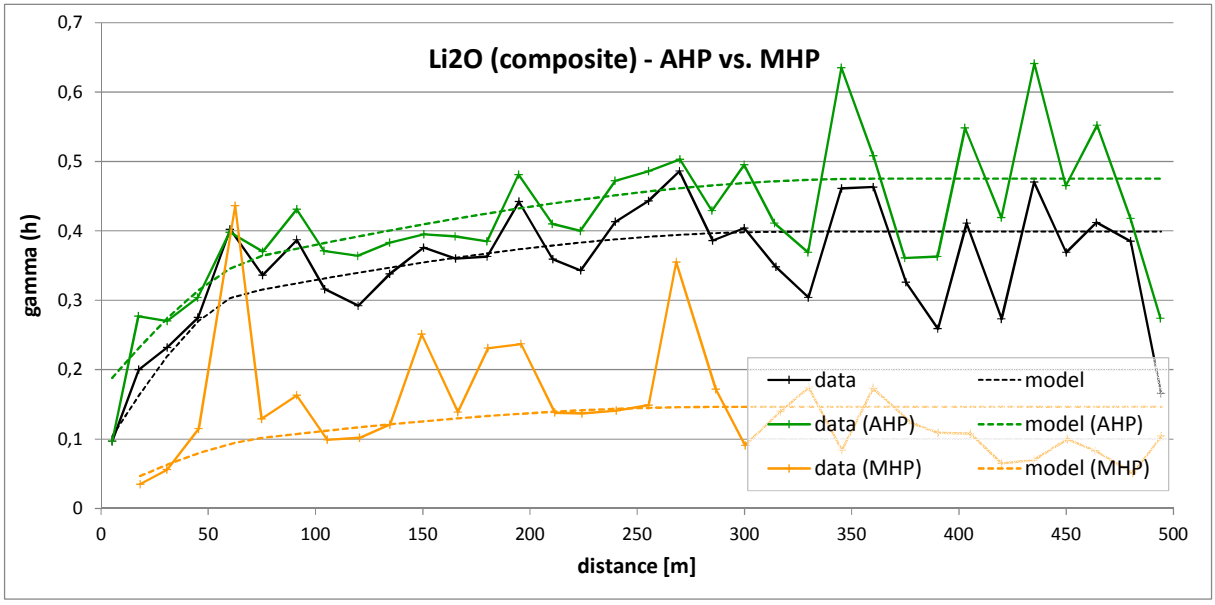

Figure 64: Variogram of lithium vein grade - comparison of amphibolite and mica schist hosted veins

The interpretation is complicated by the lack of sufficient data for MHP (99 out of 348). AHP variogram (green line) resembles the total variogram simply by the dominant number of samples. However, the MHP variogram (orange line) is pretty erratic and makes hardly possible to derive a clear variogram model. The model shown is essentially set in analogy to AHP rather than by stringent conclusion. However, what is absolutely clear is that again the total variance for MHP is significantly lower than for AHP. This correlates with the observations from the face sampling investigation and the univariate statistical analysis.

Another assumption to examine refers to the difference of vein grade (diluted by interbedding) and pegmatite grade (undiluted). Geological considerations might favor the idea that there is a higher regularity for pure pegmatite grade. To verify this the pegmatite grade has been calculated from the vein grade and interbedding factor. Their comparison is shown in Figure 65. It was performed only for the AHPs, because interbedding occurs by far dominantly in this geological setting. The result shows clearly that interbedding does not make a noteworthy difference as far as regularity is concerned. This is not very surprising because number of interbedding occurrences is not very high and interbedding factor is in most cases reduced.

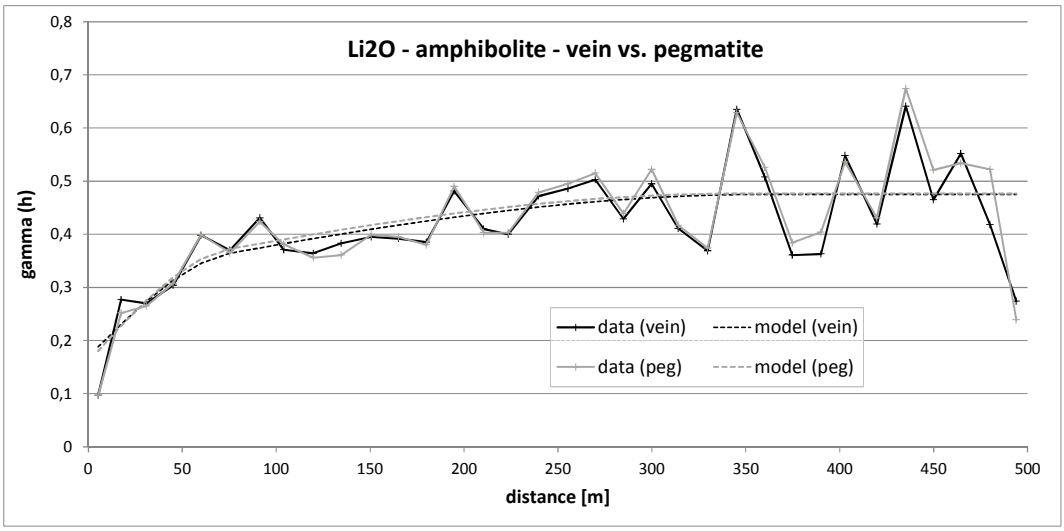

Figure 65: Variogram of lithium grade - comparison of vein and pegmatite grade.

8.2.2 Thickness investigation

Thickness characteristics are similarly important for modeling as lithium grade. However, it is not directly available in the exploration results, which hold only sample length (or vein intersection length). Thickness depends on the relative orientation of the borehole to the local orientation of the vein, which is unknown (see section 6.1 for more details on the aspects of thickness calculation). On contrast, for this analysis the use of sample length is a reasonable assumption due to in variographies only the relative difference is decisive and not the absolute value. The resulting variogram is shown in Figure 66 .

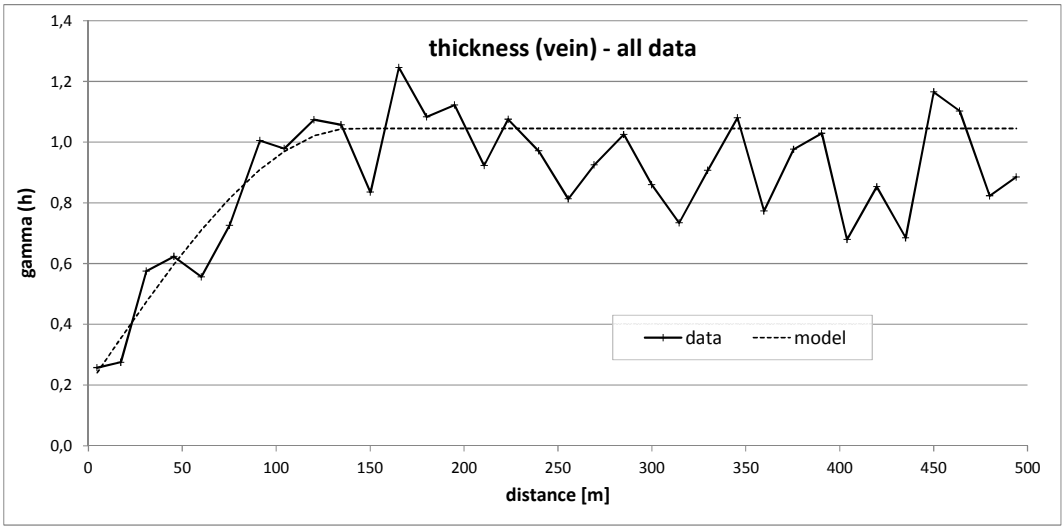

Figure 66: Variogram of vein thickness - all data.

The experimental variogram for thickness comes up with a quite standard shape. This indicates a single structure model with 20% nugget and a range well above 100 m. This is a quite positive result for modeling, even for the less densely explored areas with a 100 m spacing of the profiles.

Again, differences of AHP and MHP are investigated (Figure 67). As expected, AHP (green line) is again close to the total graph, and MHP (orange line) is again more difficult to interpret due to the lack samples (in particular in low range). Nevertheless, a similar variogram model as AHP seems to be also for MHP reasonable. Total variance is slightly lower, despite the fact the average thickness of MHP is higher. This supports the geological assumption that MHP is in general more regular than AHP.

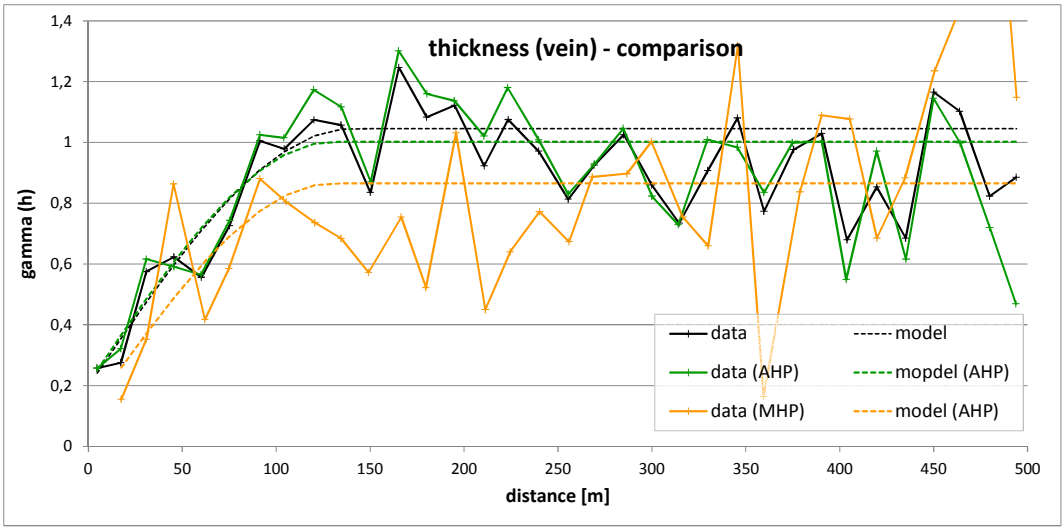

Figure 67: Variogram of vein thickness - comparison of amphibolite and mica schist hosted veins.

8.3 Variography parameters summary

The parameters of the approximated models for the various data discussed before are summarized in Table 19. It must be indicated that the choice of the model was done independently, so that comparisons are valid. MHP results must be interpreted cautiously because of low number of data.

bore hole sampling - lithium grade										
data	population		nugget	strucure 1		structure 2		rel. sill		
	s. num.	var.		sill c1	range r1	sill c2	range r2	c0	c1	c3
all	348	0,402	0,079	0,192	68	0,127	320	20%	48%	32%
AHP	249	0,493	0,170	0,192	76	0,160	360	34%	39%	33%
MHP	99	0,150	0,021	0,021	77	0,072	288	14%	14%	48%
AHP (peg)	249	0,494	0,160	0,160	75	0,154	345	32%	32%	31%
borehole sampling - thickness										
data	population		nugget	strucure 1		structure 2		rel. sill		
	s. num.	var.		sill c1	range r1	sill c2	range r2	c0	c1	c3
all	405	1,043	0,199	0,847	140			19%	81%	0%
AHP	298	0,991	0,207	0,795	130			21%	80%	0%
MHP	107	1,110	0,106	0,759	130			10%	68%	0%
face sampling - lithium grade										
data	population		nugget	strucure 1		structure 2		rel. sill		
	s. num.	var.		sill c1	range r1	sill c2	range r2	c0	c1	c3
all (detail)	693	0,420	0,181	0,120	27	0,116	250	43%	29%	28%
all (f.avg)	247	0,312	0,069	0,114	22	0,129	225	22%	37%	41%
AHP (f.avg)	179	0,304	0,086	0,150	24	0,103	180	28%	49%	34%
MHP (f.avg)	58	0,071	0,017	0,053	21			24%	75%	0%

Table 19: Results of variography.

Regarding lithium grade, most models indicate the presence of two structures. The ranges are usually pretty similar. Face sampling shows lower ranges, which is probably due to the higher spatial density and the restricted spatial extension. Range of the nugget is relatively substantial but, due to the low number of closely located samples, does not allow absolutely reliable deduction. 25% of total variance is probably a good estimate. The same applies to the sill of the other structures. The variogram model for MHP is poorly data supported but resembles in shape to AHP. For that reason, it is assumed that the basic structure is similar to AHP. For the estimate of the mean the same variogram could be applied. If the estimated variances are of relevance, the lower sill of the MHP should be taken into consideration.

Vein thickness has probably a simpler behavior. Currently, a single structure model seems to be sufficient to approximate the experimental variogram. Nugget is estimated to be in a range of 20%, possibly lower for MHP. A range of about 130 m is well supported. For calculation, again similar variogram models can be applied for AHP and MHP, with the only difference of a lower total variance for MHP (although the effect is less significant for thickness than for lithium grade).

9 Modeling

The deposit modeling should apply the results dropped from the updated data investigation. Its goal is to provide a resources calculation according to JORC complaint which later allows to generate a feasibility study including mine design. Therefore, the main outputs to obtain a final result in terms of lithium tonnage (Li_2O) must be grade and thickness distribution in the deposit. The most relevant input parameters for the resource calculation will be primary thickness (intersection length), grade, in terms of persistence and extension in volume, and interbedding. Exact spatial location of the ore body takes a minor significance for the resource calculation. On the contrary, regarding the mine design, geometry has a predominant importance. However, due to the high level of variability inside the deposit – shown through all data investigation – the accuracy in the prediction of the deposit geometry is quite limited.

9.1 Preliminary modeling

On an early attempt of modeling the Koralpe deposit, a linear interpolation of the boundaries was performed according to the vein assignment of Minerex through triangulation of solids (Figure 68). The term solid is applied by Surpac™ to a valid close surface. This definition of the ore body was based on the geological profiles and borehole data. As was described in the section 4.2.1, this pure surface modeling only provides a volume calculation or information about the deposit boundaries geometry, but not about grade distribution. Since the same reason, it does not allow any extrapolation or calculation of reliability – very important attributes for the JORC complaint. Other drawback of this method is its laborious and time-consuming characteristic. This method does not allow an appropriate automatization. On the other hand, its main advantage is that fits perfectly to the sampling data.

As it was explained in section 5.2.4, boreholes show a wide variety of quality in the data: from pure geology information without any assignment to fully tested and assigned samples. This approach basically allows to employ all information assigned to a vein. It is used to provide a general idea of the deposit characteristics. According to it, vein thickness varies from 0,25 m up to more than 5,5 m. Veins are traced over a horizontal extension of approximately 1,5 km and a depth of about

450 m. The general dip angle is around 65° and fits quite nicely to all the veins due to they are disposed rather parallel.

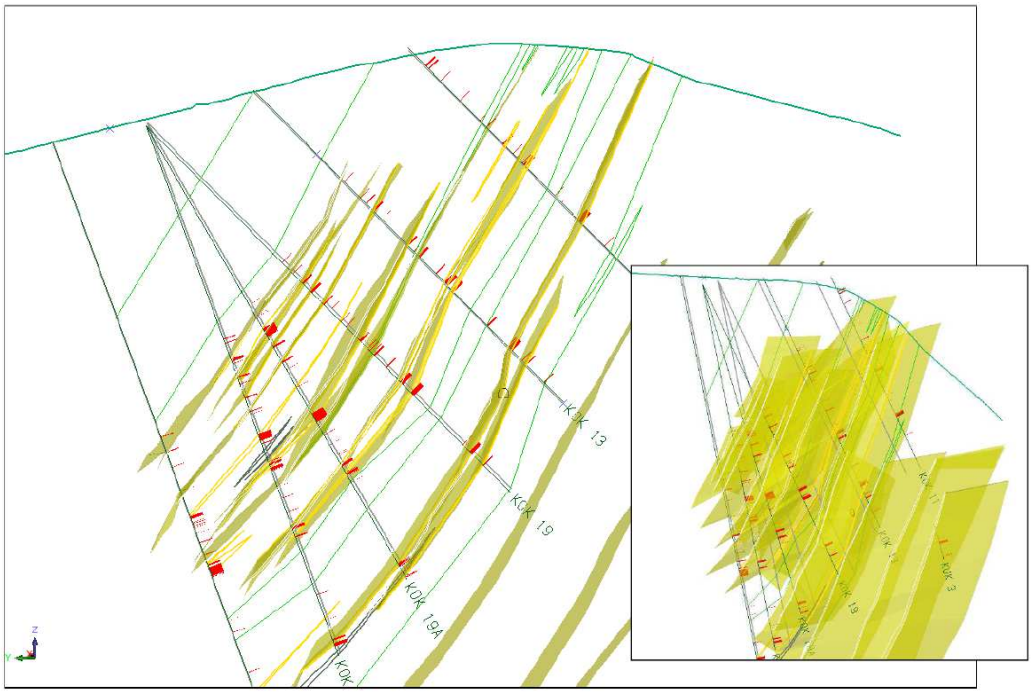

Figure 68: First surface modeling of the deposit.

9.2 Modeling approach discussion

Previous section has argued the poor adequacy of linear interpolation technique for modeling of this deposit. Others methods, such as inverse squared distance, present the advantage over the preceding one that allows extrapolation but not reliability assessment. The consideration of the reliability of the estimations of the model use for a resource calculation is essential factor for the JORC complaint. Therefore, according to the statements established at the section 4.2.3, the use of geostatistics is recommended, which allows the calculation of the reliability of results as well as extrapolation based on statistical background.

Geostatistics may be applied by the use of a block model. As discussed in section 4.1.2, block model technique is an implicit method. This involves that the whole modeling space is defined and the calculation results and capacities are directly linked to the block size.

As it was mentioned before, the size of the blocks is strongly related to the reliability of each individual estimation. If a block represents a bigger size, as it is not a real homogenic unit, the estimated value allocated omit the internal variability to a

greater extent (Figure 69). The bigger the block, the greater omission and therefore, the bigger the variance in the block. On the other hand, too small blocks provide too smooth estimations with, therefore, low precision which strongly hinders boundary definitions. Besides, the density of the data should be considered as well to select a proper block size.

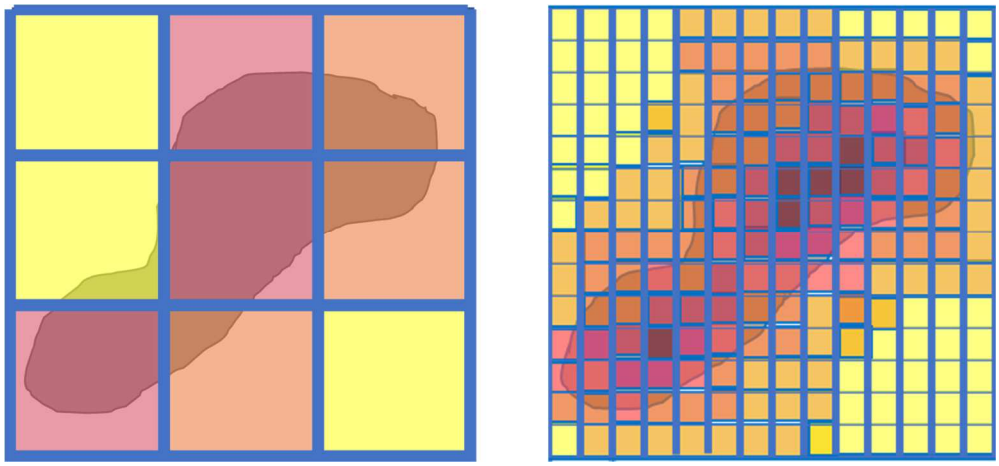

Figure 69: Influence of the block size in the estimations.

In the previous section, it has been shown that the veins are considerable thin (from 0,25 to 5,5 m). In order to model this feature, a minimum of blocks size of 0,25 m would be required. Due to veins expand along an extension over a kilometer, this would mean a huge number of blocks, beyond regular computer limitations. Besides, so reduced blocks would have very low significance in their estimations.

Observing the general shape of the veins, it may be affirmed that they strongly resemble to planes. Besides, the available data along thickness is scare. This suggests the suitableness of a 2D modeling approach. In order to obtain a tonnage value, thickness – which is missing in a 2D approach – has to be model as another property of the deposit. In this way, the modeling is focused on the variation of features along the veins neglecting the transversal changes, which has the ultimate importance due to mining methods hardly can extract in a selective way along the thickness of such thin veins.

The reduction of the problem to 2D has associated several advantages. Firstly, it permits the use of geostatistics through block model, but avoiding the need of define the whole modeling space and providing a reliability of the results. Besides, it enables to increase the blocks to a reasonable size. Another important benefit is the possibility of automatize the process.

However, a 2D representation may be insufficient for a task such as mine design or visual validation of results – intersections between veins and contradictions with

sampling data. For this purpose, a 3D representation of the results by means of linear interpolation is proposed. This is based on the better suitability of linear interpolation to describe geometry or sharp changes and faithfulness to samples location. In this sense, this method allows to apply the main advantages of both parametric and implicit methods. On the other hand, this alternative requires to adapt Surpac™ to a not intended use through a quite elaborated programming.

9.3 Data adaptation to the modeling approach

The veins of Koralpe deposit have two dominant directions which embrace several hundred of meters: strike and along dip. On the contrary, the third dimension, denominated thickness, comprises a range of few meters or less and, therefore, few data describe its variation. From a mining perspective, due to the given dimensions, a selective extraction is very unlikely, i.e. it can be assumed that when an area of a vein is mined, the full vein width will be mined. Thus, changes in along the dominant longer dimensions are much more relevant compared to changes from hangingwall to footwall. According to that, the average grade along the thickness on a certain position is probably the decisive figure for the decision whether an area should be mined. Consequently, a two-dimensional modeling perspective of the veins could present particular advantages. This method would then requires a transformation of the available sampling data from 2D to 3D and consider this conversion for the results interpretation.

9.3.1 2D transformation proposal

The reduction of 3D problems to 2D is a frequent approach in modeling because complexity is significantly decreased and it also presents advantages in topological features handling, see section 4.1.1. However, this method requires the further step of the transformation of the 2D model into 3D space, usually termed mapping. This may be a quite complicated process. Complexity of this step often determines whether a 2D approach plus mapping is preferable against a full 3D approach. The particular case of a vein mapping is relatively simple, because the topology of the vein resembles already very much to a (2D) plane.

The 2D transformation concept is sketched in Figure 70. First step is an abstraction of the 3D shape of the vein to a surface due to only 2D objects can be transferred

to a 2D plane. A surface may be deducted from reducing the hangingwall and footwall into a centerline. Thus, any location of the vein is represented by a point on this surface. The abstracted points can hold any values or descriptions required for vein representation and modelling result interpretation. These point representations are then projected on the projection plane and become in this way truly 2D (x_p/y_p coordinate instead of x/y/z).

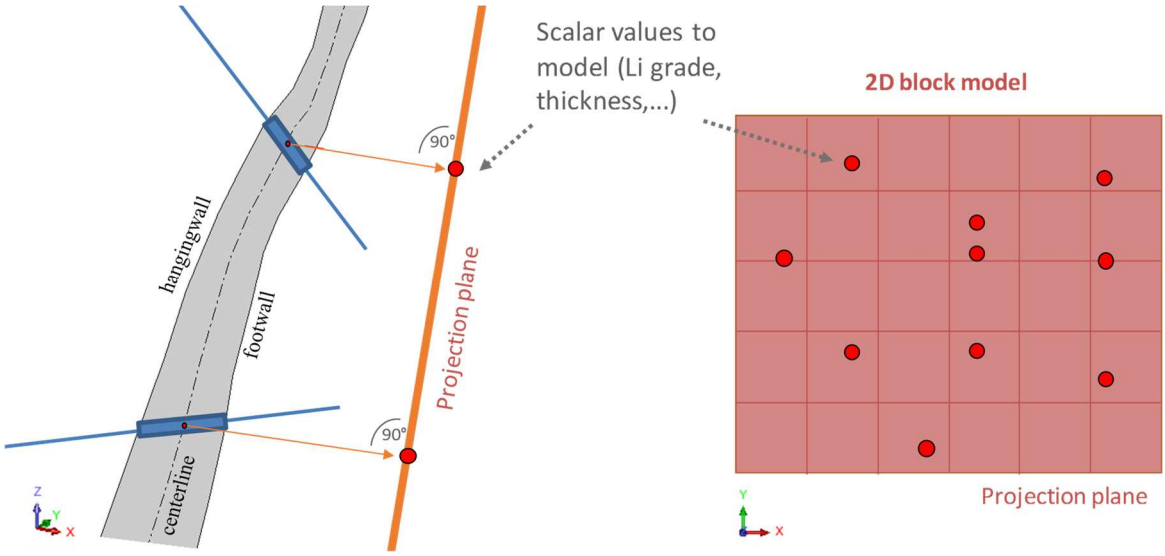

Figure 70: Concept of 2D representation

Vector parameters, such as the orientation of a fault, might be effected by this projection and possibly have to be adjusted. Scalar values such as grade are invariant to projection. As a consequence of the 2D transformation, volumes, which need three spatial dimensions, do not exist in the modeling space. The parameter thickness represents the volumetric aspect of the vein, it is a scalar value though.

The distance of the original 3D points from the projection plane can be handled as any other parameter recorded in the point description. Although it is not a vein characteristic as such, it is needed for back calculations to 3D. For new points generated in 2D during modeling, by means of, for instance, cell grid, the distance has to be estimated as well for the back-transformation of the model.

In this planar approach, every point has a singular input value or estimation for all parameters: at one position, there is one single value of thickness, one value of grade, etc. These values describe the deposit through its whole thickness at each model location.

9.3.2 Thickness

The modeling of the vein thickness is relevant to volume calculation and to evaluate the minimum accepted stope width or expected dilution. However, the definition of thickness of a layer is not clear when boundaries are not parallel. In case of deviation from parallelism, subjective aspects get involved (Figure 71b).

Generally, Koralpe veins may be associated to the type shown in Figure 71a, but other scenarios may occur. Examples such as Figure 71c, d, and e shown the occurrence of interbedding in veins. In these cases, the difference between the pegmatite and the vein thickness is the interbedding space.

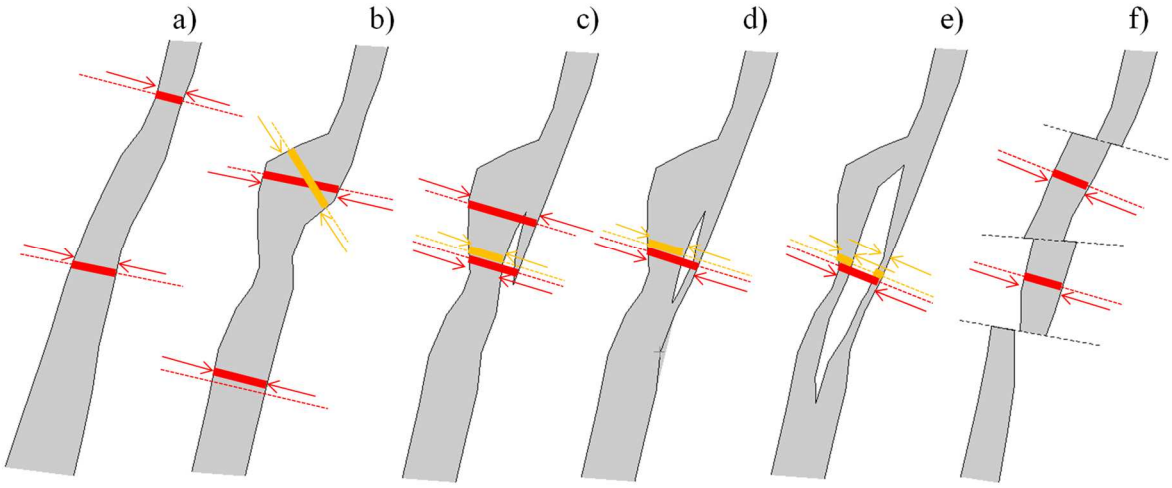

Figure 71: Interpretative aspects of vein thickness

Besides, in cases where veins are very close to each other, the differentiation between interbedding and actual space between veins is problematic. Due to vein assignment is a subject of interpretation, which may vary during the exploration works, a high level of automation is desirable.

As mentioned before, the needed block size of a model able to describe the effect of interbedding in the veins were so small (0,25-0,5 m), that the huge number of blocks required could be completely beyond computer limitations. A more handily alternative is to contemplate the vein thickness and employ the interbedding as a dilution factor of the grade.

9.3.3 Lithium grade

Lithium grade is one of the main characteristics to model. It is a scalar attribute. In a 2D model, grade has to be considered as an average value for the whole vein thickness, including the dilution due to interbedding if there is any, or referring only to the pegmatite extension. In the second case, it is needed to add a parameter representing the ratio of interbedding, so that the total grade can be calculated (see Figure 72).

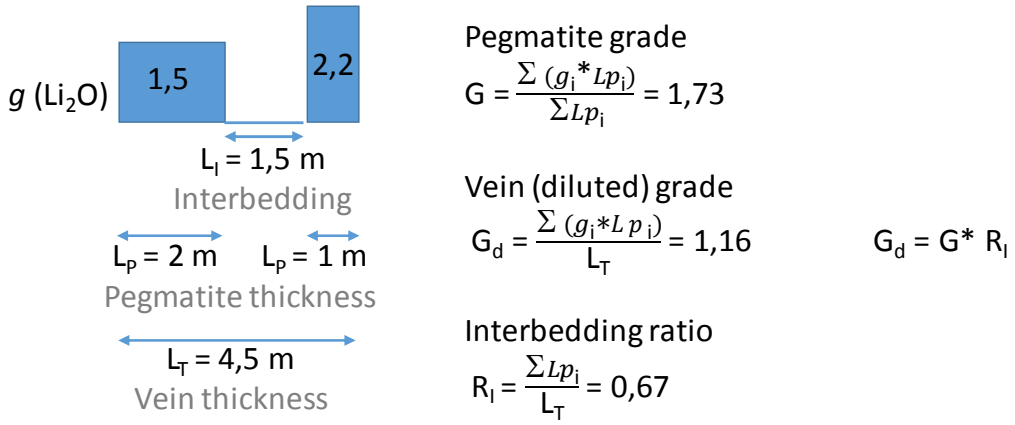

Figure 72: Example of lithium grade calculation.

From a practical point of view, the overall diluted grade is considered of prime importance. Interbedding ratio can be helpful in addition for considering of processing aspects, in particular presorting to handle internal dilution or selective drilling and blasting.

It is important to note that the sample data refer to pegmatite grade because the sampling routine excluded interbedding bigger than approximately 10 cm.

9.3.4 Volume interpretation

Regarding the resource calculation, thickness interest lies in its influence on the volume, that together with the grade estimation, will provide a resources calculation.

In vector based modeling, the volume is calculated by the space surrounded by a closed surface. In 2D modeling method where thickness represents the third dimensional extension, the volume is calculated multiplying area by thickness. As it was mentioned above, the definition of thickness is partially subjective and in

essence a vector. Hence, it is very important to define thickness in a way that volume calculation through 2D model is equal to the 3D version.

If the vein has constant thickness and linear shape and the projection plane is parallel to the vein, volume in 3D and 2D is obviously identical, see Figure 73. In case there is a deviation between vein and projection plane (denoted as α in Figure 73), the projected volume V_p is still identical to the true volume V calculated in the 3D space. However, in that case thickness is increased by a factor given by $1/\cos(\alpha)$, due to the performed projection.

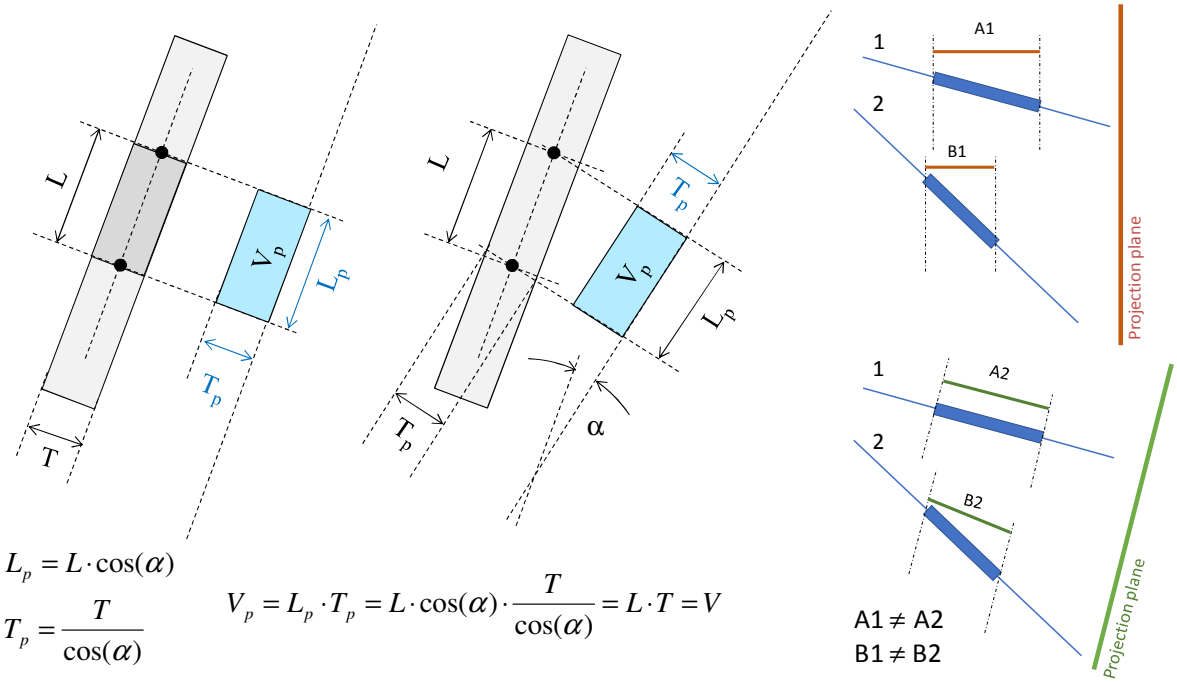

Figure 73: Relation between volume in 3D space and 2D model space and interrelation with project plane orientation.

Therefore, the modeled thickness (T_p) does not exactly correspond to the 3D thickness, which is to some degree subjective anyhow. From an interpretation point of view (e.g. stope width, dilution, etc.), this difference has to be kept in mind. From a practical point of view, the problem of different thickness interpretations is not a major problem due to the differences are very small as long as the local deviation between vein and projection plane is not significant. Figure 74 shows the difference between modeled and true thickness based on the deviation between vein orientation and projection plane orientation, which is essentially a cosine function. Subsequently, if the deviation is less than 20°, the error is very low, not exceeding 6% (which is probably less than the prediction reliability). Even for a deviation of 25°, the error is not more than 10%. It has to be emphasized that this error refers to the interpretation of the consequences of modeled thickness on mining operation,

and not to the volume (which is unique for 2D and 3D models). Therefore, the projection plane should be positioned as close as possible to the orientation of the vein to be modeled.

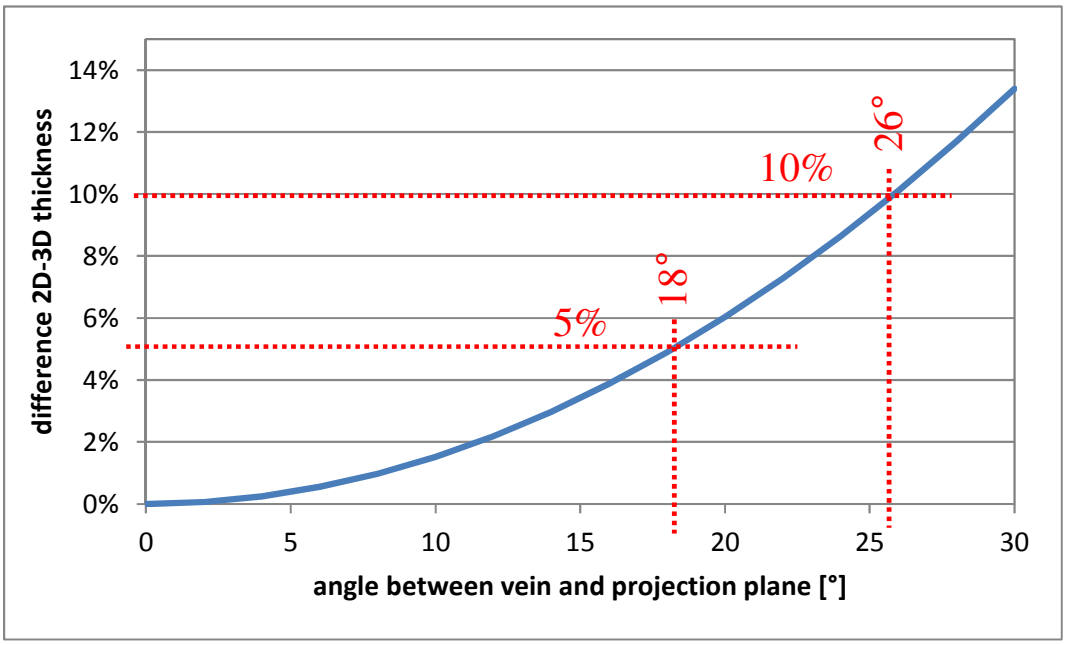

Figure 74:Relation between projected thickness (2D model) and true 3D thickness.

9.3.5 Projection plane for 2D transformation

As it is demonstrated above, the choice of the orientation of the reference plane affects the volume calculation in a minor scale. Nevertheless, the plane location is irrelevant. The setting is done therefore primarily on practical considerations.

Due to according to geological examination the veins are expected to have a similar dip and strike, the projection planes for all veins are arranged in parallel with an orientation which reflects the dominant global orientation and the main geological structure.

The position is set by a single linear position referring to a position vector. The starting point of the position vector is approximately the portal of the existing adit and the direction is essentially parallel to the profiles orientation of Minerex (i.e. perpendicular to the geological strike direction). The principles of the definition are shown in Figure 75.

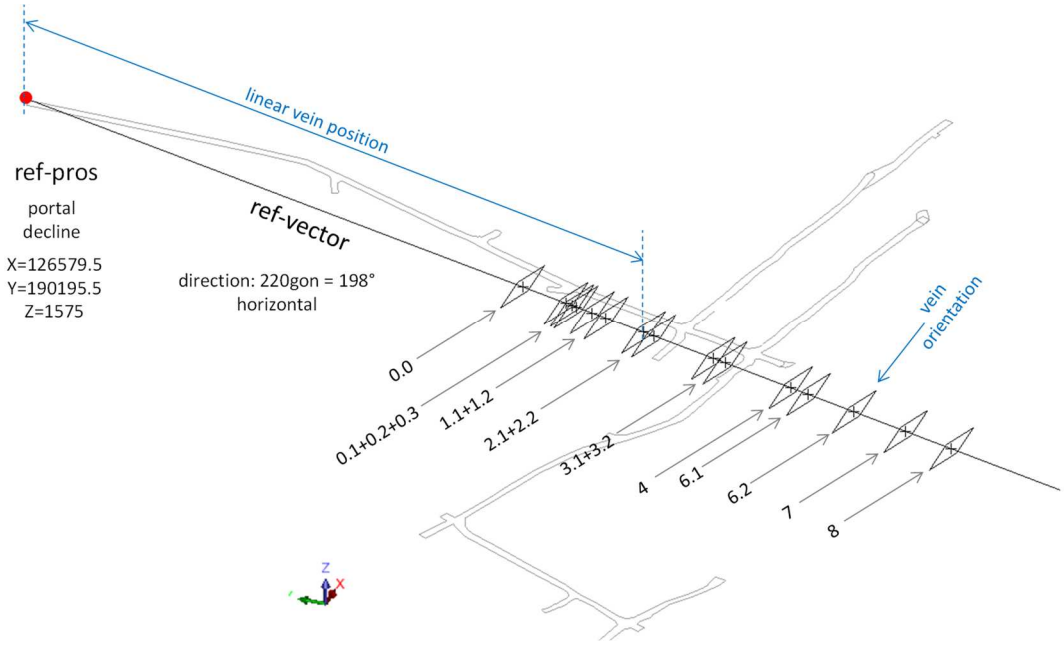

Figure 75: Principle approach of reference plane definition for 2D transformation

9.3.6 Raw thickness data acquisition

For the modeling procedure, a projected thickness onto the defined projection planes has to be generated. The main source of thickness data are the borehole samples. As mentioned in the section 6.1, sample length is only an apparent thickness as it depends on the angle of intersection of the borehole with the vein.

In order to obtain a projected thickness data, the actual thickness of the veins cannot be retrieved from an individual sample geometry because the actual orientation of the vein is unknown at this stage of the investigations. Therefore, the estimation of the orientation of the vein cannot be determined on an individual sample by sample basis, it has to consider the adjacent sample geometry as well.

Thus, the boundaries of the veins are firstly estimated as two surfaces built in terms of linear interpolation between the limits of the samples. This estimation fits completely to the samples, as demonstrated at section 4.2.1. Then, the projected thickness for modeling input is measured as the difference between the intersections of a line perpendicular to the projection plane passing through the central position of each sample with the two surfaces interpolated reflecting hanging-wall and foot-wall, see Figure 76. Input projected thickness data will be calculated only at the position of each borehole - vein intersection as the distance

between samples is too big to consider the linear interpolation an acceptable estimation of the thickness for locations in between.

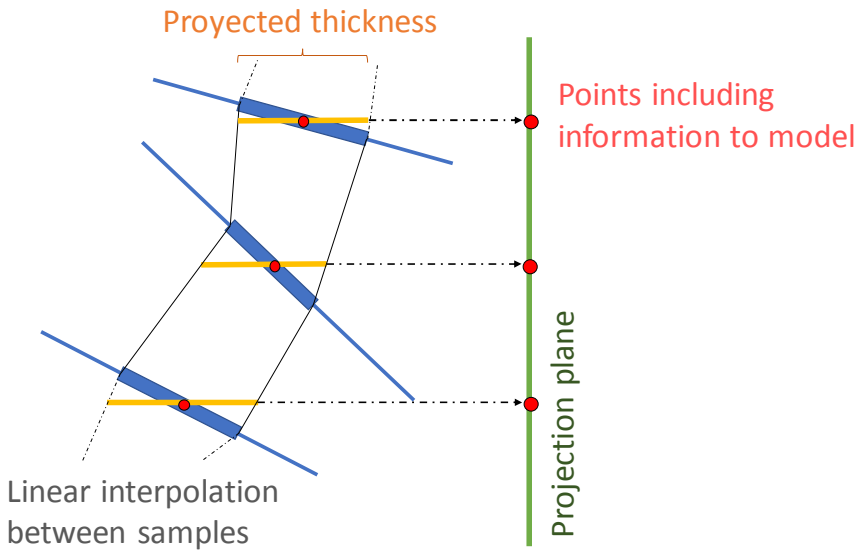

Figure 76.Calculation of projected thickness.

9.3.7 Source of input data for modeling

For modeling input, exclusively drill hole data is used. Data from the exploration drifts are not used directly for the modeling, because they are available only for a restricted area and restricted veins and, therefore, it could contribute to biased computation. Besides, the thickness was not always visible in its whole extend along the drifts, so in some of the cases the measurement applies only to the observable area - the hangingwall or footwall limit disappears beyond the face profile. Nevertheless, findings from the analysis of the spatial behavior of geometry and grade of the veins are used for defining and supporting assumptions applied during modeling.

9.4 Modeling procedure

As described previously, for modeling purposes the veins are considered as planar objects with the attributes grade and thickness to describe the vein characteristics. This is sufficient for fulfilling the resource calculation requirements. For further mine

design investigations, it is possible to include additional features such as interbedding, true position in space or respective deviation from reference plane. These additional characteristics may be applied for 3D shape representation of veins, dip estimation and relative positions between veins.

The procedure of the overall vein modeling process derives from the basic considerations and modeling approach proposed in section 9.3. Besides, the methodology is to some degree also affected by the capabilities of the employed modeling software (Geovia Surpac™). A general overview is given in the following flow sheet and will be discussed briefly in his chapter (see Figure 77).

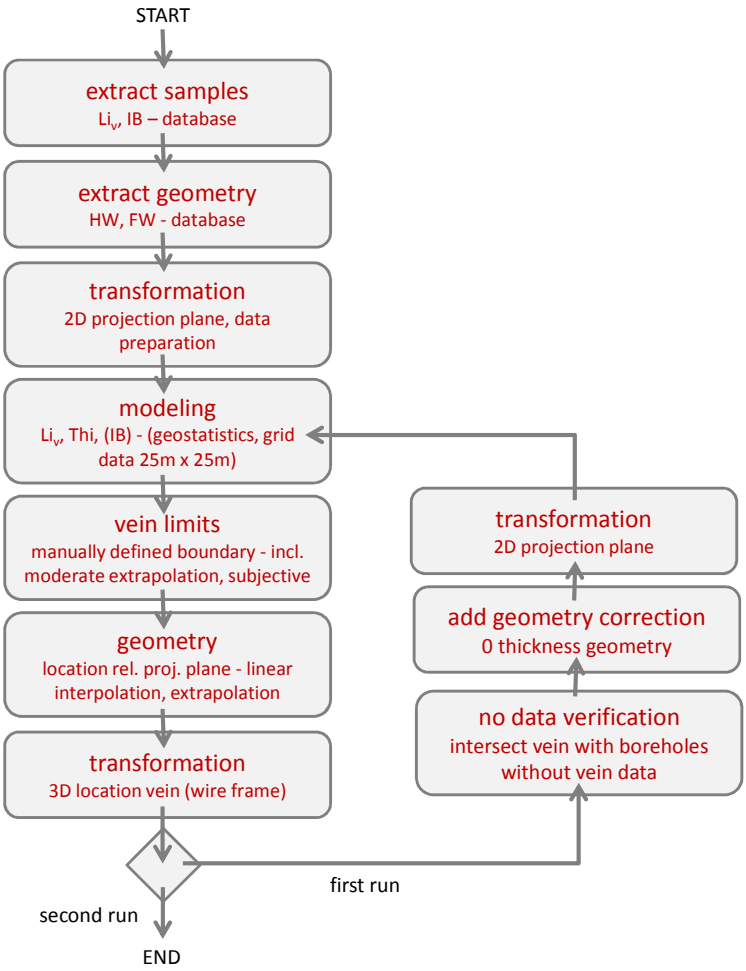

Figure 77: Flowsheet of the modeling procedure.

The flow sheet indicates that a two-cycle approach is applied. Due to the calculation is executed vein by vein, for each vein only the samples assigned to it are used for its modeling. As a consequence, in the first modeling round, interpolation between two assigned samples may happen although there was a borehole intersecting this section without including in it any pegmatite, which would be a case of an invalid

modeling or contradiction. In this case, the fact that a continuous extension of the vein in this area is unlikely and, therefore a gap in the mineralization area of the model should appear. This is represented through thickness zero at this location as a correction factor.

The prominent example from the mentioned situation is the borehole KUK-4. It did not comprise a sample of vein 7, but modeling generated a fraction of this vein which intersected the borehole. In this case, the consequences were not critical, because the twin-hole from EL campaign 2016 (P15-24A) revealed that the pegmatite was absent only due to poor drilling performance of the original Minerex borehole. This example emphasizes also that pure data processing is risky and always should be accompanied by critical human reasoning.

The established procedure is based on the argument provided during the previous investigations. Below, it is given a detailed description of each modeling step.

9.4.1 Extraction of sampling data

Sampling data is extracted from the database in form of string data of Surpac™. Sampling and geometry data are handled separately because they derive possibly from different sources, i.e. sometimes the location of a vein assignment is available without any sampling information (see section 5.2.4).

Currently only data from exploration boreholes are integrated in the database. The database already provides vein grades which include the dilution caused by interbedding factor.

9.4.2 Extraction of geometry information

Geometry data are firstly exported as geometric position of hanging-wall and foot-wall of the veins, that it is to say start and end intersection position of the borehole with each assigned vein of the ore body. In a farther processing phase, these data are converted into singular thickness according to the statements of section 9.3.6. String data is also the vehicle to incorporate this data in Surpac™.

9.4.3 2D transformation

2D transformation is a pretty straight forward process which use general concepts of coordinates transformation. This step also includes some pre-processing of input data, primarily geometric data – from thickness to projected thickness. This is because the thickness perpendicular to the projection plane can only be calculated on basis of selected plane characteristics. The result of this are truly 2D data, distributed in the coordinates *x* and *y* and *z*=0, containing lithium vein grade and projected thickness, relative to the projection plane, as single data point for each borehole-vein intersection (Figure 78). The original location of the data is also stored in mentioned points for back calculation.

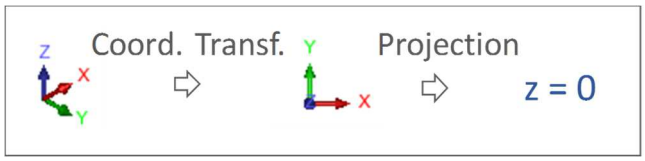

Figure 78: 2D coordinates transformation.

9.4.4 Modeling

Modeling of grade and thickness is executed using the typical mechanisms. In respect of easier handling a block model is used. The model is constituted by a compilation of blocks covering projection plane in the dimensions *x*/*y* and a single block in the *z* dimension covering 1 m of extension. This allows to use the standard evaluation and reporting tools because block volume is then nominal block volume multiplied by thickness. Vein volume or subsets of it are calculated by summing up these result volumes.

Lithium grade and thickness are modeled using geostatics, namely ordinary kriging, described at section 4.2.3. The parameters used are compiled in Table 20. The parameters of the employed variogram model are based on the assessment of variability developed in the section 8. The search radius for data selection was selected in accordance with the range of the variograms from a conservative perspective. Due to the limited number of samples, the minimum number of samples in the search radius for modeling a block is set one. The maximum is set as 15 although because the widespread exploration pattern is rarely reached. The dimensions of the block model make useless establishing an anisotropy in the z

dimension. Likewise, no relevant arguments have been found to consider anisotropy in the *x*/*y* dimension.

The importance of the block size selection to represent the grade/tonnage properly must be noted. The larger the block, the less variable or the sharper the distribution of the property to estimate due to high-grade blocks are overestimated and low-grade blocks are underestimated. On the other hand, if blocks are too small, there is an over smooth distribution of the estimated properties and, thus, very low precision. Over smoothing leads to an underestimation of high-grade blocks and an overestimation of low-grade blocks. Ideally, the block size is also related to the mining equipment planned regarding selectivity issues. In the same way, the sampling grid should be considered too. Due to the high variability on small scale and the large spacing between boreholes, blocks of 25 by 25 m in the *x*/*y* dimension are selected. Besides, this size it may be also reasonable for mining stopes in an applicable method for Koralpe deposit, as long hole open stoping. As it is a 2D modeling, the z dimension is irrelevant – 1 m is chosen for practical reasons.

	Li2O	Thickness
variogram		
nugget c0	0,087	0,2
sill structure 1	0,152	0,85
range structure 1	61,3	140
sill structure 2	0,16	-
range structure 2	250	-
data selection		
search radius	100	100
minimum sample	1	1
maximum sample	15	15
anisotropy		
anisotropy	none	none
grid		
blocksize	25 x 25	25 x 25

Table 20: Modeling parameters for lithium and thickness.

9.4.5 Vein limits

In a first step modeling includes both interpolation and extrapolation, depending on the search radius defined for the modeling. As extrapolation should be limited to a reasonable extent (significantly less than interpolation range), this limitation is done

by a manually and subjectively defined boundary. The boundary is saved and can be used or modified for subsequent runs.

9.4.6 Geometry

The results of previous steps are basically sufficient for the resource calculation. However, for visualization purposes and much more important for the checking of results against invalid interpolations; a representation of the vein in 3D is required.

This is done through several steps (Figure 79). Frist, a surface is created by linear interpolation between the center points of the sampling boreholes. Extrapolation is necessary to obtain a geometric position also for the extrapolated grade/thickness values. It should be considered that methods of linear extrapolation of a general surface are equivocal. Due to the precise location in 3D space is currently not a prime requirement, a very simple algorithm is used for this task. Secondly, at the centroid of each block of the model, results are abstracted to a point containing the modeling results. Each of those points are projected to the surface connecting the central position of the veins. Finally, the half of the estimated thickness at each point/block is applied perpendicularly to the projection plane to each face of the triangulated surface between the central positions of samples. These new points define two wiremesh surfaces representing hanging-wall and foot-wall, which can be reversely relocated to 3D original location.

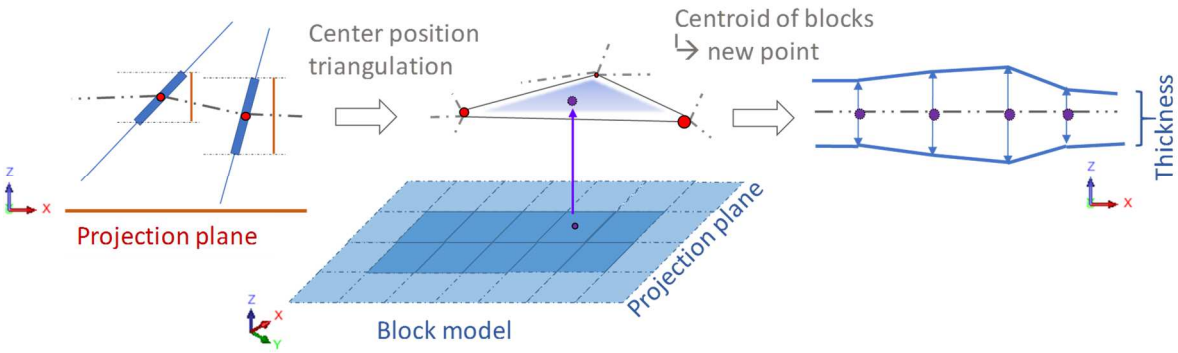

Figure 79. Representation of geometry results.

Therefore, the vertices of the two triangulated surfaces correspond to the centroid of each block of the model and are distanced the value of the thickness at each centroid. These vertices will also keep the value of the estimations of each block, such as lithium grade for instance.

The limits of these surfaces will be connected forming Surpac™ solids[4] which involving a close space, independent from other veins. This has advantages for visualization and data handling.

By the use of a linear interpolation between the central position of the samples as basis for the representation of the thickness, it is achieved a more loyal model to the actual samples than applying geo-statistic, see section 4. However, it must be kept in mind that the resulting solid may not precisely fit to the samples position of the boreholes. This is due to the estimations are calculated through geostatistic / block model. The calculation of the estimations of each block are influenced by all the samples included in the selected search ratio independently of whether the block position includes a sample of known characteristics or not. This is an inherent feature due to a block represents a piece of space, not an individual item, and therefore the estimated value is the mean of the modeled parameter to all the represented volume inside that block.

9.4.7 3D transformation

The result from the previous step is already in 3D but the created wiremesh is still oriented according to the projection plane. A back transformation to the original 3D location is then required (Figure 80).

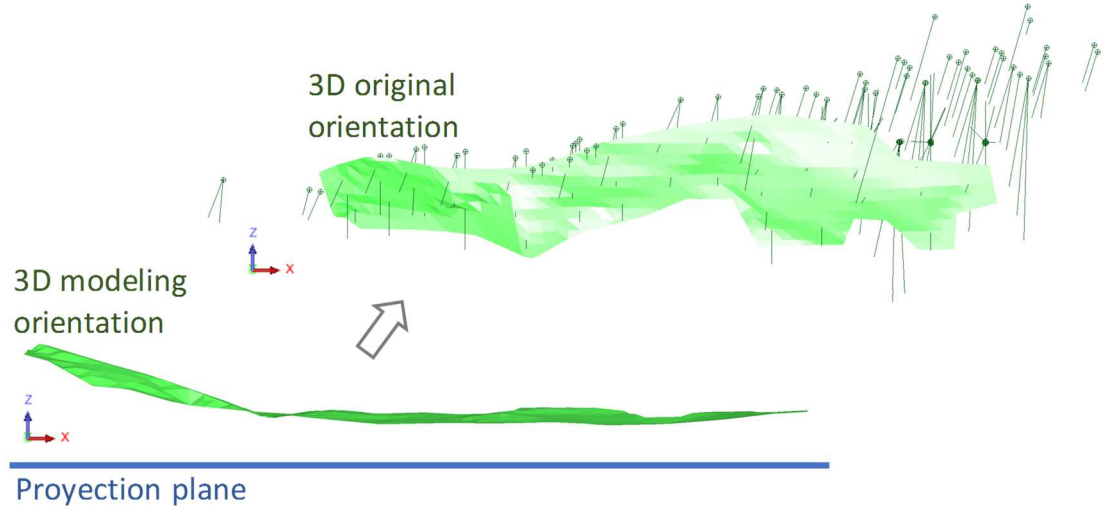

Figure 80: Transformation of the results back to 3D original location.

[4]Surpac uses the term solid to denominate a set of surfaces which envelope a close space. It does not refer to an implicit solid.

9.4.8 No data verification

For checking the wiremesh, the surface is intersected with all boreholes which do not contain an assignment of the particular vein and hence could be source of potential contradictions. If intersections with these boreholes occur, then they have to be inspected manually.

9.4.9 Add geometry correction

Allowances for these cases can be various. Ideally, a not yet assigned pegmatite (sampled or merely geologically documented) can be identified in the database and introduced as additional information. In other cases, a dummy-sample with a thickness of zero has to be introduced to take account for this situation. Alternatively, a void area, by an additional boundary, could be defined. In some cases, the problem also can be ignored if there are good reasons to do so. Typically, this can be done if the problem appears very close to the end of the borehole (i.e. it very well could be that it missed the vein), or if there are indications that borehole data are not absolutely reliable (e.g. poor documentation, indications of drilling problems, significant core loss, etc.). The described situation with borehole KUK-4 might illustrate the required interpretation work.

9.4.10 Second 2D transformation

The generated new data for modification of the model are now integrated into the dataset. The modeling process is then repeated (Figure 81). In order to do that, new data have also to be transformed previously to 2D. Both the modifications as well as the considerations for the applied or ignored modifications are documented. The result is a continuous and close wiremesh which include in each vertex of it surface the estimations for grade and thickness. Where thickness equal to zero is required, the value zero is store at the points required position, but the wiremesh will not have a gap because of Surpac™ limitations in representations of solids with holes. Instead, both hanging-wall and foot-wall surfaces will occupy the same position representing a zero thickness.

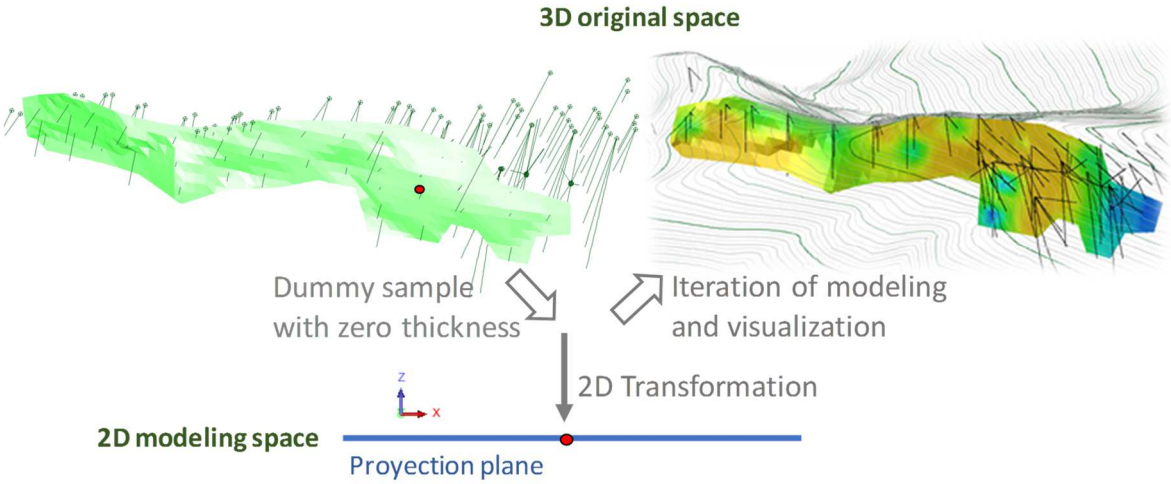

Figure 81. Validation in 3D of modeling results.

9.5 Modeling results

The results on a vein-by-vein basis are compiled in Table 21. The density used for tonnage calculation was determined by the lab analysis performed during the campaign of 2016 as 2,72 t/m^3. In addition to the stratigraphic order, the veins are also sorted by Li_2O content (tonnage*grade), with the respective characteristics in cumulative figures. This gives a better insight into the importance of the individual veins and their contribution to total deposit.

individual vein results							cumulative results sorted by Li-content				
vein	tonnage	Li2O	thickn.	ranking			vein	tonnage	contrib.	Li2O	thickn.
	t	%	m	ton.	Li-cont			t	%	%	m
0.0	116.000	0,91	0,76	11	11		7	1.777.200	27,1%	1,13	2,45
0.1	118.300	1,08	0,92	10	10		3.1	2.498.100	15,8%	1,27	2,06
0.2	56.100	1,53	0,79	15	13		2.1	3.117.900	12,7%	1,32	1,89
0.3	103.700	0,84	0,66	12	12		6.2	3.925.600	11,9%	1,27	1,76
1.1	451.200	1,13	1,18	6	5		1.1	4.376.800	6,9%	1,25	1,68
1.2	635.800	0,72	1,82	4	6		1.2	5.012.600	6,2%	1,19	1,69
2.1	619.800	1,51	1,43	5	3		3.2	5.286.700	4,8%	1,19	1,59
2.2	253.500	1,32	0,98	8	8		2.2	5.540.200	4,5%	1,20	1,55
3.1	720.900	1,62	1,48	3	2		4	5.740.000	3,1%	1,20	1,50
3.2	274.100	1,30	0,77	7	7		0.1	5.858.300	1,7%	1,19	1,48
4	199.800	1,15	0,79	9	9		0.0	5.974.300	1,4%	1,19	1,45
6.1	88.500	0,69	0,95	13	14		0.3	6.078.000	1,2%	1,18	1,42
6.2	807.700	1,08	1,39	2	4		0.2	6.134.100	1,2%	1,19	1,41
7	1.777.200	1,13	2,45	1	1		6.1	6.222.600	0,8%	1,18	1,40
8	80.800	0,60	1,32	14	15		8	6.303.400	0,7%	1,17	1,40

Table 21: Summary of modeling results vein-by-vein and cumulative.

The total tonnage is categorized in classes for both thickness and grade. This is a first step to consider mining aspects, i.e. calculation of reserves. It has to be emphasized that the class thresholds are based on rough assumptions of mining relevant scales and do not incorporate any economical evaluations. Similar to previous results, figures in Table 22 show that a rather high ratio of the deposit is related to situations preferable for mining operations.

incremental							
ratio(vol)	avg.thick	**thickness**					
10^3 tons	avg.grade	<1m		1-1.5m		>1.5m	
garde	< 0.75%	3,3%	0,69m	3,2%	1,23m	6,1%	2,42m
		209	0,57%Li	**203**	0,61%Li	**386**	0,48%Li
	0.75-1%	4,7%	0,71m	4,2%	1,22m	6,8%	2,22m
		293	0,89%Li	**266**	0,89%Li	**430**	0,92%Li
	> 1%	14,5%	0,75m	11,6%	1,22m	45,4%	2,36m
		915	1,37%Li	**730**	1,41%Li	**2858**	2,36%Li
cumulative							
ratio(vol)	avg.thick	**thickness**					
10^3 tons	avg.grade	all		>1m		>1.5m	
garde	all	100,0%	1,32m	77,5%	1,92m	58,4%	2,35m
		6.291	1,17%Li	**4.874**	1,18%Li	**3.674**	1,18%Li
	>0.75%	87,3%	1,33m	68,1%	1,93m	52,3%	2,34m
		5.492	1,26%Li	**4.285**	1,27%Li	**3.288**	1,27%Li
	>1%	71,6%	1,49m	57,0%	1,98m	45,4%	2,34m
		4.503	1,34%Li	**3.588**	1,34%Li	**2.858**	1,32%Li

Table 22: Characteristics of classes using thickness and grade cut-offs in combination.

Figure 82 shows the modeling results of the lithium grade estimation in the largest vein in extension and volume, the vein 7, mica schist hosted.

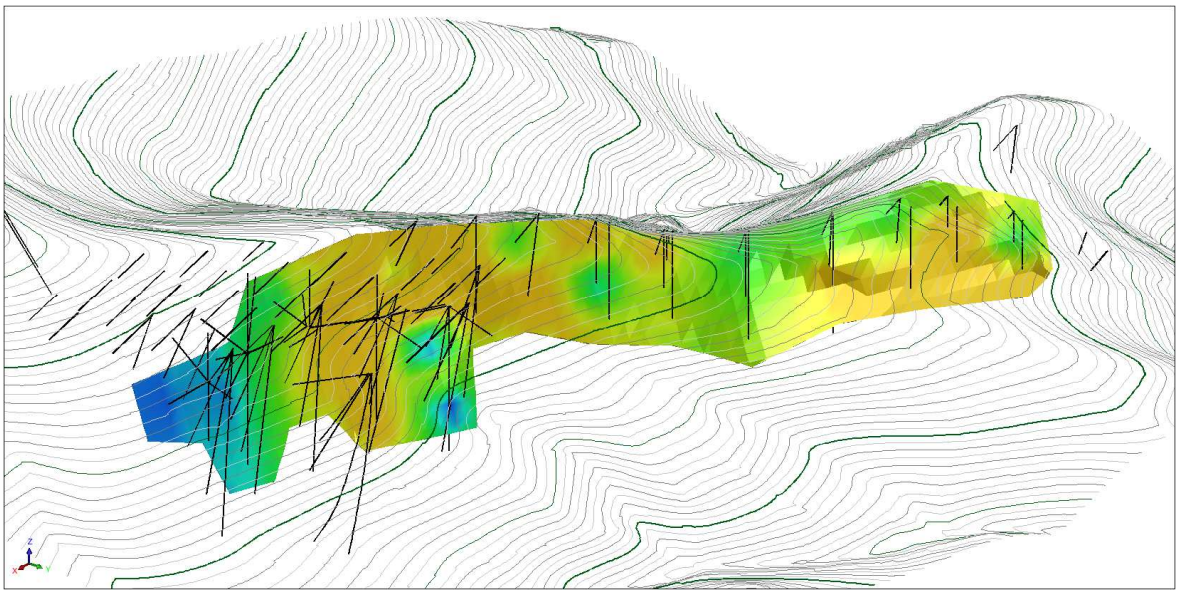

Figure 82: Example of 3D modeling result of vein 7 including boreholes visualization.

The resource calculation is based on the statement of the geologist competent person, A.J. Maynard, mentioned below:

> *[…] the resources in the veins immediately above and below the underground workings to the extent of the underground drilling could probably expected to be in the Measured category, the veins intersected by at least three drill holes no further than 50 m apart on the main cross sections to be indicated and to the extent of the remainder of the drilling along strike and at depth not included in the Measured and Indicated resource estimates to be Inferred.* (Al Maynard & Associates Pty Ltd 2014, p. 39)

Accordingly, the resources were discriminated by two main criteria: location within underground workings (where the spacing of profiles based on boreholes was 50 m), and distinction between interpolation and extrapolation, as shown in Figure 83. Measured resources are those resources calculated by interpolation in the area where profiles spacing was 50 m - excluding extrapolation. The resources in this area calculated by extrapolation were considered indicated resources, as well as all the calculated resources in the area where the profile spacing is wider – including interpolation and extrapolation. This classification is supported by the extensive degree of documentation performed by Minerex.

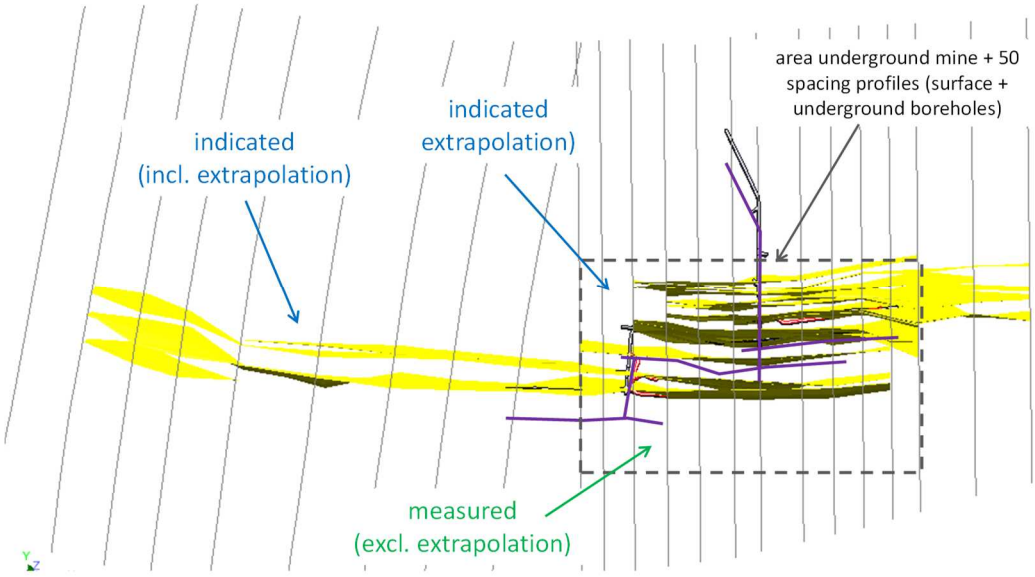

Figure 83: Illustration of the criteria used for resource categorization.

Results of measured and indicated resources are shown in Table 23 by stratigraphic order. The total of measured resources is 2.861.800 tons with an average Li_2O grade of 1,28 % and average thickness of 1,31 m. Regarding indicated results, the total tonnage is 3.444.500 and average grade and thickness are 1,08 % and 1,49 m respectively.

vein	measured resources			indicated resources		
	tonnage	Li2O	thick	tonnage	Li2O	thick
0.0	51.800	0,85	0,80	64.200	0,96	0,73
0.1	34.400	1,03	0,96	83.900	1,10	0,90
0.2	27.000	1,57	0,88	29.200	1,49	0,72
0.3	41.800	1,01	0,68	61.900	0,73	0,65
1.1	298.900	1,23	1,29	152.400	0,93	1,01
1.2	361.400	0,63	1,79	274.400	0,83	1,86
2.1	442.500	1,61	1,58	177.300	1,25	1,16
2.2	156.100	1,30	0,97	97.400	1,35	1,01
3.1	628.300	1,63	1,53	92.600	1,52	1,21
3.2	118.800	1,31	0,74	155.300	1,29	0,79
4	110.200	1,21	0,83	89.600	1,07	0,74
6.1	6.700	0,90	0,66	81.700	0,67	0,98
6.2	276.200	1,17	1,22	531.500	1,04	1,50
7	307.800	1,12	1,79	1.469.400	1,13	2,65
8	0			80.800	0,60	1,32
total	2.861.800	1,28	1,31	3.441.500	1,08	1,49

Table 23: Resources by vein and category (measured, indicated).

9.6 Reliability of modeling results

In this chapter, an interpretation of the modeling results and their reliability is performed. Deposit regularity is regarded a very important aspect for mining operation. In this respect, the inherent smoothing effect of modeling must be considered.

Firstly, blocks represent an extension – 25 m x 25 m in this case – at which is attributed a common estimation, but, in the actual deposit, includes a local variability. This variability is an output of the block model in terms of variance.

Secondly, the geostatistical estimation approach makes smoothing effect inevitable due to it is basically a weighted average method. Averaging mechanisms always leads to some smoothing, see 4.2.3. Geostatistics is unbiased for the mean, but not unbiased for the distribution (spread of population), see Figure 84. As a result, figures around the mean of the population are overestimated and extremes are underestimated. The magnitude of this effect is again driven by the shape of the variogram and spatial sample distribution. It is as well reflected in the estimation error or kriging variance, which is a result so essential as the estimate of the expected mean. As it has been discussed in detail in chapter 8, the variograms of lithium and thickness are not ideal for accurate modeling (high nugget, steep increase at small distances). Consequently, the reliability of the predicted figures for one single block is very low (see detailed information at section 9.6.2).

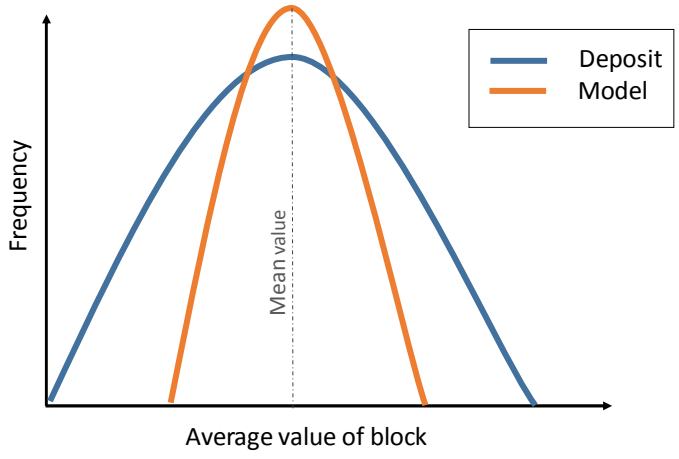

Figure 84: Representation of the averaging effect of geostatistics in the distribution of the estimated parameters.

As far as only the mean is of relevance, this effect can be ignored. However, if the estimated parameters are categorized in classes (such as that cut-offs are applied), it is advisable to consider to this effect. For this reason, it is employed the modeling

method so-called indicator kriging (see description in section 4.2.3) applied to particular thresholds (only with exemplary purposes because cutoffs are not known yet).

9.6.1 Indicator kriging

As discussed above, the estimated block values of the model concentrate around the mean, whilst more extreme values (both on the lower and higher tail) will rarely appear. On a global basis, such as resource estimation, this will be of minor relevance. However, for aspects related to mine design, this can take importance. Thus, the modeling method indicator kriging (see section 4.2.3) is applied for several classes or possible cutoffs.

Figure 85 shown the histograms and cumulative curve for the results of Li_2O grade estimations according to ordinary (blue figures) and indicator kriging (orange figures). As expected, it shows clearly that standard calculation, ordinary kriging, overestimates ratios around the mean lithium grade and does not reflects distribution at the tails. This means that there are portions in the deposit with rather low grade which seem to be not existing by standard modeling. In volumetric terms, these low-grade portions are however compensated by some high-grade areas. Cumulative curve of ordinary kriging is therefore steeper for central values and almost horizontal in the tails.

Due to the limitations inherent to mining methods, it may happen that the extraction of a high grade/thickness areas involves as well extraction of low grade/thickness sections. This is basically a question of mine design. Therefore, the interpretation of a cutoff-ratio curve (or cutoff tonnage curve) must be done carefully.

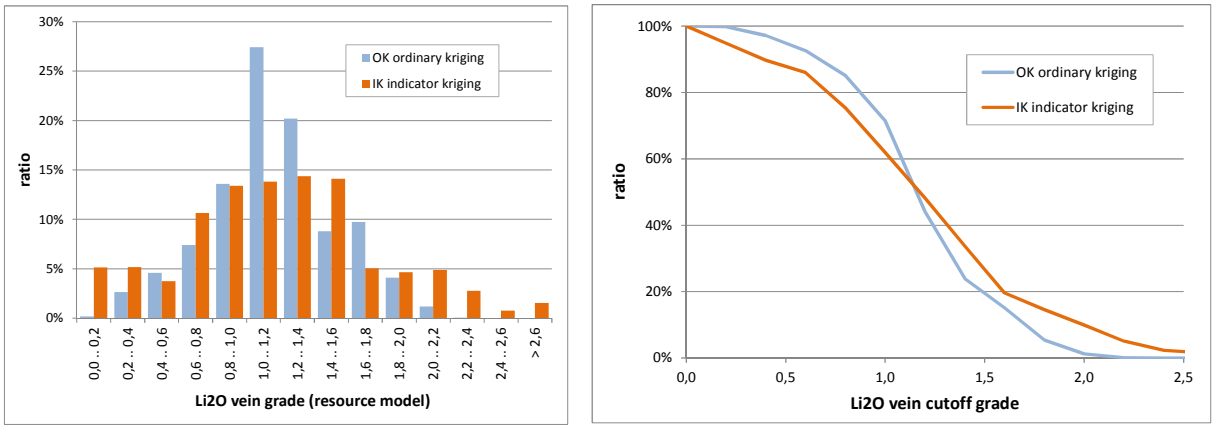

Figure 85: Lithium distribution by ordinary and indicator kriging.

The results considering vein thickness (Figure 86) show a similar situation. As described previously only pegmatite intersection with a length greater than 0,5 were sampled and, therefore, used as basis for the modeling. Due to the fact that true thickness can be smaller than the apparent thickness from sampling and also because occasionally additional auxiliary data were introduced to reflect a thinning out area of a vein – no data verification -, estimation results below 0,5 m can occur theoretically. In alignment with the underlying idea of the 0,5 m sample limit, these blocks have been excluded from the resource classification. Hence the standard model (blue bar/line in Figure 86) gives a 0% ratio for thicknesses below 0,5 m. The indicator model, however, returns even for this low-thickness class a notable ratio. This can be interpreted such that in areas with an average thickness above 0,5 m still fractions with lower thicknesses must be expected. Similar to the statement made for the grade the consequences from this is a question related with the mine design.

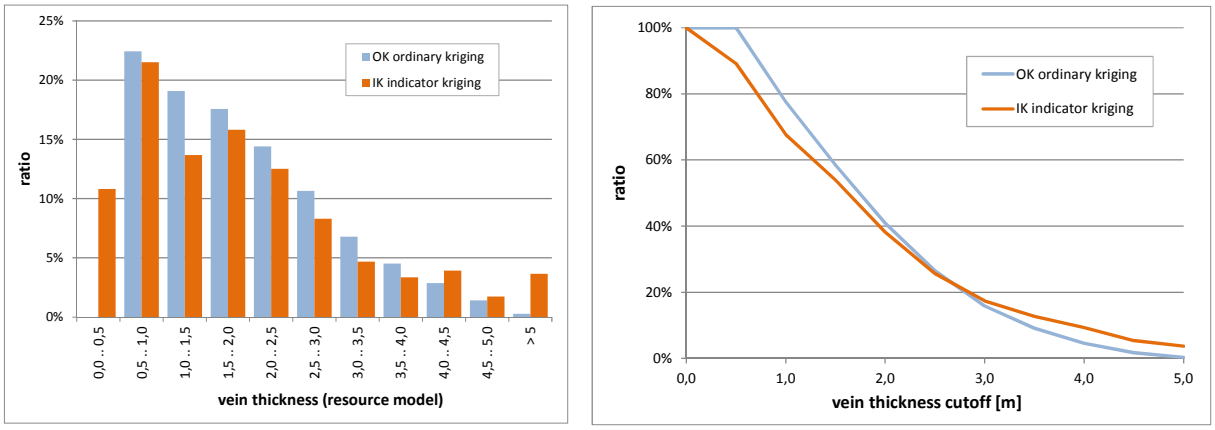

Figure 86: Thickness distribution by ordinary and indicator kriging.

9.6.2 Local reliability

Individual reliability is supported by the statistical analysis of the block estimation error. For an overview this analysis covers all blocks of all veins. This calculation was executed both for Li_2O grade and thickness. The results of the estimated error expressed as standard deviation (square root of kriging variance) are shown in Figure 87. Standard deviation allows to calculate confidence intervals, namely the 95 % reliability confidence interval can be estimated by two times either side of the estimated mean.

For the lithium grades with frequencies higher than 6 % there is already a standard deviation larger than 0,275. If it is considered the range of the Li_2O grade mean

(from 0,6, to vein 8, to 1,62, to vein 3.1, see Table 21), this makes in comparison interval confidences very wide, even taking only one time the standard deviation either side of the estimated mean (from 0,325-0,875 to 1,345-1,895), where the intervals would represent between 34% and 91% of the mean value. Similar it is the situation for the estimation of thickness - frequencies higher than 8 % have a standard deviation larger than 0,7 - where intervals based on plus/minus one standard deviation represent between 57 % and 212 % of the mean value (ranges from 0,66, to vein 0.3, to 2,45, to vein 7, see Table 21). This accentuates that local predictions have to be interpreted with caution.

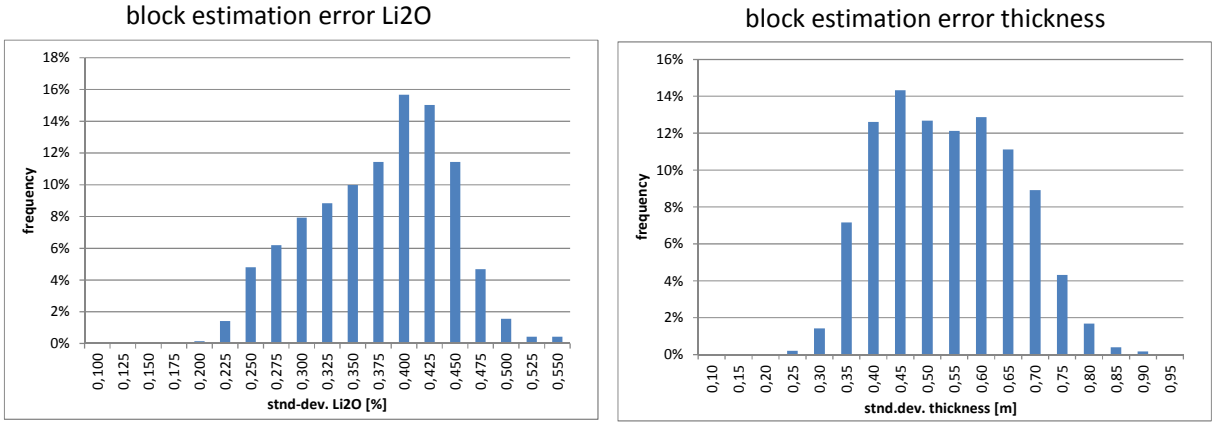

Figure 87: Global statistics of block estimation error for lithium and thickness.

This refers exclusively to local estimates. On a more regional or global aspect the reliability is much higher due to the existence of samples and veins in the analysis area is ensured. Besides and more important, local estimation errors are compensated in large scale (underestimation in one location is balanced with overestimation somewhere else).

For this reason, below it is checked the reliability for global or regional areas (e.g. per vein). This done by analyzing many potentially possible realizations of the model through the method usually called conditional simulation or Monte Carlo method.

9.6.3 Global reliability

In order to assess the global consistency of the modeling results in spite of the difficulties for the local prediction, it is applied the Monte Carlo simulation.

This is an iterative technique which use random numbers to evaluate a deterministic model. After a large number of iterations, the set of obtained results allows to

describe the likelihood of results in the model. It is used to compare the observed data with random number samples generated in accordance with the hypothesis being tested – in this case, the mean and standard deviation of each block.

The use of random tests has become very popular in the era of the high-speed computers. However, an excessive number of random samples may make these methods unnecessary complicated. Monte Carlo procedures similarly but using a smaller size of reference set. Mentioned size depends on the significance level chosen for testing and the procedure adopted for judging significance. (Hope, 1968)

This method strongly depends on the fast production of streams of random numbers. In general, the random number sequences needed for simulation purposes should be uniform, uncorrelated, and with an extremely long period, i.e. do not repeat over long intervals. Generation of random numbers is a problematic which has not been fully solved. The use of tables of random numbers is very impractical because of the big amount needed. Due to the fact that random generation through computers depends on algorithms which are actually deterministic, the produced numbers are only “pseudo-random”. Studies have pointed out that no generator can be consider completely safe for simulation purposes. Therefore, the quality of the random generator must be tested. (Landau et al., 2009, p. 34)

In order to Monte Carlo simulation application to check the global or regional reliability of modeling results, it has been created a normal distribution to each block according to the provided parameters, namely estimated mean and standard deviation (square root of block variance). This has been done for the attributes thickness and lithium grade. Then, it has been carried out one hundred iterations generating a random number per each block from its allocated distribution. The only limitation applied to the random generation has been excluding negative values because of their lack of meaning as thickness and lithium grade. From the output of each iteration, it has been calculated a simulated tonnage per block. Afterwards, a mean value and standard deviation of the set of one hundred simulated tonnages has been calculated to each vein separately and to the whole deposit.

The results are shown in Table 24 regionally by vein by vein and globally considering the deposit as a whole unit in terms of tonnage obtained from the volume calculated with the simulated grade thickness. Notice that the reliability of the simulation is based on the variogram parameters and does not include potential hidden errors such as erroneous vein assignment, major fault structures, etc.

vein	Stnd. estimate		conditional simulation			95% conf. interval	
			mean	stdev	rel.stdev	low	high
7	1.777.200		1.779.900	24.460	1,4%	1.728.300	1.826.100
6.2	807.700		821.600	21.050	2,6%	765.600	849.800
3.1	720.900		724.200	17.550	2,4%	685.800	756.000
1.2	635.800		638.200	10.950	1,7%	613.900	657.700
2.1	619.800		613.700	13.210	2,1%	593.400	646.200
1.1	451.200		455.600	12.430	2,8%	426.300	476.100
3.2	274.100		286.800	12.880	4,7%	248.300	299.900
2.2	253.500		256.900	11.910	4,7%	229.700	277.300
4	199.800		203.400	11.680	5,8%	176.400	223.200
0.1	118.300		122.000	8.830	7,5%	100.600	136.000
0.0	116.000		120.500	8.330	7,2%	99.300	132.700
0.3	103.700		108.400	7.590	7,3%	88.500	118.900
6.1	88.500		91.000	6.570	7,4%	75.400	101.600
8	80.800		80.700	6.060	7,5%	68.700	92.900
0.2	56.100		58.100	5.380	9,6%	45.300	66.900
Total	6.303.300		6.357.900	49.870	0,8%	6.203.600	6.403.000

Table 24: Reliability analysis on a global and vein-by-vein basis.

Logically, the vein-by-vein perspective reveals lower reliability than the global calculation although it is still in a very acceptable level. This is in particular correct for the largest veins which have a significant tonnage. For theses (vein 7, 6.2, 3.1, 1.2, 2.1, accounting for more than 2/3 of total resource) the relative standard deviation is not more than 2,6 % of the estimated mean. For smaller veins, the relative standard deviation is higher because less chance to compensate (and possible adverse sample situation).

As expected, the reliability of the model in global terms is very high, with a 0,8 % of standard deviation relative to estimated mean. According to this, the total resource varies by ±100.000 tons with a 95 % of confidence interval.

The global reliability check is also applied to the investigation on grade and thickness classes (cutoffs). The results of the deterministic analysis are shown in Table 22, which is exclusively based on the estimation mean. The stochastic approach provides slightly different results. The essential figures are compiled in Table 25. For a better overview and comparison, the results from the deterministic approach (considering only estimate mean) are included as well in black font. Mean and standard deviation of the conditional simulation are identified by blue color. The green data are the high and low limits of the confidence interval with 95 % reliability (i.e. mean ± two times standard deviation).

		thickness							
		<1m		1-1.5m		>1.5m		all	
grade	< 0.75%	3,3%		3,2%		6,1%		12,7%	
		3,3%	0,2%	**4,1%**	0,3%	**14,5%**	0,8%	**21,8%**	0,8%
		2,9%	3,7%	3,6%	4,7%	13,0%	16,1%	20,2%	23,4%
	0.75-1.0%	4,7%		4,2%		6,8%		15,7%	
		2,2%	0,2%	**2,8%**	0,3%	**10,6%**	0,9%	**15,6%**	0,8%
		1,8%	2,5%	2,3%	3,4%	8,9%	12,3%	14,1%	17,1%
	>1.0%	14,5%		11,6%		45,4%		71,6%	
		8,4%	0,3%	**11,8%**	0,6%	**42,2%**	1,1%	**62,7%**	0,9%
		7,8%	9,1%	10,7%	12,9%	40,1%	44,4%	60,9%	64,4%
	all	22,5%		19,1%		58,4%		det.ratio	
		13,9%	0,4%	**19,0%**	0,7%	**67,2%**	0,7%	**cs-ratio**	cs-stdev
		13,0%	14,7%	17,6%	20,3%	65,9%	68,5%	cs-conf.int. (low/high)	

Table 25: Conditional simulation results for ratios for lithium grade and thickness classes.

Results slightly vary between deterministic and stochastic perspective. The attribute thickness seems to be shifted to higher thickness classes (< 1 m class is decreased while > 1, 5 m class is increased). It must be reminded that sampling took place only for lengths > 0,5 m, and therefore no smaller samples are represented in the model. On the contrary, the attribute grade seems to be shifted to low classes in the conditional simulation.

10 Conclusions

Koralpe deposit, located in Austria, consists on a lithium concentration in form of thin pegmatite veins hosted in amphibolite and mica schist rock. In order to bring the deposit into operation, a resource calculation according to JORC compliant is required.

Exploration data of the deposit obtained during the 1980ies by the company Minerex have been thoroughly examined and statistically assessed to prove its acceptance according to up-to-date standards. For this purpose, new exploration data from the year 2016 – consisting of twin holes and channel samples at the existing drifts – have been compared to the former one on an individual and global basis. Internal and external duplicates of laboratory analysis performed in the past have been also statistically evaluated to sustain the conclusions.

The investigation of the data has shown a high variability of the deposit on the small scale which is balanced by a very good continuity on the large scale. This has

supported the validation of the data, which have a very good similarity with new data on general basis, but diffused on a detailed comparison. The consideration of former duplicates provides as well satisfactory results. This work has concluded with the acceptance of the Minerex data as input to a resources calculation.

Main aspects to model are lithium (Li_2O) grade and thickness in order to obtain a tonnage measurement. Therefore, the evaluation of the influence of the geology in the deposit has been focused on these two features. Amphibolite hosted veins have a higher lithium grade and thinner thickness than mica schist hosted.

The modelling approach has consisted on an innovative method combining the benefits of the use of geostatistics for calculation of the features of interest and linear interpolation for 3D representation and verification of the results. The calculation has been developed through the use of a 2D block model that avoids the problematic of too small block size required to model such thin veins (0,25 - 5,5 m). Thickness has been modeled as well through geostatistics instead of as a conventional geometric characteristic. In this sense, both estimations, thickness and grade, are based on a statistical background and a measurement of the reliability of the results is obtained. It consideration is extremely valuable for risk aspects as mine design or overall economics. On the other hand, the use of linear interpolation cushion the smoothing effect of geostatistics to provide a more geometrically accurate 3D visualization, faithful to the samples location to a greater extend. The procedure is based on a geological vein assignment, which is the main reason for the need of a 3D validation of the results.

This method has been developed in a way that allows a high level of automatization. This aspect is especially relevant for a fast incorporation of new exploration data and geological interpretations.

The modeling results are obtained applying ordinary kriging. The analysis of its reliability shows a consistency in the results good enough for a resources calculation in terms of mean value. The global results are 6,3 Mt with 1,17 % of Li_2O and 1,32 m thickness. However, it has been noted the need of a tool, such as indicator kriging, to measure different classes or cut-offs, which are omit by the standard calculation.

The local reliability of the results has been assessed in terms of kriging variance, which shows that results at this scale must be interpreted cautiously. On a global analysis, Monte Carlo simulation is suggested as conditional simulation of bigger areas.

Data validation and modeling results have been approved by a competent person according to the JORC organization.

11 Bibliography

Al Maynard & Associates Pty Ltd: Competent Person's Report – Austrian Lithium Project, April 2014.

Beck-Mannagetta, P.: Die Koralpe. In: Oberhauser, R. (ed.) Der geologische Aufbau Osterreichs. Geol. Bundesanstalt Wien, p. 386 – 392, 1980.

Berg, M.; Cheong, O.; van Kreveld, M.: Computational geometry, algorithms and applications, 2008.

Botsch, M.; Kobbelt, L.; Pauly, M.: Polygon mesh processing, A K Peters, Ltd, 2010.

Cerny, I; Moser, P; Nedeff, P.: Das Projekt "Lithium Koralpe". BHM, 134. Jg. (1989), Helf 6.

Glacken, I. M.; Snowden, D. V.: Mineral Resource Estimation, in Mineral Resource and Ore Reserve Estimation – The AusIMM Guide to Good Practice (Ed: A C Edwards), p. 189-198 (The Australasian Institute of Mining and Metallurgy: Melbourne), 2001.

Göd R.: The spodumen deposit at „Weinebene", Koralpe, Austria. Mineralium Deposita 24, p. 270-278, 1989.

Götzinger, M.: "Verein zur Verbreitung naturwissenschaftlicher Kenntnisse", http://www.univie.ac.at/Verbreitung-naturwiss-Kenntnisse/min_s.html (22.08.2016)

Hope, A. C.: A simplified Monte Carlo significance test procedure. Journal of the Royal Statistical Society. Series B (Methodological), Vol. 30, No. 3 (1968), 582-598.

Horman, K.; Lévy, B.; Sheffer, A.:Course presented at ACM SIGGRAPH, 2007.

Jaskula, B. W.: Lithium. U. S. Geological Survey, Mineral Commodity Summaries, p. 100 – 101, January 2016

JORC (The Joint Ore Reserves Committee of The Australasian Institute of Mining and Metallurgy, Australian Institute of Geoscientists and Minerals Council of Australia): Australasian Code for Reporting of Exploration Results, Mineral Resources and Ore reserves – The Jorc Code, 2004 Edition, 2004.

Landau, D., Binder, K.: A Guide to Monte Carlo Simulations in Statistical Physics. Cambridge University Press, New York, 2009.

Mohr, S.H.; Mudd, G.M.; Giurco, D. Lithium Resources and Production: A Critical Global Assessment; Report prepared for CSIRO Minerals Down Under Flagship. Department of Civil Engineering, Monash University Institute for Sustainable Futures, University of Technology: Sydney, Australia, 2010.

Mohr, S.; Mudd, G.; Giurco, D.: Lithium Resources and Production: Critical Assessment and Global Projections. Minerals 2012, 2, p. 65 – 84.

Queen´s University: Geostatistics and resource estimation techniques. Mine Design Project Wiki. 2014 http://minewiki.engineering.queensu.ca/mediawiki/index.php/Geostatistics_and_resource_estimation_techniques (19.09.2016)

Rostami, N.; Habibi, V.; Kamali R.: Comparing Deterministic and Geostatistical Methods in Spatial Distribution Study of Soil Physical and Chemical Properties in Arid Rangelands (Case Study: Masileh Plain, Qom, Iran) in Journal of Rangeland Science, 2015, Vol. 5, No. 3, p. 181-191.

Wolfram Research: Voroni Diagram, 2016. http://mathworld.wolfram.com/VoronoiDiagram.html (15.09.2016).

Zorin, D.; Schröder, P.; DeRose, T.: Subdivision for modeling and animation. In ACM SIGGRAPH 2000 Courses. New York: ACM, 2000.

12 List of Figures

13 List of Tables

14 List of Abbreviations

ARS	Bundesversuchs- und Forschungsanstalt Arsenal (arsenal research)
ASX	Australian Securities Exchange
BEV	Austrian Surveying Service
BMFWF	Bundesministerium für Wissenschaft, Forschung und Wirtschaft
EL	European Lithium
JORC	Code for Reporting of Exploration Results
KMI	Kärntner Montanindustrie GmbH
MRL	North Carolina State University, Minerals Research Laboratory